1. Synthesis of New Polyfluoroaryl Materials.
2. New Transition Metal Catalysts for Enantioselective C – H Bond Functionalization.

by
Thien Ngoc Lieu

A dissertation submitted to the Department of Chemistry,
College of Natural Sciences and Mathematics
in partial fulfillment of the requirements for the degree of

Doctor of Philosophy

in Chemistry

Chair of Committee: Dr. Olafs Daugulis

Committee Member: Dr. Ognjen Miljanic

Committee Member: Dr. Judy Wu

Committee Member: Dr. Thomas Teets

Committee Member: Dr. Jeffrey Rimer

University of Houston
December 2021

ACKNOWLEDGMENTS

First of all, I would like to express my profound and heartfelt thanks to my advisor Dr. Olafs Daugulis for giving me a chance to join his research group. His guidance, support, and forgiveness are so meaningful to me during the entire time I worked in his group.

I also want to thank Dr. Ognjen Miljanic and Dr. Zhenglin Zhang for a great time working with me in my collaboration project. In addition, I would like to thank Dr. Smith for his advice with NMR spectroscopic analysis.

To my committee members Dr. Ognjen Miljanic, Dr. Judy Wu, Dr. Thomas Teets, and Dr. Jeffrey Rimer, I really appreciate your time for reading my thesis and giving me valuable comments. I also want to acknowledge Department of Chemistry staffs for all the helps and kindness you gave to me.

I would like to thank my former group members, Dr. Milad Mesgar, Dr. Tung Nguyen, Dr. Andrew Kocen, Dr. Sehun Kwak, Dr. Quan Tran, Dr. Sabrina Aderibigbe, Dr. Julius Heidlas, and Dr. Hanh Nguyen, for sharing knowledge with me and giving me advice so that I can improve myself. I will cherish every moment we had and wish you guys all the best. To my current group members, although we just met recently, I am still thankful for working with me.

To my undergraduate mentors at BKU-HCMC, Dr. Thanh Truong, Dr. Nam Phan, Dr. Khoa Nguyen, and Dr. Chung Nguyen, thank you for your encouragement and advice during the years.

Finally, I would like to thank my mom, my dad, and my sister, for all the love you give me.

ABSTRACT

1. Synthesis of new polyfluoroaryl materials.

Polyfluorinated porous materials are essential in sequestration of fluorine pollutants due to their high water resistance and fluorophilic ability. In 2014, our and Dr. Miljanic group introduced a triangular porous material prepared from perfluoro organic compounds, showing remarkably selective adsorption toward halogenated hydrocarbons.

Based on the precedent published in 2014, we attempted to increase the pore size of this material by inserting 2,2'-bipyridine groups on each linkage arm. Furthermore, modification of central arene groups was accomplished by using 1,3,5-triazine or 1,3,5-trifluorobenzene. In addition, ferrocene-based fluorine material and two tetragonal fluorine compounds containing pyrene and tetraphenylethylene core were successfully synthesized by using copper catalysis as a main step. Among these compounds, tetraphenylethylene-based structure showed different emissive behaviors under 'wet' and 'dry' conditions.

Other fluorinated tetraphenylethylene compounds such as (Z)/(E)-bis(pentafluorophenyl)stilbene, and tris(pentafluorophenyl)ethylene were synthesized using copper catalysis. In addition, their reactivity and selectivity in photocyclization reactions was also explored.

2. New transition metal catalysts for enantioselective C – H bond functionalization.

Enantioselective carbon-hydrogen bond functionalization using transition metal catalysis is one of the most powerful tools in organic synthesis. This method offers a straightforward route to obtain enantiopure isomer compounds. Thus, in the second part of this

dissertation, two new types of potential chiral catalysts were developed and their reactivity was explored.

A series of new C_3-symmetric tridentate sulfur-containing ligands were synthesized. Various transition metals such as rhodium, iridium, ruthenium, and copper were coordinated to these ligands. In addition, catalytic activity of copper(I) and ruthenium (II) complexes was proved in carbene and nitrene C-H insertion reactions.

Finally, aminoquinoline-directed enantioselective coupling of sp^2 C-H bonds with alkenes using new cobalt catalyst was explored. The catalyst tolerates a broad substrates scope such as styrenes and aliphatic alkenes, giving low to medium level of enantioselectivity. This result may open an opportunity in asymmetric functionalization using bidentate directing groups, which sp far has proven very difficult.

TABLE OF CONTENTS

LIST OF ABBREVIATION

^{13}C NMR	Carbon-13 nuclear magnetic resonance
^{19}F NMR	Fluorine-19 nuclear magnetic resonance
^{1}H NMR	Proton nuclear magnetic resonance
ee	Enantiomeric excess
MOFs	Metal-organic frameworks
DABCO	1,4–diazobicyclo[2.2.2]octane
DMF	N,N–dimethyl formamide
TGA	Thermogravimetric analysis
BET	Brunauer-Emmett-Teller
COFs	Covalent organic frameworks
nCOFs	Noncovalent organic frameworks
TPE	Tetraphenylethylene
AIE	Aggregation-induced emission
DIPA	Diisopropyl amine
Cp	Cyclopentadienyl
Cp*	Pentamethyl cyclopentadienyl
LDA	Lithium diisopropylamide
DEAD	Diethyl azodicarboxylate
DIAD	Diisopropyl azodicarboxylate
EDA	Ethyldiazoacetate
KHMDS	Potassium bis(trimethyl silyl) amide
DGs	Directing groups
HFIP	Hexafluoroisopropanol
TFE	1,1,1-Trifluoroethanol
CSP	Chiral stationary phase

LIST OF SCHEMES

LIST OF FIGURES

LIST OF TABLES

Chapter 1. Fluorinated Porous Materials

1.1 Introduction

Recent decades have witnessed an increase of fluorine containing compound use in synthetic chemistry. Indeed, these compounds are important in materials science, catalysis, medicine, and biochemistry since reactivity as well as properties of molecules and ions change dramatically in the presence of fluorinated moieties.[1] The interest in fluorinated molecules is attributed to the unique properties of carbon – fluorine bonds.[2] Due to high electronegativity of fluorine, the C – F bonds are polar, short, and possess low lying $\sigma^*_{C\text{-}F}$ antibonding orbital.[3] Furthermore, fluorine containing substrates are generally considered to be weak Lewis bases. Fluoride ion is known as a poor leaving group, resulting in high thermodynamic stability and kinetically inert carbon-fluorine bonds. Consequently, fluorination is one of the most versatile methods for changing electron-density distribution in molecules without a large impact on steric aspect.[3]

Since fluorine containing compounds possess exceptional properties, the fluorochemical industry has vastly expanded in last 100 – 150 years and numerous fluorinated products have become essential.[4] For instance, hydrogen fluoride, prepared by treating fluorospar (CaF_2) with sulfuric acid, is the key intermediate in the synthesis of cryolite for aluminum production and fluorocarbons including chlorofluorocarbons (CFCs), and hydrofluorocarbons (HFCs), mainly used as refrigerants.[5] Additionally, elemental fluorine is used in nuclear industry, to enrich ^{235}U by using gas centrifugation of uranium hexafluoride, derived from reaction between UF_4 and fluorine gas.[6] Similarly, fluoropolymers have also gained a lot of attention from chemists due to their attractive properties including chemical resistance, thermal and weather stability, flame resistance, good mechanical properties, and

high dielectric breakdown voltage which has widened their usages in industry.[7] Furthermore, fluorine containing pharmaceuticals are important due to their ability to enhance bioactivity and metabolic stability.[2] Recent reports have shown that approximately 25% of small molecule drugs in clinic contain fluorine moiety while 25 – 30% newly established drugs have fluorine atoms in structure.[8] Last but not least, since "fluorination" differentiates physicochemical properties of active compounds such as lipophilicity, water solubility, and metabolic stability, fluorine containing molecules are also used in agricultural industry to provide selective crop-protection agents.[9]

In spite of the fact that fluorinated compounds are widely used today, there are still some inherent potential problems associated with them. First, the oxidation potential of fluorine is much higher than that of other halogens at -3.06 V. Consequently, enzymatic fluorination is not feasible.[10] Due to its slow release, fluoride can accumulate in human body, causing dental fluorosis in children or skeletal fluorosis in both children and adults. The main source of fluoride pollution comes from aluminum industry and phosphate fertilizers. In addition, the later one normally accounts for majority of fluoride content which is 1 – 3% in the case of superphosphate.[11] Although fluoride pollutant adheres strongly to a soil, it can still present a threat to grazing livestock.[11] Furthermore, community water fluoridation, long-term controversial topics in medicine, also contributes to the drastic increase in the amount of fluoride intake.[12] Finally, the over-exploitation of polyfluoroalkyl substrates and their derivatives has created other dangers since these compounds are inert to degradation, resulting in their accumulation in the environment.[13] For example, refrigerants (**R-134a, R-12, R-40**), propellants (**HFC-227ea**, **HCFC-225ca**), blowing agents for foams (**CFC-113**) and electronics industry (CF_4, SF_6, perfluorohexane) are greenhouse gases and cause ozone depletion in the

upper atmosphere.[14] These substances have been replaced by less harmful fluorocarbons, yet the alternatives still remain potent greenhouse gases. In the past, numerous polychlorinated substrates such as DDT, γ-hexachlorocyclohexane, and polychlorinated biphenyl have clearly showed harmful effects on environment.[15] This raises a significant interest in the capture and sequestration of another potentially hazardous group of compounds, namely polyfluorinated compounds.

There are significant challenges in selectively capturing toxic chemicals listed above due to their low concentration in air (part-per-million), as well as the atmospheric presence of other active molecules such as water.[16] Traditionally, one of the cheapest and most readily available absorbents, activated carbon, was employed in filtering both chemical warfare agents and toxic industry chemicals, yet this material shows only weak interactions with many toxic chemicals, leading to medium to low uptake capacities.[17] Additionally, adsorption of polar toxic agents is even more ineffective because of nonpolar surfaces of activated carbon. To enhance the uptake capacity of diluted toxic chemicals, activated carbon has been blended with transition metals including zinc, copper, silver, molybdenum, or basic organic compounds such as triethylenediamine or 1,4-diazabicyclo[2,2,2]octane.[18] However, this is not a long-term solution due to the lack of crystallinity and compositional tunability, leading to difficulties in further improvement for targeted toxic substance adsorption. To this end, metal-organic frameworks (MOFs), a hybrid material created from metal cations or clusters and organic linkers, appears to be an ideal solution to address these limitations owing to its high crystallinity and synthetic versatility.[19-21] Furthermore, open metal sites on MOFs can act as Lewis acid sites for strong selective adsorption, even at low concentrations.[22] Finally, the easy modification of pore sizes,

and surface areas is an additional attractive feature of MOFs, since it can be predicted as well as calculated to enhance selectivity and uptake capacity of targeted molecules.

Regardless of promising performance in adsorption and separation, there has been a downside in practical applications of MOFs, mainly due to their high water sensitivity.[23] Most MOFs are labile or hemilabile,[24] and humidity affects them by coordination bond cleavage, which prohibits their usage in many cases. There are two common degradation mechanisms when MOFs are exposed to humidity, namely ligand displacement and hydrolysis.[25] After being attacked by water, a hydrated cation is formed, releasing free ligand. This process is called ligand displacement. The other possibility is known as water dissociation. In this case, the release of hydroxylated cations and free protonated ligands leads to hydrolytic cleavage of metal-ligand coordination bonds.[26] Mechanistically, this phenomenon can be prevented if metal-ligand coordination bonds are strong which can be achieved by either increasing electronegativity of ligands or installing hydrophobic agents (normally fluorine atoms) to retard hydrolytic attack.[26] The replacement of hydrogen by fluorine in ligands not only helps to increase the robustness toward moisture, but also increases the fluorophilicity of those MOFs, resulting in enhancement in selective adsorption of halogenated pollutants.

1.2 Mesoporous Fluorinated Metal Organic Frameworks

It is undeniable that installation of fluorine in polymers[27] and drugs[28] dramatically changes their properties. In the same manner, the incorporation of fluorine atoms in MOFs also increases their stability, specifically in terms of robustness toward humidity, resulting in chemical resistance. This trend has attracted a lot of attention from chemists since the introduction of FMOF-1, prepared from silver (I) and 3,5-bis(trifluoromethyl)-1,2,4-triazolate (**Scheme 1.1**). This material showed remarkable oxygen and hydrogen gas uptake.[29] Authors

believe that high gas uptake is attributed to the presence of fluorine atoms in the linkers of FMOF-1.[29] The thermal and chemical stability,[29,30] as well as hydrophobicity increase of these "Teflon coated"-MOFs were also examined and highlighted. [31]

Scheme 1.1. Building block of FMOF-1.

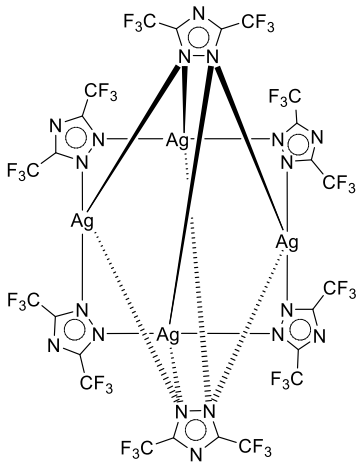

In 2013, our and Dr.Miljanic groups reported three perfluorinated copper-based MOFs, made from copper (II) nitrate and ligand **3** or **4** with assistance of 1,4-diazabicyclo[2.2.2]octane (DABCO).[32] The synthesis of fluorinated polyaryl ligands **3** and **4** is illustrated in **Scheme 1.2**. The C – H bond functionalization reaction using copper (I) iodide catalyst between compound **1** and 2,3,5,6-tetrafluoro-4-iodobenzonitrile gave compound **2** in good yield. This methodology was reported by our group in 2008,[33] affording a fast, convenient, and cheap route to obtain **2**. Then, compound **2** was either treated with sodium azide in acid solution, giving **4** or hydrolyzed under strong acid conditions to afford diacid **3** in excellent yield. After that, the linkers was heated with copper salts in *N.N*-dimethylformamide (DMF), methanol, and water at 40 °C for several days to obtain well-defined crystals. Thermal stability of those "Teflon-coated" MOFs was evaluated using thermogravimetric analysis (TGA), showing all of them are stable up to 220 °C, while nitrogen adsorption/desorption test revealed that they were mesoporous with the

Brunauer–Emmett–Teller (BET) surface areas value around 400 to 600 m^2 g^{-1}. The most important feature of these MOFs is their hydrophobicity. This property was examined by water contact angle measurements. The results illustrate that all the materials are water-repellent with the contact angle fluctuating from 108 to 151 °, proving the essential role of fluorine atoms in the structure. Additionally, further evidence showing the super-hydrophobic behavior of those materials was uncovered by water adsorption. Even at 90% relative humidity all prepared MOFs only adsorbed negligible amount of water, compared to FMOF-1.[34] Presumably, the larger perfluorinated ligand results in more hydrophobic material.

Scheme 1.2. Synthesis of ligands **3** and **4**.

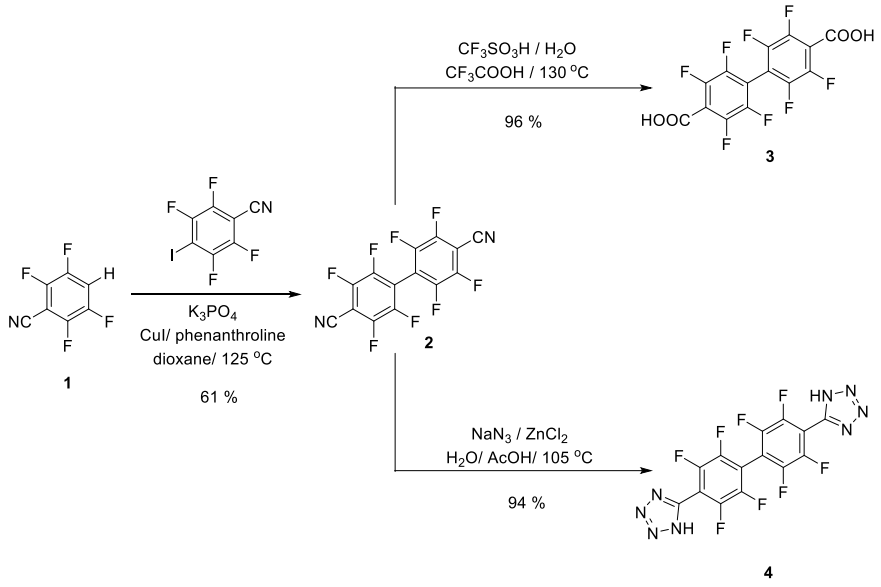

In 2016, the Douglas group reported other fluorinated MOFs based on indium. The YCM-101 was synthesized by using solvothermal method between indium (III) chloride and 2,3,5,6-tetrafluoroterephthalic acid in DMF, 2-propanol, and water.[35] Although the material was not super-hydrophobic due to the lack of C – F bonds on each linker, the authors showed that this material is capable of removing pharmaceuticals from water streams. Specifically, the

strong electron deficiency of linker enables beneficial π-π stacking interactions with electron rich arenes present in most polycyclic aromatic hydrocarbons and numerous pharmaceuticals. Furthermore, the authors reported that the uptake of tetracycline was up to 32 mg per 1 g of MOF, compared to no tetracycline uptake in MIL-68, which contains no fluorinated carboxylic linker.[35]

Another type of fluorinated MOFs were reported in 2018.[36] Treating zinc (II) salts with octafluorobiphenyl-4,4'-dicarboxylate under various conditions, a series of six zinc (II) coordination polymers wer obtained with different dimensions (1D, 2D, and 3D). However, only two of them were shown to be porous with BET surface area around 450 m^2 g^{-1}. Interestingly, these materials were more efficient in selective adsorption of carbon dioxide over nitrogen and methane at room temperature. Additionally, the measurements of water contact angles and low water uptake also confirmed the hydrophobic characteristic of those MOFs.

1.3 Covalent and Noncovalent Fluorinated Organic Frameworks

Unlike MOFs, covalent and noncovalent organic frameworks (COFs and nCOFs) consist of only light elements, typically H, B, C, N, and O. These kinds of materials were first pioneered by Yaghi group in 2005.[37] Since then, numerous COFs have been reported. The highly ordered internal structures of COFs are mainly formed by strong covalent bonds through some chemical reactions including boronic acid trimerization,[38,39] boronated ester formation,[40,41] nitrile trimerization,[42,43] and nitroso self-addition,[44] while the main factors constructing nCOFs are non-covalent bonds such as hydrogen bonding or π-π stacking interactions.[45] Basically, COFs and MOFs share similar properties, but an interesting question is how fluorine atoms influence the crystal structures as well as physicochemical properties of COFs.

In 2018, Pascal and co-workers reported the effect of fluorine on adsorption properties of covalent triazine frameworks.[46] The materials were synthesized from monomer, perfluoro-4,4'-biphenyldicarbonitrile, under ionothermal conditions at 400 °C, using molten zinc (II) dichloride catalyst (**Scheme 1.3**) to obtain F-DCBP-CTF in good yield. The non-halogenated compound, DCBP-CTF, was prepared from 4,4'-biphenyldicarbonitrle monomer. After characterization, results indicated that DCBP-CTF had higher surface area and pore volume compared to fluorinated compound, 2437 $m^2 g^{-1}$ and 1.41 $cm^3 g^{-1}$ compared to 1574 $m^2 g^{-1}$ and 0.51 $cm^3 g^{-1}$, respectively.[46] In contrast, F-DCBP-CTF showed remarkably interesting selective gas adsorption properties. This material can reach up to 1.77 (wt%) of hydrogen uptake at 77 K, while only a negligible amount of H_2 uptake was observed in the case of DCBP-CTF. Furthermore, the selective adsorption ratio between CO_2 and N_2 showed that fluorine-containing CTF possesses relatively high selectivity towards CO_2, compared to non-functionalized one at, 31 and 13 ratios, respectively.

Scheme 1.3. The synthesis of F-DCBP-CTF.

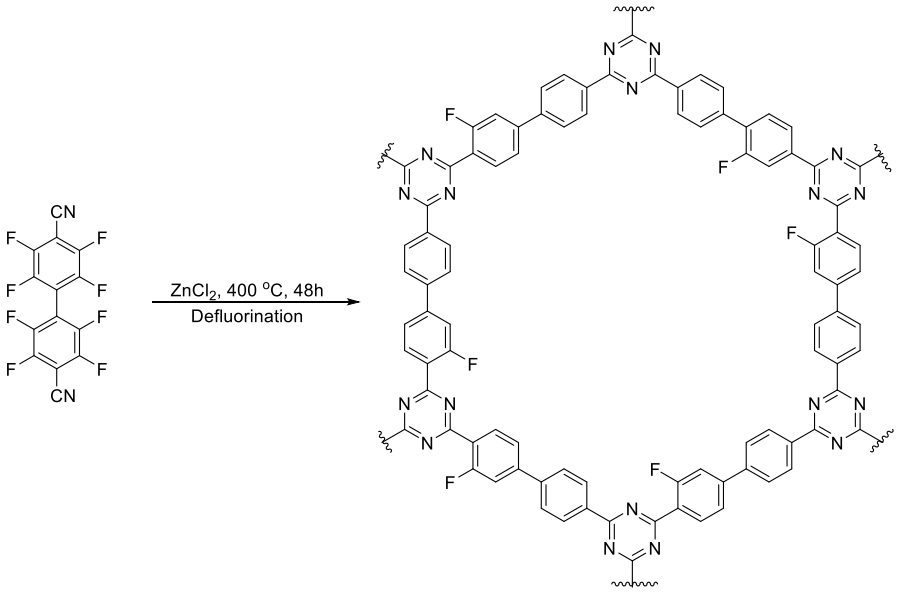

In same year, Justin and co-workers explored the influence of fluorine atoms on structure and properties of COFs.[47] A series of fluorinated and non-fluorinated COFs was synthesized using simple imine condensation reaction (**Scheme 1.4**). In contrast to the work by Pascal group, this paper indicated that FASt-COF material possesses the highest BET surface area and pore volume, 1700 $m^2 g^{-1}$ and 1.09 $cm^3 g^{-1}$, respectively, while only 970 $m^2 g^{-1}$ and 0.4 $cm^3 g^{-1}$ was observed for Base-COF.[47] The dramatic increase in surface area and pore volume of partially fluorinated COF, FASt-COF, was rationalized by strongly enhanced stability imposed by fluorine atoms and the rotated stacking structure, resulting in phenyl-perfluorophenyl interactions in alternating layers compared with non-alternating COF analogues.[47] This observation also suggests ways how to increase surface area and stability in these materials.

Scheme 1.4. Synthesis of imine-based 2D COFs.

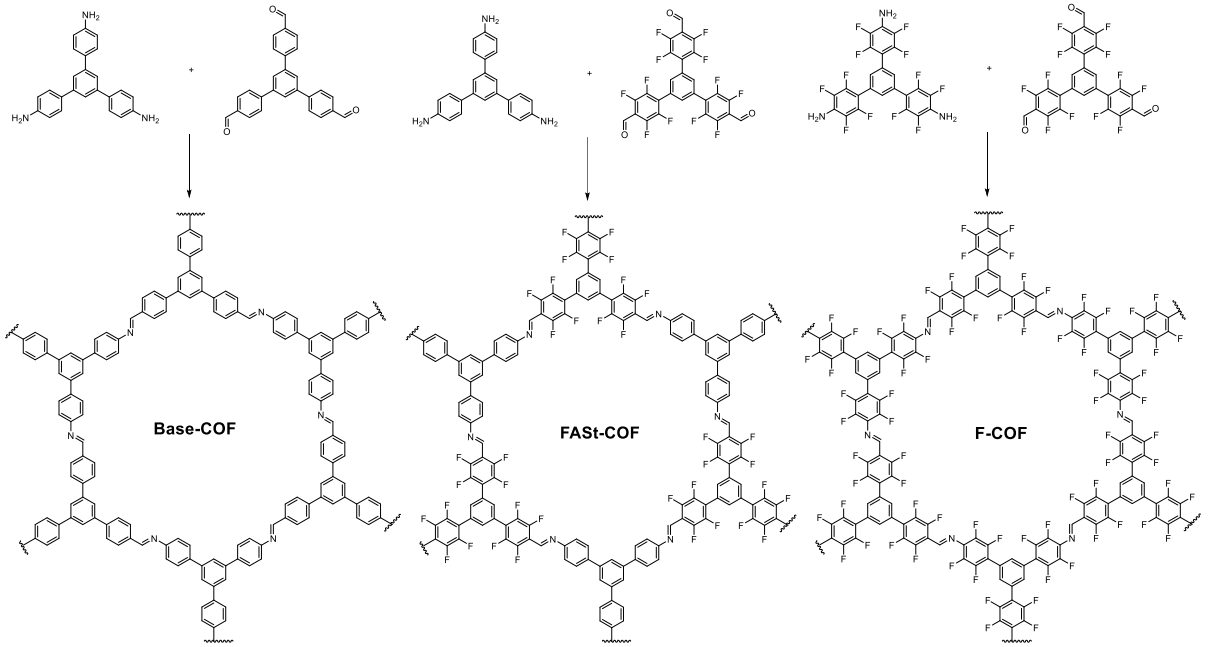

Only few publications report synthesis and use of noncovalent organic frameworks due to the fairly weak interactions, associated with noncovalent bonding. In 2014, our and

Dr.Miljanic groups introduced a nCOF, mainly formed by hydrogen bonding and π-π stacking interactions.[45] The synthesis of linker is described in **Scheme 1.5**. Compound **5** was protected by a trityl group, then a series of palladium catalyzed C – H bond functionalizations with the assistance of copper (I) chloride and a strong base were performed to obtain **8**. Subsequently, protecting group replacement gave compound **9**. This step was used to prepare for the removal of protecting group using simple heating to produce final product **10**. Compound **10** was then recrystallized to form porous crystals.

Scheme 1.5. Synthesis of nCOF **10.**

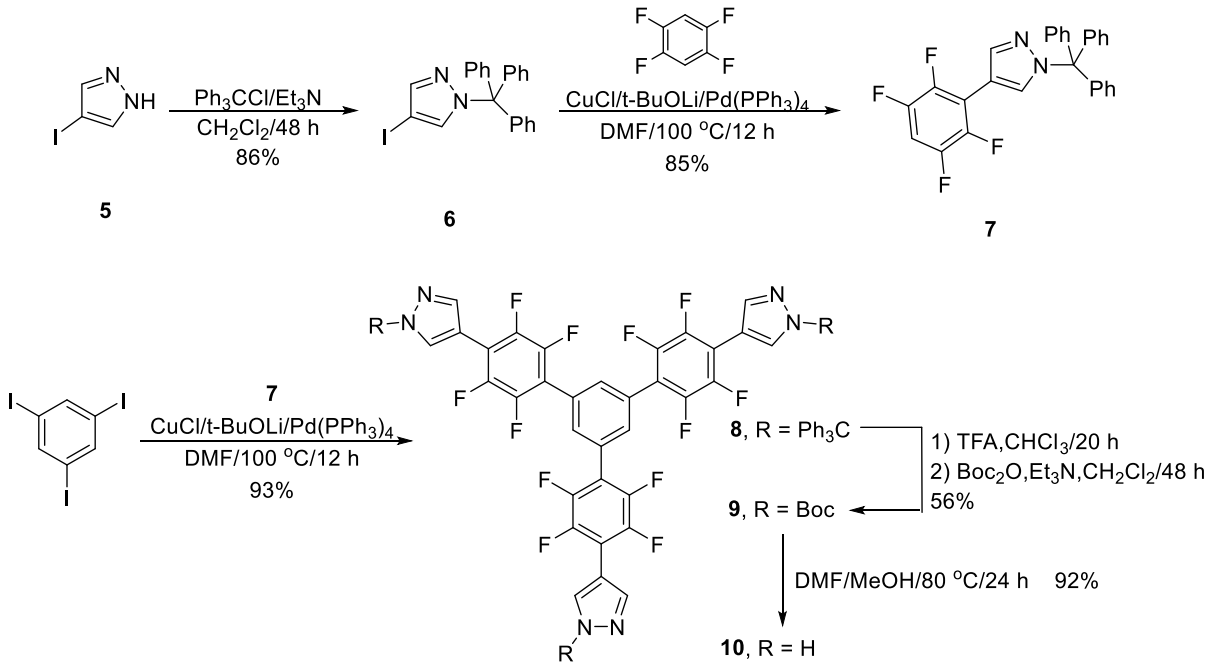

The crystal structure of nCOF **10** was analyzed by using X-ray diffraction (**Figure 1.1**). The crystals of this material art mainly formed by [N-H ⋯ N] hydrogen bonding among the pyrazole groups and each unit comprises of triplet of hydrogen bonds with the length of 1.85 Å to form one layer. Layers were held by [π ⋯ π] stacking interactions between electron rich pyrazole with its six neighbors, electron poor pentafluorobenzene rings. Other physicochemical

characterizations were performed and the results showed that this nCOF **10** is stable up to 250 °C. The BET surface area of **10** was 1,159 m^2 g^{-1}, determined by nitrogen adsorption, and pore volume was around 51%. Furthermore, the water contact angle of 132 ± 1° confirmed the hydrophobic behavior of **10**. Interestingly, this material also showed the efficiency in selective adsorption toward halogenated hydrocarbons. Specifically, crystal **10** could reach up to 74 (wt%) of perfluorohexane uptake while only 27.7 (wt%) of hexane uptake was adsorbed. Moreover, the uptake of potent greenhouse gases including **CFC-113** (Cl_2FC-$CClF_2$) and **HCFC-225ca** ($CF_3CHF_2CHCl_2$) were also investigated, reaching 66 (wt%) and 58 (wt%), respectively.

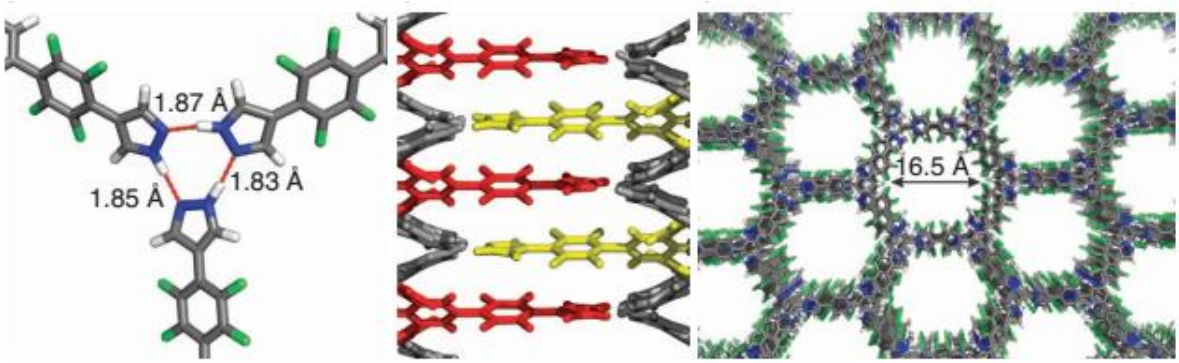

Figure 1.1. Crystal structure of compound **10**. [45]

To conclude, both fluorinated MOFs as well as COFs possess advantages and disadvantages in either structure design or physicochemical properties. To this end, nCOFs appear to offer a potential solution for problems inherent in these materials. First, nCOFs material do not require the incorporation of transition metals within the structure but they can still achieve remarkably selective adsorptions. Second, metal-free structure and presence of only covalent bonds result in wider solvent options for these structure, leading to easier characterization as well as their destruction and recovery when in need. Next, since most of noncovalent bond distances are known, the channels inside materials can be calculated or

predicted prior experiments. However, due to fairly weak interactions and limited number of noncovalent bonds, there are only few options in designing these structures, which results in lack of variety. This drawback seems to be less important due to extraordinary unique properties of nCOFs. Consequently, synthesis and studies of nCOF materials is still a hot topic in finding solutions for environmental issues. Thus, synthesis and exploration of nCOF materials is the main purpose of the first project in this thesis.

Chapter 2: Synthesis and Characterization of Fluorinated Linkers for nCOFs Synthesis

2.1 Synthesis of Triangular Based Fluorinated Linkers

2.1.1 Introduction

The work in this chapter was performed to increase the surface area and pore volume of the material by lengthening the size of each arm in the original molecule, which has been prepared earlier.[45] There have been several examples which show that the length of the linkers correlates with better physicochemical properties of materials. An example is COF-5, synthesized by condensation reaction of phenyl-1,4-diboronic acid and hexahydrotriphenylene. This material showed a remarkable crystal structure with the BET surface area of 1590 $m^2 g^{-1}$, corresponding to a mesopore volume of 0.998 $cm^3 g^{-1}$ and pore size of 26 Å.[37] Meanwhile, by inserting an extra phenyl ring in boronic acid fragment, the properties of COF-10 were enhanced significantly. Specifically, owing to strong Lewis acid-base interaction, COF-10 showed the highest ammonia uptake capacity (15 mol kg^{-1}, 298 K, 1 bar) of any porous materials, including microporous 13X zeolite (9 mol kg^{-1}), Amberlyst 15 (11 mol kg^{-1}), and mesoporous silica MCM-41 (7.9 mol kg^{-1}) at that time.[48] Furthermore, the pore size distribution was increased up to 34 Å, compared to COF-5. **Scheme 2.1** depicts the structures of COF-5 and COF-10.

Scheme 2.1. Structure of COF-5 and COF-10.

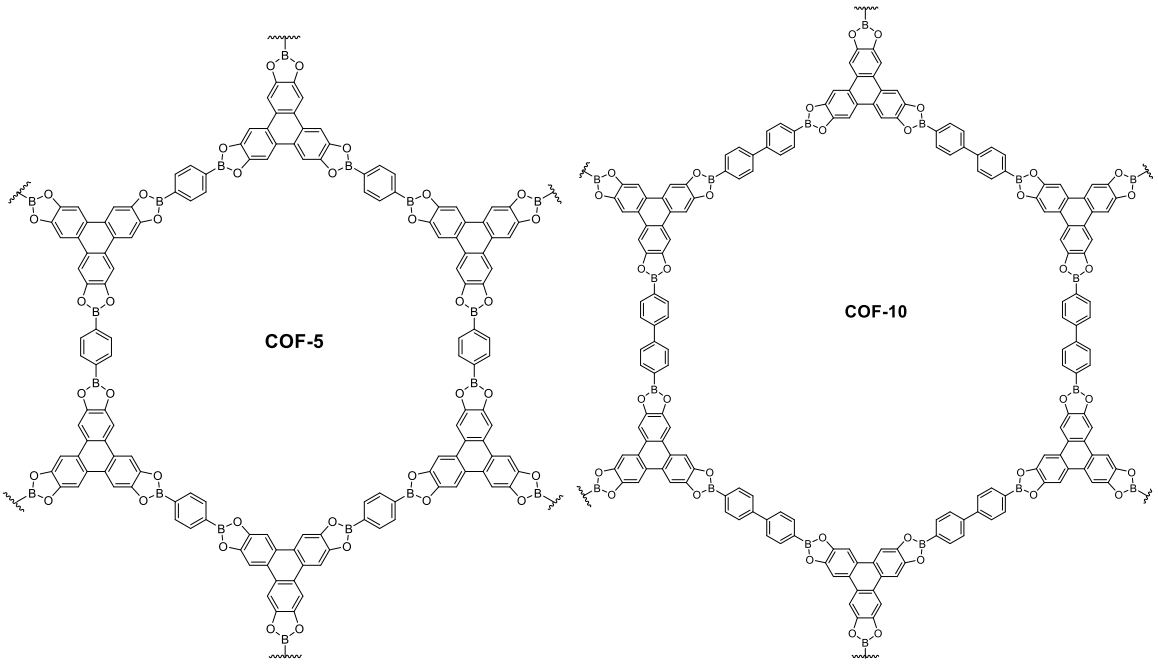

We speculated that 4,4'-bipyridine linker would potentially induce some useful properties in the material (**Scheme 2.2**). First, this bipyridine elongates the molecule and may enhance the π···π interactions in the structure. Second, two nitrogen groups may act as ligands for most common transition metals.

Scheme 2.2. New nCOFs design.

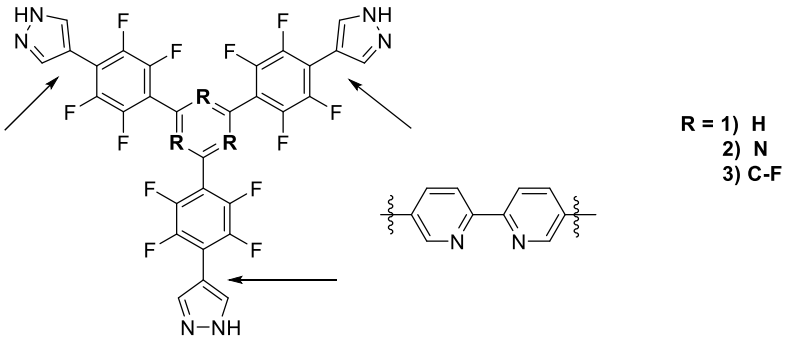

Use of metal coordination in porous materials has been reported. For example, in 2010, Yaghi group reported MOF-253, [Al(OH) (BPYDC), BPYDC = 2,2'-bipyridine-5,5'-dicarboxylate], (**Figure 2.1**) in which the ligands connected with alumina rods were metalated with copper (II) or palladium (II). The products show a remarkable ability in gas separation. A 4-fold increase of selectivity in N_2/CO_2 separation was observed.[49]

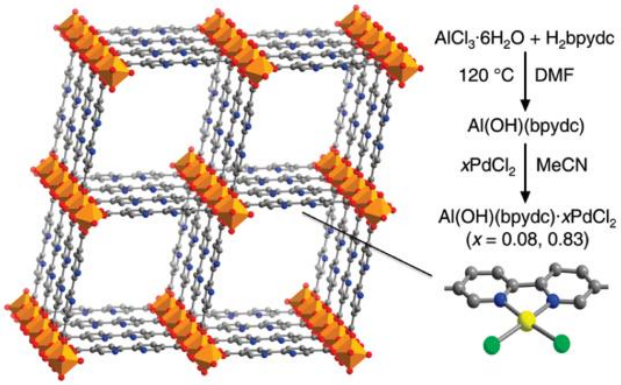

Figure 2.1. Synthesis and representative structure of Al(OH)(bpydc) (MOF-253) with subsequent insertion of $PdCl_2$ into open bpy ligand sites.[49]

In 2012, Fabian and coworkers claimed that metal coordinated porous materials can be used in catalytic reactions as well. Specifically, the authors investigated oxidation reaction of alcohols.[50] The researchers used ruthenium doped MOF-235 to catalyze the transformation of alcohols to aldehydes or ketones in the presence of $PhI(OAc)_2$ as oxidant at low temperatures. The catalyst worked surprisingly well for oxidation of both benzylic and alkyl alcohols, giving excellent yields and good turnover frequencies. **Table 2.1** summarizes some of the substrate scope. In addition, authors also applied this methodology in oxidizing cholestanol to cholestanone in good yield (**Scheme 2.3**). Presumably due to the small size of cholestanol (8.1 x 6.5 Å) compared to Ru-doped MOF-235 (11 x 13 Å), the substrate was able to enter the pores

and react.[50] Independent work in 2015 reported that Ru complex on MOF-235 has potential for photocatalytic CO_2 reduction under visible light.[51]

Table 2.1. Oxidation of various alcohols by using MOF-235-Ru

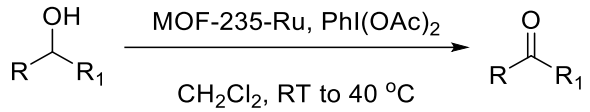

Entry	Product	t [h]	T [°C]	Conversion/Yield [%]	TOF [h^{-1}]
1	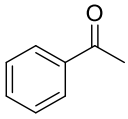	2	40	97/97	97
2	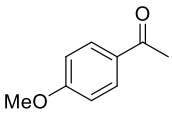	2	40	99/99	99
3	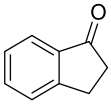	2	40	92/92	92
4		3.5	40	98/98	56
5	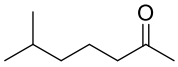	2	40	99/99	99
6		2	40	95/88	96

Scheme 2.3. Oxidation of cholestanol to cholestanone catalyzed by MOF-235-Ru.

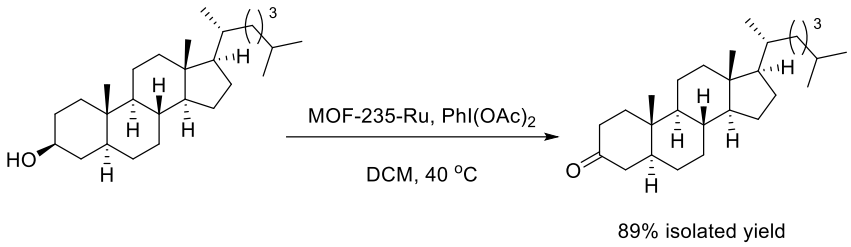

Lastly, we also tested the influence of the middle benzene ring on the properties of material. Since the main interaction in these materials are the π···π stacking interactions, the electronic nature of this benzene ring would probably result in different pore size which has been noticed in previous work. Therefore, several models need to be examined including one containing benzene, 1,3,5-triazine, and 1,3,5-trifluorobenzene substituents (**Scheme 2.2**).

2.1.2 Synthetic Route

The key step in the synthesis of these new compounds is copper-catalyzed C – H bond functionalization developed by our group in 2008.[33] The synthetic route is summarized in **Scheme 2.4**.

Scheme 2.4. Synthesis of Y-shaped compound with benzene ring at core.

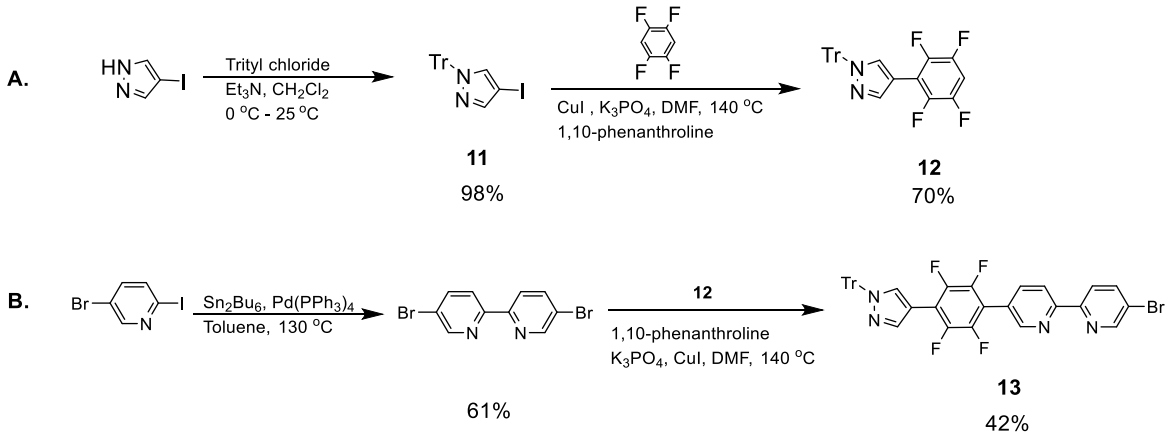

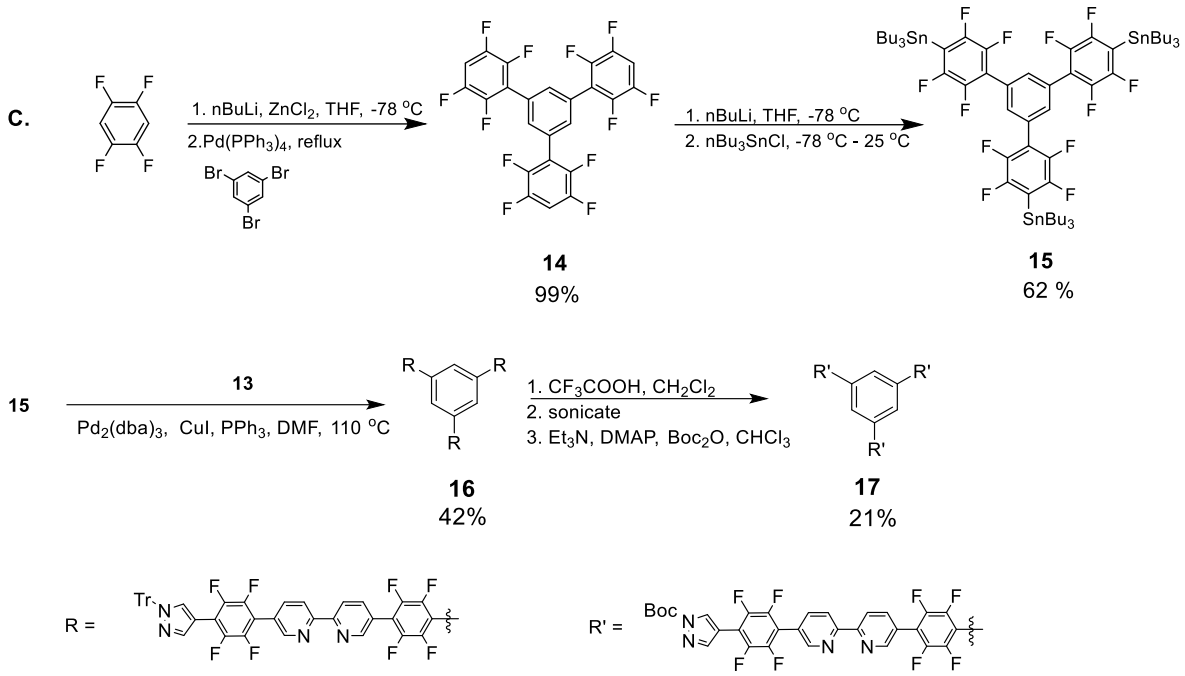

The procedure commenced with 4-iodopyrazole protection by trityl group giving quantitative yield of product **11**. This protecting group was chosen owing to its ability to endure harsh conditions later in synthetic scheme. Then, C – H functionalization reaction of **11** with 1,2,4,5-tetrafluorobenzene using copper catalyst in the presence of bidentate ligand 1,10-phenanthroline and potassium phosphate base afforded compound **12** in 70% yield. Next, 5,5-dibromo-2,2-bipyridine was synthesized in a one-pot Stille coupling reaction by using a literature method, in which organotin reagents were generated and consumed during the reaction.[52] The yield of this reaction strongly depends on the quality of tin reagent, with higher purity normally affording better yields. In addition, small scale reactions also offered higher yields. After that, using copper catalyzed methodology, compound **13** was obtained in moderate yield. Additionally, bis-coupling by-product was observed no matter how large of excess of bipyridine was used. In parallel, compound **14** was synthesized using Negishi coupling in which 1,2,4,5-tetrafluorobenzene was treated with nBuLi and zinc (II) dichloride to generate

organozinc reagent and subsequently coupled with 1,3,5-tribromobenzene using palladium (0) complex, giving **14** in quantitative yield. Compound **14** is fairly insoluble in most common organic solvents so it could be collected by simple filtration. Presumably, due to its insolubility, the initial approach for compound **14** using copper catalysis methodology failed. All the efforts using direct C – H functionalization from **14** and **13** to produce **16** were unsuccessful. In contrast, Stille coupling was a good option to solve this problem. The organotin reagent was generated by lithiation of **14**, followed by quenching with tin reagent, giving **15** in moderate yield. The Stille coupling between **15** and **13**, using palladium (0) complex with assistance of copper salt and phosphine ligand afforded **16** in 42% yield. Finally, deprotection of **16** and addition of Boc protecting group gave target **17** in 21% yield. The sonication step is crucial; otherwise the addition will not occur due to insolubility of deprotected intermediate.

To test the influence of central ring on the crystal properties, two more molecules were prepared. In one, benzene is replaced by 1,3,5-triazine, and in the other 1,3,5-trifluorobenzene core is used. The synthetic procedure for the former compound is described in **Scheme 2.5**.

Scheme 2.5. Synthesis of Y-shaped compound with 1,3,5-triazine core.

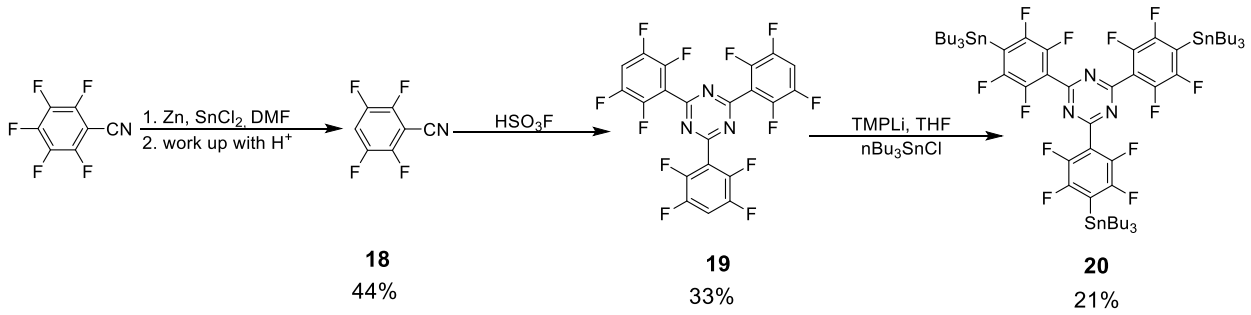

18 44%

19 33%

20 21%

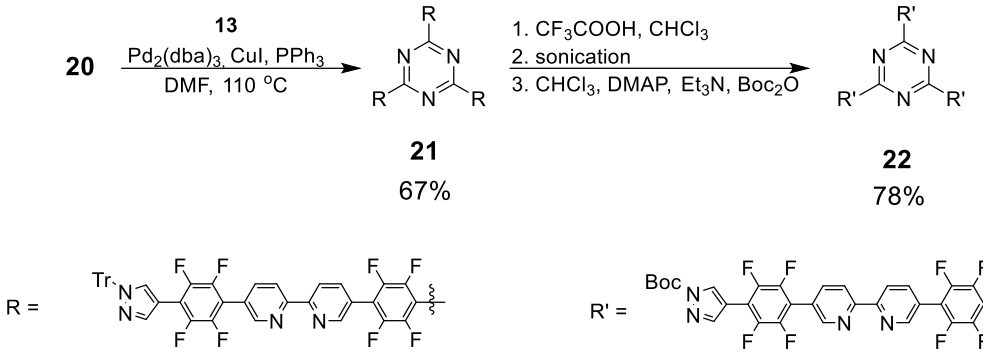

The triazine core-containing compound **18** was synthesized by defluorination of pentafluorobenzonitrile.[53] Using zinc metal with tin (II) dichloride followed by quenching with aqueous hydro chloric acid gave compound **18** in moderate yield. The next step is trimerization using strong acid for several days, gave compound **19**.[54] The product **19** was soluble in various common organic solvents in contrast to the insolubility of compound **14**. This phenomenon shows the influence of core ring on the properties of the molecule. To prepare precursor for Stille coupling, bulky base was used to deprotonate compound **19**, giving **20** in 21% yield. Next, the Stille coupling between compound **20** and **13** using palladium (0) complex catalyst afforded **21** in 67% yield. The last step of this procedure is deprotection of trityl protecting group, followed by addition of Boc protecting group, which gave **22** in 78% yield. Again, sonication determined the success for this step.

All efforts to attach 1,2,4,5-tetrafluorbenzene to 1,3,5-trifluorobenzene moiety were unsuccessful, presumably due to electronic and steric repulsions. Hence, the model was changed to overcome the problem, and fragment **13** was directly coupled to 1,3,5-trifluorobenzene, resulting in a shorter ligand. The procedure for preparation of new compound is described in **Scheme 2.6**. Initially, 1,3,5-trifluorobenzene was deprotonated by TMPLi in the presence of nBu_3SnCl generating organotin compound **23**. Then, **23** was coupled with **13** in the

presence of palladium (0) catalyst, copper salt, and phosphine ligand, producing intermediate **24** in a 30% yield. The final step was deprotection, sonication and addition of new protecting group, giving final product **25** in 42% yield.

Scheme 2.6. Synthesis of Y-shaped compound containing trifluoroarene core.

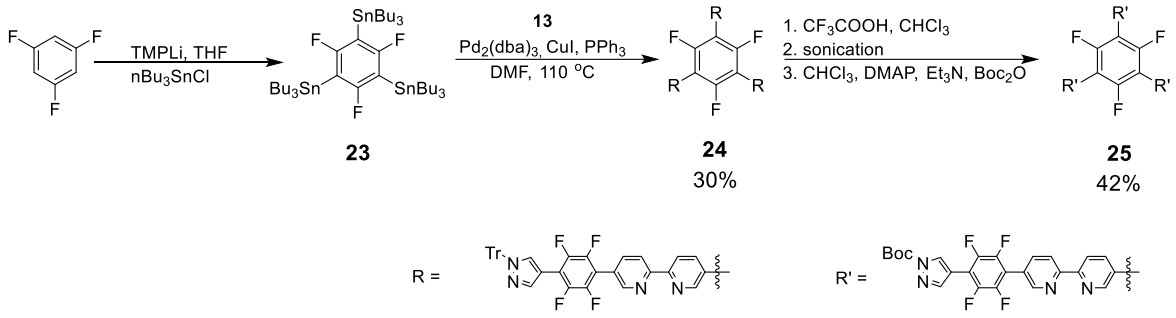

2.2 Synthesis of Tetragonal Fluorinated Linker

2.2.1 Introduction

Pyrene is an organic chromophore which is capable of absorbing particular wavelengths of visible light and its photophysical nature has been extensively investigated.[55] Due to its interesting properties, compounds made from pyrene have attracted significant attention from chemists.[56] For example, in 2016, Farha's group developed a 3-D Zr-based MOF constructed from a tetratopic pyrene-containing linker and metal salt.[57] This material was applied as catalyst for oxidizing sulfur mustard, a chemical warfare agent, by a singlet oxygen owing to low energy triplet state together with effective intersystem crossing from singlet to triplet state of pyrene compounds.[58] Pyrene and its derivatives are also widely used in other COFs as well. In 2014, a series of four different pyrene based 2D COFs were created with BET surface areas up to 2300 $m^2 g^{-1}$ and pore volumes up to 1.85 $cm^3 g^{-1}$.[59] In 2016, Cheng group developed 3D pyrene based COFs by the treatment of tetra(p-aminophenyl)methane with 1,3,6,8-terakis(4-formylphenyl)pyrene.[60] The BET surface area and pore volume of this 3D COFs were measured

to be 1290 $m^2 g^{-1}$ and 0.72 $cm^3 g^{-1}$, respectively.[60] The most interesting property of this material is that 3D-py-COF is the first ever fluorescent 3D COF with a yellow-green luminescence. Additionally, authors also suggested their potential application in explosive detection due to its fluorescence behavior.

Inspired by interesting properties of pyrenes, we prepared other pyrene materials, which would possess noncovalent interactions such as hydrogen bonds and π···π stacking.

2.2.2 Synthetic Route

The synthesis of new linker is summarized in **Scheme 2.7**. Initially, 1,4,6,9-tetrabromopyrene was synthesized by bromination under reflux in nitromethane solvent, yielding 89 % of the product.[61] The product is insoluble in all common organic solvents, limiting its characterization. The next step in sequence was C – H bond functionalization using copper catalysis in the presence of potassium phosphate and 1,10-phenanthroline, affording **26** in 54% yield. Reaction time and proper temperature were the key factors determining the yield due to the insolubility of starting material. Finally, protecting group exchange gave product **27** in 16% yield.

Scheme 2.7. Synthesis of pyrene based compound.

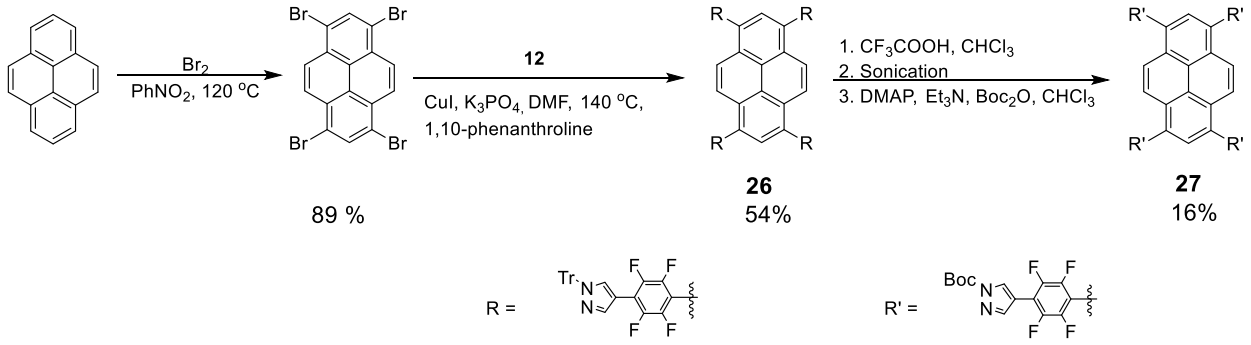

2.3 Synthesis of Ferrocene Based Linker

To date, there are very few reports on preparation and applications of ferrocene-based nanoporous frameworks.[62] Therefore, it would be valuable to prepare porous materials based on ferrocene since they may have characteristics of both metal organic and covalent organic frameworks. In addition, iron (II) based MOFs are fairly rare due to weak oxidative stability of iron (II), so material which overcome that issue may be of interest. The synthesis of ferrocene-containing compound is summarized in **Scheme 2.8**. First, 1,1'-diiodoferrocene was synthesized by deprotonation of ferrocene using TMEDA and nBuLi followed by quenching with iodine to obtain product in 58% yield. This method has been reported in literature.[63] Then, compound **16** was obtained by using copper catalysis methodology as shown previously; however, the yield was only about 20%. On the other hand, using Stille coupling, the yield of the product could be improved to 77 % and the last step involving protecting group exchange gave compound **29** in moderate yield.

Scheme 2.8. Synthesis of ferrocene based linker.

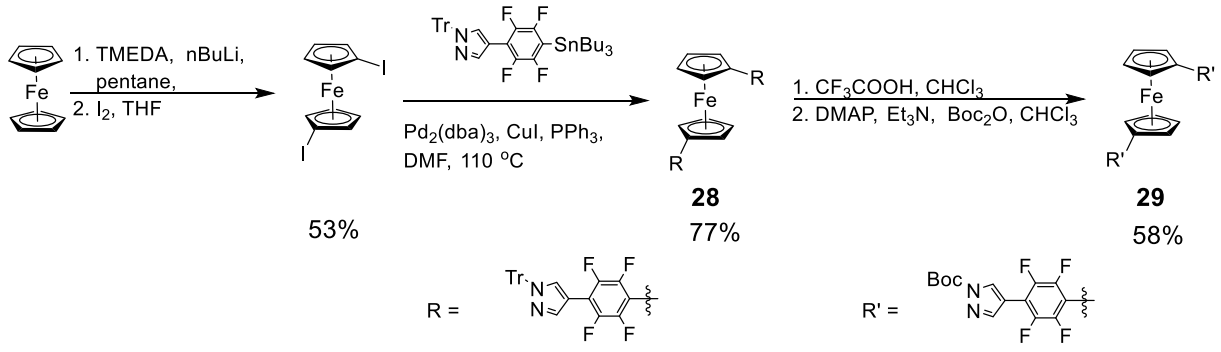

2.4 Summary

We have prepared various compounds for nCOFs synthesis. Specifically, triangular linkers with different in core rings, tetragonal linker, and ferrocene based linker were synthesized. These compounds will be used in Dr. Miljanic group for crystal growth. The bipyridine-containing compounds will be coordinated or doped with transition metals and their catalytic activities will be explored.

2.5 Experimental Section

General

Reactions were performed using standard glassware or were run in 2-dram vials with PTFE/Liner screw caps and 8-dram vials w/polyseal screw caps. Column chromatography was performed on 60Å silica gel (Dynamic Adsorbents Inc.). ^{1}H, ^{13}C, ^{19}F-NMR spectra were recorded on JEOL EC-400, JEOL EC-500, JEOL EC-600 spectrometers. Analytical thin layer chromatography was performed on silica gel IB-F (Baker-flex) by J. T. Baker. All procedures were performed under nitrogen unless otherwise noted. Reagents and starting materials were obtained from commercial sources and used without further purification unless otherwise noted.

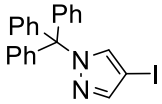

N-Trityl-4-iodopryazole 11.

4-Iodopyrazole (19.4 g, 100 mmol) was dissolved in the mixture of dry CH_2Cl_2 (250 mL) and NEt_3 (27.9 mL, 200 mmol) under a nitrogen atmosphere. The solution was cooled using the ice bath to 5 $^{\circ}C$ (measurement inside flask) and trityl chloride (30.7 g, 110 mmol) was added in small portions over 20 min. The cooling bath was removed and the mixture was left overnight. The mixture was poured into water (200 mL) and $NaHCO_3$ sat. (200 mL) was added slowly. The suspension was extracted with CH_2Cl_2 (4 x 150 mL), dried over $MgSO_4$, filtered and evaporated. The crude product was recrystallized from CH_2Cl_2. Yield 43.0 g (98%) of a white crystalline solid. Compound **11** is known.[45]

^{1}H NMR (500 MHz, $CDCl_3$) δ 7.67 (s, 1H), 7.41 (s, 1H), 7.33 – 7.31 (m, 9H), 7.14 – 7.10 (m, 6H).

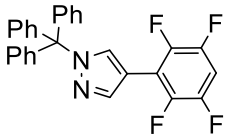

Compound 12.

Compound **11** (4.36 g, 10 mmol) was placed in an opened pressure vessel at room temperature. The vessel was then placed in glove box. After that, copper (I) iodide (0.191 g, 1.0 mmol), 1,10-phenanthroline (0.18 g, 1.0 mmol), potassium phosphate (4.24 g, 20 mmol), 1,2,4,5-tetrafluorobenzene (4.5 g, 30 mmol), and DMF (6 mL) were added. The vessel was sealed and taken out of the glove box followed by placing in oil bath at 130 °C for one day. After the indicated time, the reaction mixture was diluted with chloroform (50 mL) and filtered through Buchner filter funnel. The collected solid was then washed with chloroform (3 x 10 mL). The combined filtrate was washed with concentrated aqueous NH_4Cl (3 x 50 mL) followed by drying over $MgSO_4$, filtration and evaporation under vacuum. The product was purified using column chromatography with hexane/ethyl acetate (4/1) eluent. Rf = 0.67 (hexane/ ethyl acetate = 4/1). Yield 3.20 g (70%) of a light yellow solid. This compound is known.[45]

^{1}H NMR (500 MHz, $CDCl_3$) δ 8.15 (s, 1H), 7.91 (s, 1H), 7.36 – 7.29 (m, 9H), 7.21 – 7.16 (m, 6H), 6.93 – 6.84 (m, 1H). 19F NMR (471 MHz) δ -139.7 – -139.9 (m, 2F), -141.1 – -141.3 (m, 2F).

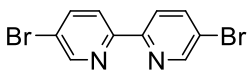

5,5-Dibromo-2,2-bipyridine.

5-Bromo-2-iodopyridine (33.47 g, 77.57 mmol), Sn_2Bu_6 (22.50 g, 38.78 mmol), $Pd(PPh_3)_4$ (1.79 g, 1.55 mmol), toluene (200 mL) and a rod shaped stir bar were sealed into 400

mL pressure flask inside the glovebox. The flask was placed inside oil bath (130 °C) for 72 h and then stirred overnight at RT. Precipitated solid was filtered and washed with ice cold toluene (50 mL). The crude product was recrystallized from toluene using hot filtration-recrystallization technique with charcoal. Yield 7.44 g (61 %) of yellow powder. This compound is known.[52]

^{1}H NMR (600 MHz, $CDCl_3$) δ 8.71 (d, J = 2.1 Hz, 1H), 8.29 (d, J = 8.4 Hz, 1H), 7.94 (dd, J = 8.4, 2.1 Hz, 1H).

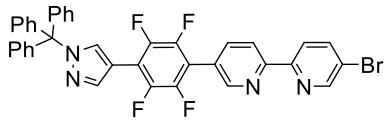

Compound 13.

To the pressure vessel, compound **12** (1.37 g, 3.0 mmol) and 5,5'-dibromo-2,2'-bipyridine (1.88 g, 6.0 mmol) were added at room temperature. The vessel was then placed in glove box. After that, copper (I) iodide (0.12 g, 20 mol%), 1,10-phenanthroline (0.11 g, 20 mol%), potassium phosphate (1.27 g, 6.0 mmol), and DMF (9 mL) were added. The vessel was sealed and taken out of the glove box followed by placing in oil bath at 140 °C for 20 h. After indicated time, the reaction mixture was cooled and diluted with chloroform (50 mL) and filtered. The solid was washed with chloroform (3 x 10 mL). The combined filtrate was washed with concentrated aqueous NH_4Cl (3 x 40 mL) followed by drying over $MgSO_4$, filtration, and evaporation. The product was purified using column chromatography with hexane/ethyl acetate (9/1), R_f = 0.23 (SiO_2, Hexane/EtOAc = 9/1). Yield 0.87 g (42%) of a light yellow solid. The total amount of recovered of 5,5'-dibromo-2,2'-bipyridine was 0.21 g.

^{1}H NMR (500 MHz, $CDCl_3$) δ 8.78 (s, 1H), 8.74 (d, J = 2.3 Hz, 1H), 8.51 (d, J = 7.9 Hz, 1H), 8.37 (d, J = 8.3 Hz, 1H), 8.22 (s, 1H), 7.99 – 7.93 (m, 3H), 7.38 – 7.33 (m, 9H), 7.23 – 7.19 (m,

6H). $^{13}C\{^{1}H\}$ NMR (126 MHz, $CDCl_3$) δ 155.4, 154.0, 150.5, 150.1, 145.7 – 143.3 (m), 145.2 – 142.8 (m), 142.8, 139.9 (t, J = 6.7 Hz), 139.8, 138.6, 133.1 (t, J = 7.2 Hz), 130.3, 128.2, 128.1, 124.5, 122.7, 121.8, 120.8, 113.7 (t, J = 16.5 Hz), 113.1 (t, J = 15.6 Hz), 107.9, 79.5. ^{19}F NMR (470 MHz, $CDCl_3$) δ -140.5 (dd, J = 21.8, 11.4 Hz, 2F), -144.6 (dd, J = 21.8, 11.4 Hz, 2F).

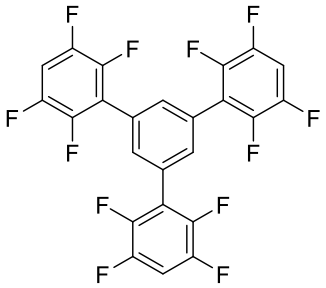

Compound 14.

In the flame-dried Schlenk flask (500 mL, nitrogen atmosphere) equipped with a magnetic stir bar, 1,2,4,5-tetrafluorobenzene (6.0 mL, 53.6 mmol) was dissolved in THF (200 mL) and the mixture was cooled to -78 °C using EtOAc/N_2 bath. Then nBuLi (1.6 M in hexane, 33.5 mL, 1.0 equiv) was added in 1 hour and reaction was kept at -78 °C for 30 min. Subsequently, a solution of $ZnCl_2$ (1M in THF, 53.6 mL, 1.0 equiv) was added during 5 min. This solution was generated by drying $ZnCl_2$ at 150 °C under vacuum overnight then stirring with THF for 8 h. The mixture was then slowly warmed up to room temperature. To the mixture, a solution of 1,3,5-tribromobenzene (2.54 g, 8.0 mmol) and $Pd(PPh_3)_4$ (0.44 g, 0.38 mmol) in THF (20 mL) was added while stirring. The system was connected with a reflux condenser under nitrogen stream. The reaction mixture was refluxed in the oil bath (bath temperature 75 °C) under nitrogen overnight. Subsequently, white precipitate was formed in the flask. The oil bath was removed and flask was cooled to room temperature in 1 h. The mixture was then filtered and the solid was washed with fresh THF (5 x 50 mL) until it turned white. Precipitate

was dried under vacuum. Yield 5.69 g (91%) of white solid. This compound is insoluble in most common solvents, making it difficult to characterize.

^{1}H NMR (600 MHz, $CDCl_3$) δ 7.9 (s, 3H), 7.6 (s, 3H). ^{19}F NMR (600 MHz, $CDCl_3$) δ -140.4 to -140.5 (m, 6F), -144.9 to -145.0 (m, 6F).

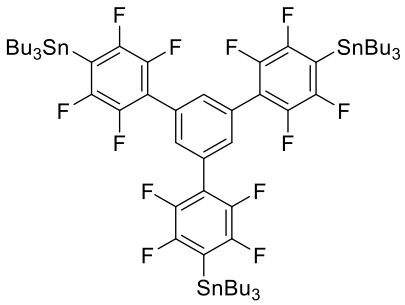

Compound 15.

In a flame-dried Schlenk flask (100 mL) equipped with magnetic stir bar, lithium 2,2,6,6-tetramethylpiperidine (LiTMP) (0.88 g, 6.0 mmol) was dissolved in THF (20 mL) under nitrogen, and the flask was cooled down to -78 °C using EtOAc/N_2 bath. After LiTMP dissolved, the solution was added to the mixture of compound **15** (0.52 g, 1.0 mmol) dispersed in THF (50 mL) at -78 °C, using cannula transfer. The mixture was then kept at -78 °C for 30 min, then nBu_3SnCl (1.64 mL, 6.0 mmol) was added in one portion. The flask was slowly warmed up to room temperature in 2 h and stirred overnight. After one night, dry silica was added and solvent was removed under vacuum. Column chromatography with hexane afforded the product, R_f = 0.8 (SiO_2, Hexane). Yield 0.86 g (62%) of colorless oil.

^{1}H NMR (400 MHz, $CDCl_3$) δ 7.69 (s, 3H), 1.48 – 1.42 (m, 18H), 1.32 – 1.23 (m, 18H), 0.92 – 0.86 (m, 18H), 0.79 (t, J = 7.3 Hz, 27H). ^{19}F NMR (400 MHz, $CDCl_3$) δ -121.2 to -121.3 (m, 6F), -142.9 to -143.0 (m, 6F).

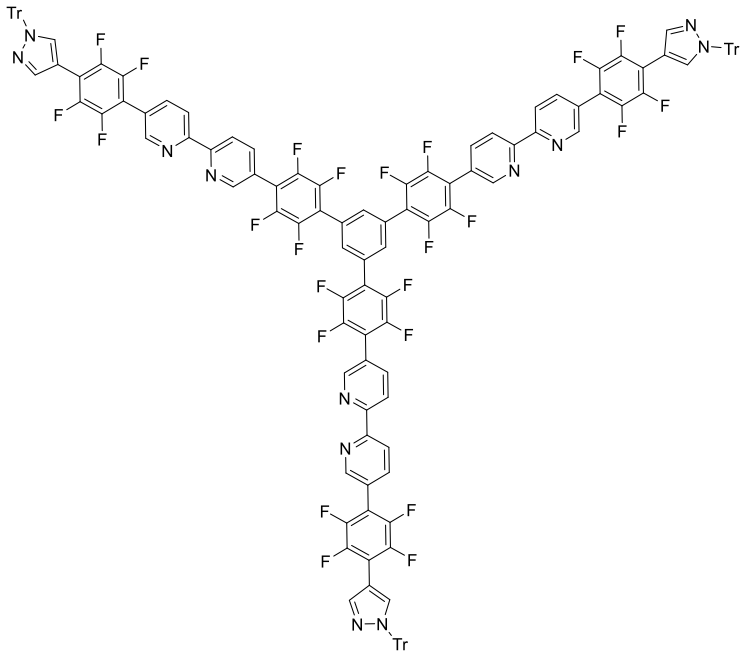

Compound 16.

Schlenk flask (25 mL) equipped with a magnetic stir bar was charged with **13** (0.4 g, 0.58 mmol), **15** (0.14 g, 0.1 mmol), Pd_2DBA_3 (0.008 g, 8.8 mol%), CuI (0.0067 g, 35 mol%), and PPh_3 (0.0184 g, 70 mol%). The flask was refilled with nitrogen, and then anhydrous DMF (5 mL) was added. The mixture was placed in an oil bath preheated to 110 °C for 24 h. The crude mixture was diluted with chloroform (100 mL), washed with solution containing NaOH (0.8 g), EDTA (75 mg), and H_2O (40 mL) three times, dried over $MgSO_4$, filtered, and concentrated. Column chromatography (silica gel, hexane/$CHCl_3$/EtOAc 85/0/15 → 80/0/20, then 0/90/10 → 0/50/50) gave **16**, R_f = 0.41 (SiO_2, Chloroform/EtOAc = 10%). The product was dried in vacuum oven (65 °C, 10 mbar) for 3 days. Yield 0.10 g (42 %) of a light yellow powder.

^{1}H NMR (500 MHz, $CDCl_3$) δ 8.91 (s, 1H), 8.84 (s, 1H), 8.71 – 8.58 (m, 2H), 8.23 (s, 1H), 8.07 (d, J = 8.4 Hz, 1H), 8.00 (s, 2H), 7.90 (s, 1H), 7.39 – 7.32 (m, 9H), 7.25 – 7.18 (m, 6H). ^{13}C{^{1}H} NMR (500 MHz, $CDCl_3$) δ 156.0, 155.4, 150.2, 150.2, 145.8 – 143.2 (m), 145.2 – 142.8 (m), 142.7, 139.9 (t, J = 6.7 Hz), 138.7, 133.1 (t, J = 7.1 Hz), 132.9, 130.3, 128.7 (t, J = 5.7 Hz), 128.2, 128.1, 124.7, 124.2, 121.2, 121.2, 119.0 (t, J = 15.8 Hz), 117.3 (t, J = 16.1 Hz), 113.7 (t, J = 16.6 Hz), 113.1 (t, J = 15.6 Hz), 107.9, 79.5. ^{19}F NMR (500 MHz, $CDCl_3$) δ -140.4 to -

140.7 (m, 6F), -142.6 to -142.8 (m, 6F), -142.8 to -143.1 (m, 6F), -144.5 to -144.8 (m, 6F).

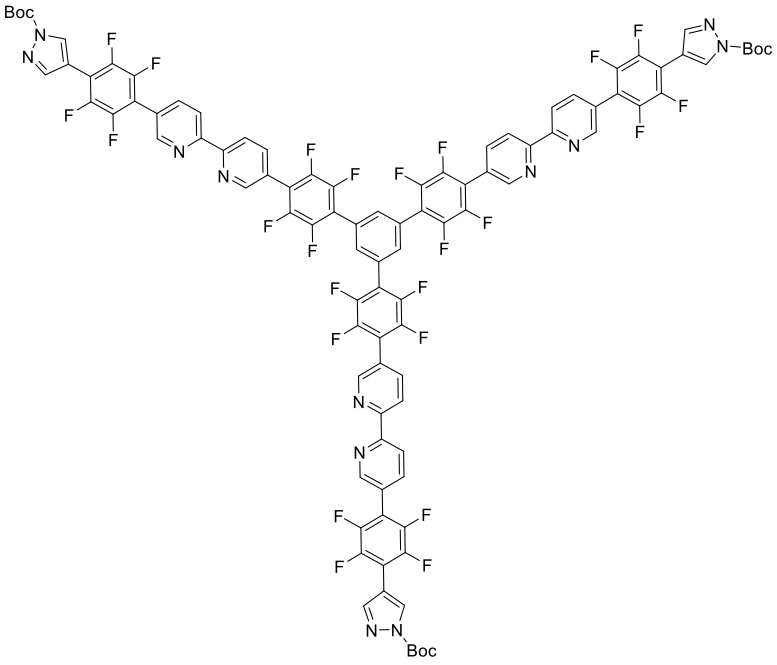

Compound 17.

In a round bottom flask equipped with a magnetic stir bar, compound **16** (0.24 g, 0.1 mmol) was dissolved in chloroform (15 mL). Then trifluoroacetic acid (2 mL, 26 mmol) was added under ambient atmosphere and left overnight at room temperature. After one night, the mixture was diluted with pentane (20 mL), precipitated solid was filtered and washed with pentane (3 x 10 mL). Subsequently, the solid was transferred to a Schlenk flask (100 mL) and chloroform (50 mL) was added under nitrogen atmosphere. The suspension was put in sonicator bath for 36 h. After indicated amount of time, the flask was taken out and connected to Schlenk line under nitrogen atmosphere. A solution of triethyl amine (2 mL, 14 mmol), 4-dimethylaminopyridine (DMAP, 0.15 g, 1.2 mmol), di-tert-butyl dicarbonate Boc_2O (2 g, 9.2 mmol) in chloroform (20 mL) was added to the flask and mixture was stirred at room temperature overnight. The volatiles were evaporated and the product was isolated by column chromatography (chloroform/EtOAc 1 to 10%), R_f = 0.5 (SiO_2, Chloroform/EtOAc = 10%). Yield 0.04 g (21%) of a light yellow solid.

^{1}H NMR (600 MHz, $CDCl_3$) δ 8.91 – 8.86 (m, 6H), 8.67 – 8.65 (m, 9H), 8.23 (s. 3H), 8.08 – 8.02 (m, 6H), 7.87 (s, 3H), 1.70 (s, 27H). ^{19}F NMR (600 MHz, $CDCl_3$) δ -139.8 to -139.9 (m, 6F), -142.6 to -142.7 (m, 6F), -142.8 to -142.9 (m, 6F), -143.5 to -143.6 (m, 6F).

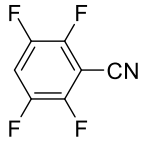

3-Cyano-1,2,4,5-tetrafluorobenzene 18.

To a 20 – dram vial, 1-cyanopentafluorobenzene (0.76 mL, 6.0 mmol), zinc (1.95 g, 30 mmol), tin (II) dichloride (0.19 g, 1.0 mmol), and DMF (8 mL) were added inside the glove box. The vial was then sealed and taken outside of the glove box and stirred at room temperature in 24 h. After indicated time, the vial was put in ice bath and aqueous HCl 1M (3 mL) was slowly added. Subsequently, the mixture was diluted with diethyl ether (50 mL) and extracted with water (3 x 30 mL) then dried over Na_2SO_4, filtered and concentrated to afford the product. Yield 0.46 g (44%) of a white solid. This compound is known.[64]

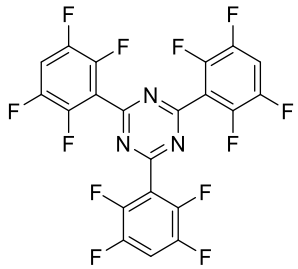

Triazine 19.

To the round bottom flask, 3-cyano-1,2,4,5-tetrafluorobenzene (0.88 g, 5.0 mmol) and fluorosulfuric acid (0.87 mL, 15 mmol) were added. The mixture was stirred at room temperature for 3 days. After that, the flask was placed in ice bath and ice water was added to quench the unreacted acid. Then, water (10 mL) was added and the mixture was filtered, residue

washed with water (2 x 10 mL), ethanol (2 x 10 mL), and diethyl ether (2 x 10 mL). Washing were discarded and the solid was dried at 60 °C under vacuum for one day. Yield 0.29 g (33%) of a white solid. This compound is known.[54]

^{1}H NMR (600 MHz, $CDCl_3$) δ 7.47 – 7.28 (m, 3H). ^{19}F NMR (600 MHz, $CDCl_3$) δ -136.8 to -136.9 (m, 6F), -141.0 to -141.1 (m, 6F).

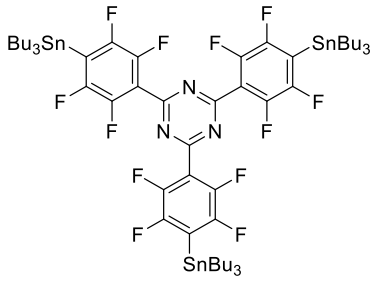

Compound 20.

In a flame-dried Schlenk flask (100 mL) equipped with magnetic stir bar, lithium 2,2,6,6-tetramethylpiperidine (0.44 g, 3.0 mmol) was dissolved in THF (30 mL). The flask was then cooled to -78 °C using EtOAc/N_2 bath. The clear solution was added to compound **19** (0.26 g, 0.5 mmol) dispersed in THF (30 mL) at -78 °C by using cannula transfer. The mixture was then kept at -78 °C for 30 min, then nBu_3SnCl (0.81 mL, 3.0 mmol) was added in one portion. The flask was slowly warmed up to room temperature in 2 h and was stirred overnight. Subsequently, dry silica was added and solvent was removed under vacuum. Column chromatography using hexane/EtOAc (9/1), R_f = 0.75 (SiO_2, Hexane), was used to purify the product. Yield 0.15 g (21%) of colorless oil.

^{1}H NMR (600 MHz, $CDCl_3$) δ 1.61 – 1.47 (m, 18H), 1.36 – 1.30 (m, 18H), 1.29 – 1.20 (m, 18H), 0.89 (t, J = 6.6 Hz, 27H). ^{19}F NMR (400 MHz, $CDCl_3$) δ -119.9 to -120.0 (m, 6F), -141.0 to -141.1 (m, 6F).

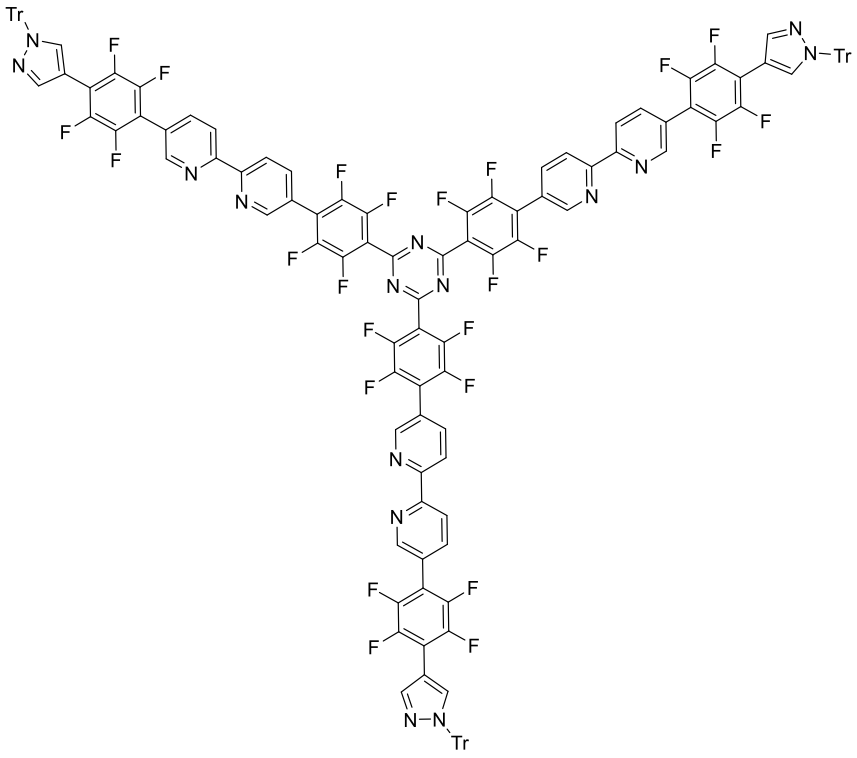

Compound 21.

Schlenk flask (25 mL) equipped with a magnetic stir bar was charged with **13** (0.40 g, 0.58 mmol), **20** (0.15 g, 0.1 mmol), Pd_2DBA_3 (0.008 g, 8.8 mol%), CuI (0.0067 g, 35 mol%), and PPh_3 (0.0184 g, 70 mol%). The flask was refilled with nitrogen, and then anhydrous DMF (5 mL) was added. The mixture was placed in an oil bath preheated to 110 °C for 24 h. The crude mixture was diluted with chloroform (100 mL), washed with solution containing NaOH (0.8 g), EDTA (75 mg), and H_2O (40 mL) three times, dried over $MgSO_4$, filtered, and concentrated. Column chromatography (silica gel, hexane/$CHCl_3$/EtOAc 85/0/15 → 80/0/20, then 0/90/10 → 0/50/50), R_f = 0.23 (SiO_2, Hexane/EtOAc = 9/1) gave **21**. The product was dried in vacuum oven (65 °C, 10 mbar) for 3 days. Yield 0.16 g (67 %) of a light yellow powder.

^{1}H NMR (600 MHz, $CDCl_3$) δ 8.91 (s, 1H), 8.84 (s, 1H), 8.68 – 8.62 (m, 2H), 8.22 (s, 1H), 8.07 (d, J = 7.2 Hz, 1H), 8.00 (s, 2H), 7.90 (s, 1H), 7.39 – 7.30 (m, 9H), 7.24 – 7.18 (m, 6H). ^{19}F NMR (600 MHz, $CDCl_3$) δ -140.1 to -140.3 (m, 6F), -140.4 to -140.5 (m, 6F), -141.4 to -141.7 (m, 6F), -144.4 to -144.7 (m, 6F).

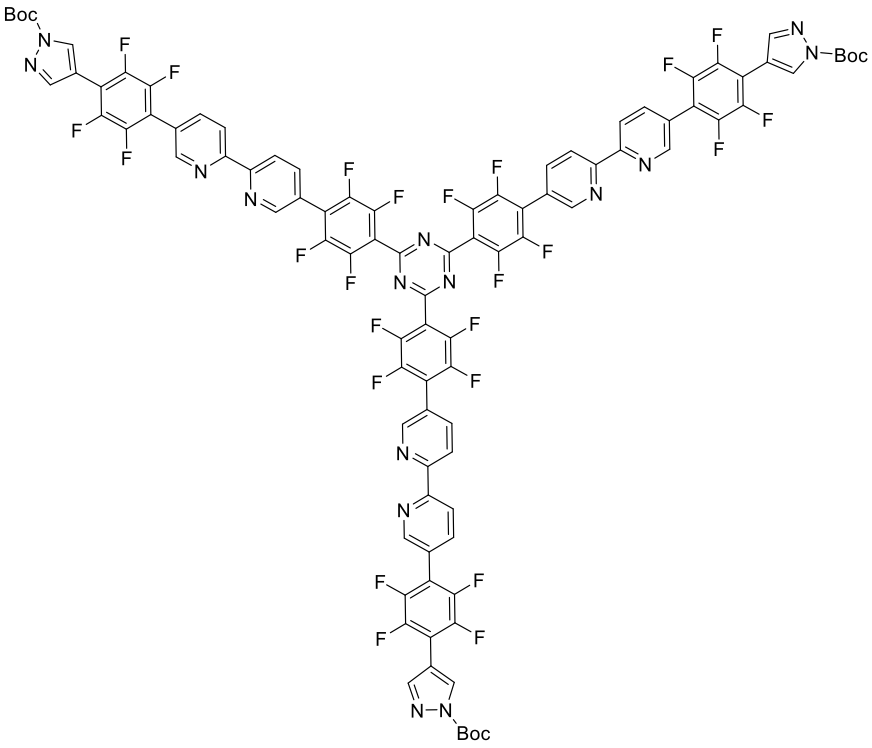

Compound 22.

In a round bottom flask equipped with a magnetic stir bar, compound **21** (0.16 g, 0.06 mmol) was dissolved in chloroform (15 mL). Then trifluoroacetic acid (2 mL, 26 mmol) was added under ambient atmosphere and mixture was kept overnight at room temperature. After that, the mixture was diluted with pentane (20 mL), precipitated solid was filtered and washed with pentane (3 x 10 mL). Subsequently, the solid was transferred to a Schlenk flask (100 mL) and chloroform (50 mL) was added under nitrogen atmosphere. The suspension was put in sonicator bath for 36 h. Subsequently, the flask was taken out and connected to Schlenk line under nitrogen atmosphere. A solution of triethyl amine (2 mL, 14 mmol), DMAP (0.15 g, 1.2 mmol), and Boc_2O (2 g, 9.2 mmol) in chloroform (20 mL) was added to the flask and the mixture was stirred at room temperature overnight. Then volatiles were evaporated and the product was isolated by column chromatography (chloroform/EtOAc 1 to 10%), R_f = 0.65 (SiO_2, Chloroform/EtOAc = 9/1). Yield 0.09 g (78%) of light yellow solid.

^{1}H NMR (600 MHz, $CDCl_3$) δ 8.91 (s, 3H), 8.87 (s, 3H), 8.69 – 8.66 (m, 9H), 8.24 (s, 3H), 8.08 (d, J = 8.4 Hz, 3H), 8.03 (d, J = 7.2 Hz, 3H), 1.66 (s, 27H). ^{19}F NMR (600 MHz, $CDCl_3$) δ -

139.7 to -139.9 (m, 6F), -140.2 to -140.3 (m, 6F), -141.4 to -141.6 (m, 6F), -143.4 to -143.6 (m, 6F).

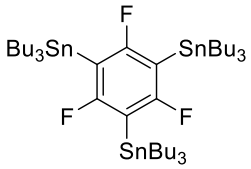

Compound 23.

To a flame-dried Schlenk flask (100 mL), 1,3,5-trifluorobenzene (1.0 mL, 10 mmol) and THF (30 mL) were added. The flask was cooled to -78 °C using EtOAc/N_2 bath. After that, nBuLi (1.6 M in hexane, 21.9 mL, 35 mmol) was added to the solution in 45 min. The flask was kept at -78 °C for one hour and nBu_3SnCl (9.3 mL, 35 mmol) was added in one portion and mixture was slowly warmed up to room temperature and stirred overnight. Subsequently, solvent was evaporated and the crude product was purified using column chromatography in hexane. All fractions, containing product were collected and dried under vacuum to afford a colorless oil. ^1H NMR analysis showed incomplete reaction.

In the flame-dried Schlenk flask (200 mL, nitrogen atmosphere) equipped with magnetic stir bar, lithium 2,2,6,6-tetramethylpiperidine (2.20 g, 15.0 mmol) was dissolved in THF (100 mL). The flask was then cooled to -78 °C using EtOAc/N_2 bath. The solution of product from above in THF (30 mL) was added to solution of LiTMP at -78 °C, using cannula transfer. The temperature was decreased to -100 °C and mixture was kept for 30 min at that temperature. Then nBu_3SnCl (3.11 mL, 13.0 mmol) was added in one portion. The flask was slowly warmed to room temperature in 2 h and stirred overnight. Dry silica was added and solvent was removed under vacuum using roto-vap. Column chromatography using hexane was

used to afford the product R_f = 0.9 (SiO_2, Hexane). This product was used for the next step without characterization due to presence of impurities.

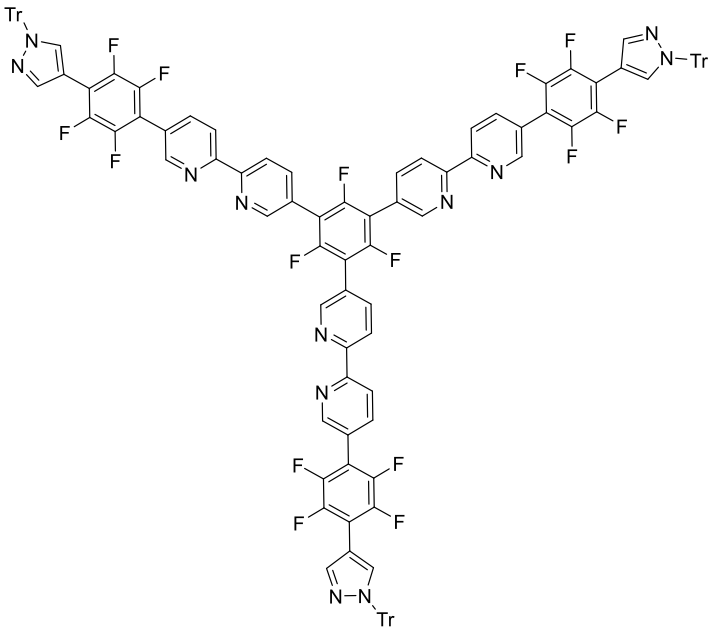

Compound 24.

Schlenk flask (25 mL) equipped with a magnetic stir bar was charged with **13** (0.83 g, 1.2 mmol), **23** (0.30 g, 0.3 mmol), Pd_2DBA_3 (0.024 g, 8.8 mol%), CuI (0.02 g, 35 mol%), and PPh_3 (0.055 g, 70 mol%). The flask was refilled with nitrogen, and then anhydrous DMF (10 mL) was added. The mixture was placed in an oil bath preheated to 110 °C for 24 h. The crude mixture was diluted with chloroform (150 mL), washed with solution containing NaOH (1.2 g), EDTA (0.15 g), and H_2O (60 mL) three times, dried over $MgSO_4$, filtered, and concentrated. Column chromatography (silica gel, hexane/$CHCl_3$/EtOAc 85/0/15 → 80/0/20, then 0/90/10 → 0/50/50), R_f = 0.75 (SiO_2, Chloroform/EtOAc = 9/1) gave **24**. The product was dried in vacuum oven (65 °C, 10 mbar) for 3 days. Yield 0.18 g (30 %) of a light yellow powder.

^{1}H NMR (600 MHz, $CDCl_3$) δ 8.82 (s, 3H), 8.78 (s 3H), 8.61 – 8.56 (m, 6H), 8.23 – 8.20 (m, 3H), 8.01 – 7.91 (m, 9H), 7.39 – 7.34 (m, 30H), 7.26 – 7.18 (m, 15H). ^{19}F NMR (600 MHz, $CDCl_3$) δ -110.0 to -110.1 (m, 3F), -140.0 to -141.0 (m, 6F), -144.5 to -145.6 (m, 6F).

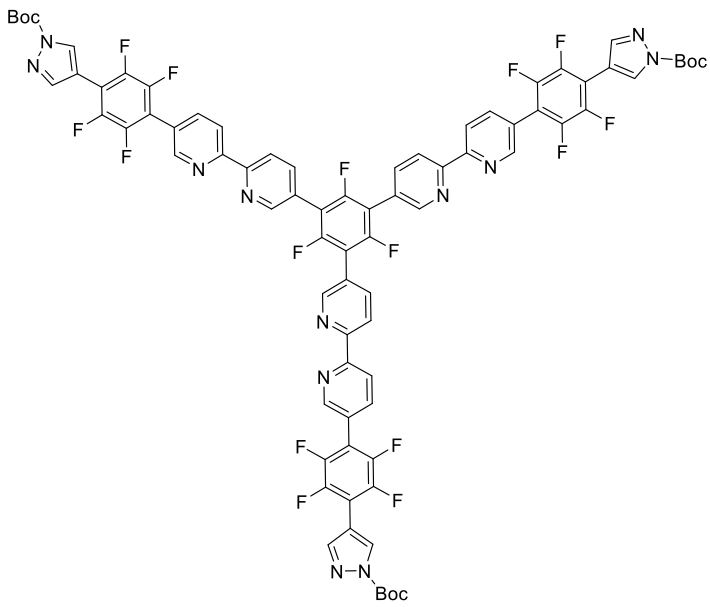

Compound 25.

In a round bottom flask equipped with magnetic stir bar, compound **24** (0.53 g, 0.27 mmol) was dissolved in chloroform (50 mL). Then trifluoroacetic acid (2 mL, 26 mmol) was added under ambient atmosphere and mixture was left overnight at room temperature. After one night, the mixture was diluted with pentane (20 mL) and precipitated solid was filtered and washed with pentane (3 x 10 mL). Subsequently, the solid was transferred to a Schlenk flask (100 mL) and chloroform (50 mL) was added under nitrogen atmosphere. The suspension was placed in sonicator bath in 36 h. After indicated amount of time, the flask was taken out and connected to Schlenk line under nitrogen atmosphere. A solution of triethyl amine (4 mL, 28 mmol), DMAP (0.3 g, 2.4 mmol), and Boc_2O (2 g, 9.2 mmol) in chloroform (20 mL) was added to the flask and mixture was stirred at room temperature overnight. Then volatile were evaporated and the product was isolated by column chromatography (chloroform/EtOAc 1 to 10%), R_f = 0.8 (SiO_2, Chloroform/EtOAc = 9/1). Yield 0.17 g (42%) of a light yellow solid.

^{1}H NMR (600 MHz, $CDCl_3$) δ 8.90 – 8.86 (m, 6H), 8.66 – 8.61 (m, 9H), 8.24 (s, 3H), 8.07 – 8.00 (m, 6H). ^{19}F NMR (600 MHz, $CDCl_3$) δ -114.1 to -115.0 (m, 3F), -139.8 to -139.9 (m, 6F), -143.5 to -143.6 (m, 6F).

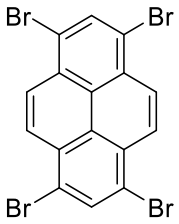

1,4,6,9-Tetrabromopyrene.

A two-necked 500 mL round bottom flask equipped with a condenser and magnet stir bar was charged with pyrene (5.0 g, 25.0 mmol) and nitrobenzene (150 mL). An addition funnel was then used to add Br_2 (0.24 M in nitrobenzene, 110 mmol) to the suspension. After the addition was complete, the yellow suspension was heated at 120 °C for 18 h and then cooled to room temperature. The precipitate was then collected by Buchner filtration and washed with ethanol (3 x 50 mL). The precipitate was dried under vacuum. Yield 11.6 g (89%) of a pale yellow-green solid. This compound was found to be insoluble in all common organic solvents, preventing it characterization. This compound is known.[61]

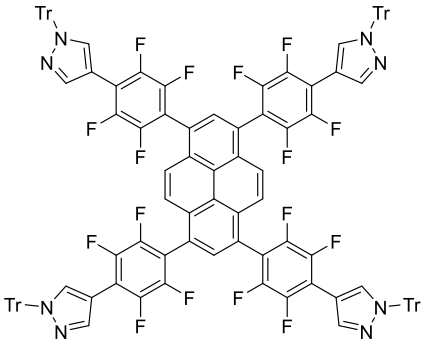

Compound 26.

To the pressure vessel, compound **12** (0.96 g, 2.0 mmol) and 1,3,6,8-tetrabromopyrene (0.16 g, 0.3 mmol) were added at room temperature. The vessel was then placed in glove box. After that, copper (I) iodide (0.023 g, 40 mol%), 1,10-phenanthroline (0.022 g, 40 mol%), potassium phosphate (0.48 g, 2.0 mmol), and DMF/m-xylene (1/1, 2 mL) were added. The

vessel was sealed and taken out of the glove box followed by placing in oil bath at 140 °C for 36 h. After indicated time, the reaction mixture was diluted with chloroform (50 mL) and filtered through Buchner filter funnel. The solid was then washed with chloroform (3 x 10 mL). The combined filtrate was washed with concentrated aqueous NH_4Cl (3 x 40 mL) followed by drying over $MgSO_4$, filtration, and evaporation. The product was purified using column chromatography with hexane/$CHCl_3$/EtOAc 85/0/15 → 80/0/20, then 0/90/10 → 0/50/50), R_f = 0.7 (SiO_2, Chloroform/EtOAc = 9/1). Yield 1.12 g (54%) of a light yellow solid.

^{1}H NMR (600 MHz, $CDCl_3$) δ 8.20 (s, 4H), 8.06 (s, 2H), 8.02 (s, 4H), 7.98 (s, 4H), 7.36 – 7.31 (m, 36 H), 7.22 – 7.18 (m, 24H). ^{19}F NMR (600 MHz, $CDCl_3$) δ -141.4 to -141.5 (m, 8F), -141.8 to -141.9 (m, 8F).

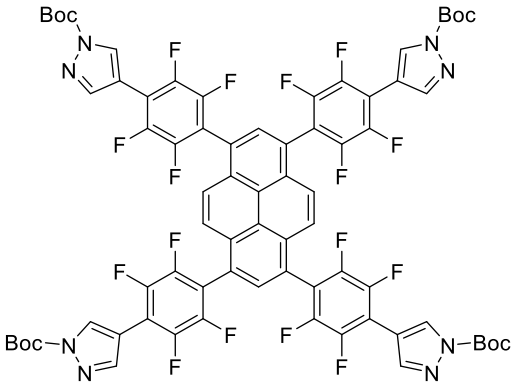

Compound 27.

To a round bottom flask equipped with a magnetic stir bar, compound **26** (1.21 g, 0.60 mmol) was dissolved in chloroform (20 mL). Then trifluoroacetic acid (1.8 mL, 23 mmol) was added under ambient atmosphere and mixture was left overnight with stirring at room temperature. After one night, the mixture was diluted with pentane (20 mL) and precipitated solid was filtered and washed with pentane (3 x 10 mL). Subsequently, the solid was transferred to a Schlenk flask (100 mL) and chloroform (80 mL) was added under nitrogen atmosphere.

The suspension was placed in sonicator bath in 24 h. After indicated amount of time, the flask was taken out and connected to Schlenk line under nitrogen atmosphere. A solution of triethyl amine (2 mL, 24 mmol), DMAP (0.58 g, 4.6 mmol), Boc_2O (1 g, 4.6 mmol) in chloroform (20 mL) was added to the flask and stirred at room temperature overnight. The volatiles were evaporated and the product was isolated by column chromatography (chloroform/EtOAc 1 to 10%), R_f = 0.6 (SiO_2, Chloroform/EtOAc = 9/1). Yield 0.14 g (16%) of a light yellow solid. ^{1}H NMR (600 MHz, $CDCl_3$) δ 8.67 (s, 4H), 8.24 (s, 4H), 8.14 (s, 4H), 8.06 (s, 4H), 1.66 (s, 36H). ^{19}F NMR (600 MHz, $CDCl_3$) δ -140.5 to -140.7 (m, 8F), -140.8 to -141.0 (m, 8F).

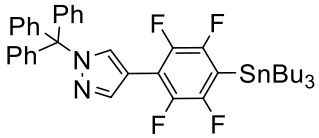

Compound 30.

In the Schlenk flask (500 mL, nitrogen atmosphere) equipped with magnet stir bar, **12** (8.40 g, 18.3 mmol) was dissolved in Et_2O/THF (1/3, 225 mL) and mixture was cooled to -78 °C using EtOAc/N_2 bath. nBuLi (1.6M, 20.6 mL, 33.0 mmol) was added within 30 min, and then nBu_3SnCl (8.2 mL, 30 mmol) was added in one portion. The cooling bath was then removed and flask was left stirring at room temperature for 2 h. The content of the Schlenk flask was poured into 1 L round bottom flask, diluted with Et_2O (100 mL), silica gel (75 g) was added and solvent was evaporated using rotary evaporator. The product was isolated using dry-filing column chromatography (silica gel, hexane/CH_2Cl_2 25 → 50%), R_f = 0.8 (SiO_2, Hexane/CH_2Cl_2 = 50%) Yield 11.97 g (87%) of white solid.

^{1}H NMR (600 MHz, $CDCl_3$) δ 8.15 (s, 1H), 7.90 (s, 1H), 7.35 – 7.31 (m, 9H), 7.21 – 7.17 (m, 6H), 1.59 – 1.46 (m, 6H), 1.36 – 1.29 (m, 6H), 1.27 – 1.15 (m, 6H), 0.88 (t, J = 7.3 Hz, 9H). ^{19}F NMR (600 MHz, $CDCl_3$) δ -122.4 to -122.9 (m, 2F), -140.0 to -140.6 (m, 2F).

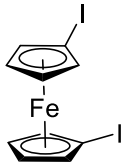

1,1'-Diiodoferrocene.

A flame-dried 200 mL Schlenk flask equipped with a magnetic stir bar was charged with ferrocene (0.5 g, 2.69 mmol), TMEDA (1.0 mL, 6.72 mmol), and pentane (38 mL). A solution of nBuLi (1.6 M in hexane, 4.2 mL, 6.72 mmol) was slowly added to the reaction mixture at room temperature and stirred for 16 h, after which a thick pale orange precipitate had formed. The suspension was cooled to -78 °C and THF (50 m) was added dropwise in 1 hour using a syringe. A solution of iodine in THF (1.5 g, 5.92 mmol in 20 mL THF) was added to the mixture via cannula. The cooling bath was removed, solution was slowly warmed up to room temperature and stirred for additional 2 h. After indicated time, the reaction was washed with $Na_2S_2O_3$ solution (2 x 50 mL), and the organic phase was separated and dried over Na_2SO_4. Solvent was evaporated using rotary evaporator and product was purified using column chromatography in pentane. Yield 0.53 g (53%) of a light brown solid. This compound is known.[63]

^{1}H NMR (600 MHz, $CDCl_3$) δ 4.36 (s, 4H), 4.17 (s, 4H). ^{13}C{^{1}H} NMR (600 MHz, $CDCl_3$) δ 77.6, 72.4, 40.4.

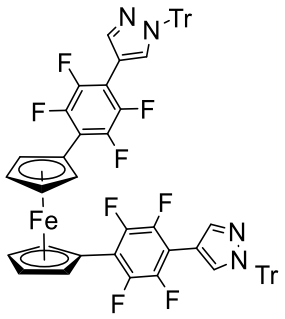

Compound 28.

A 20 dram vial equipped with a magnetic stir bar was charged with diiodoferrocene (0.26 g, 0.6 mmol) and **30** (1.47 g, 2.0 mmol). The vial was placed in the glovebox and Pd_2DBA_3 (0.014 g, 2.5 mol%), CuI (0.012 g, 10 mol%), PPh_3 (0.032 g, 20 mol%), and anhydrous DMF (7.5 mL) were added. The mixture was taken out of the glovebox and placed in an oil bath preheated to 110 °C for 24 h. The crude mixture was diluted with chloroform (70 mL), washed with solution containing NaOH (0.6 g), EDTA (0.08 g), and H_2O (30 mL) three times, dried over $MgSO_4$, filtered, and concentrated. Column chromatography (silica gel, hexane/$CHCl_3$/EtOAc 85/0/15 → 80/0/20, then 0/90/10 → 0/50/50), R_f = 0.75 (SiO_2, Chloroform/EtOAc = 9/1) gave **28**. Yield 0.49 g (77 %) of a brownish red powder.

^{1}H NMR (600 MHz, $CDCl_3$) δ 8.08 (s, 2H), 7.89 (s, 2H), 7.44 – 7.32 (m, 18H), 7.29 – 7.12 (m, 12H), 4.78 (s, 4H), 4.35 (s, 4H). ^{19}F NMR (600 MHz, $CDCl_3$) δ -141.3 to -141.4 (m, 4F), -142.4 to -142.5 (m, 4F).

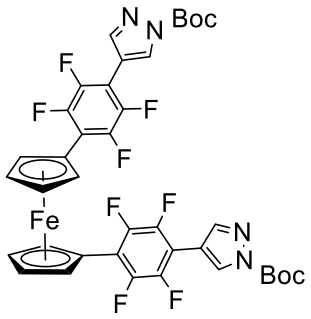

Compound 29.

In a round bottom flask equipped with magnetic stir bar, compound **28** (0.49 g, 0.45 mmol) was dissolved in chloroform (20 mL). Then trifluoroacetic acid (0.5 mL, 6.4 mmol) was added under ambient atmosphere and mixture was left stirring overnight at room temperature. After one night, the mixture was diluted with pentane (20 mL), precipitated solid was filtered and washed with pentane (3 x 10 mL). Subsequently, the solid was transferred to a Schlenk flask (100 mL) and chloroform (50 mL) was added under nitrogen atmosphere. The suspension was placed in sonicator bath for 24 h. After indicated amount of time, the flask was taken out and connected to Schlenk line under nitrogen atmosphere. A solution of triethyl amine (2 mL, 24 mmol), DMAP (0.15 g, 1.23 mmol), and Boc_2O (1 g, 4.6 mmol) in chloroform (20 mL) was added to the flask and mixture was stirred at room temperature overnight. The volatiles were evaporated and the product was isolated by column chromatography (chloroform/EtOAc 1 to 10%), R_f = 0.6 (SiO_2, Chloroform/EtOAc = 9/1). Yield 0.21 g (58%) of a light red solid.

^{1}H NMR (600 MHz, $CDCl_3$) δ 8.27 (s, 2H), 7.99 (s, 2H), 4.92 (s, 4H), 4.49 (s, 4H), 1.71 (s, 18 H). ^{19}F NMR (600 MHz, $CDCl_3$) δ -140.2 to -140.3 (m, 4F), -141.9 to -142.0 (m, 4F).

Chapter 3: Synthesis of Tetragonal Fluorinated Compound and Its Application as a Stimuli-Responsive Materials.

Reproduced in part with permission from Zhang, Z.; Lieu, T.; Wu, C.-H.; Wang, X.; Wu, J. I.-C.; Daugulis, O.; Miljanic, Solvation-Dependent Switching of Solid-state Luminescence of a Fluorinated Aromatic Tetrapyrazole. *Chem. Commun*. 2019, 55, 9387–9390.

DOI: 10.1039/C9CC03932E

3.1 Introduction

Solid-state materials that respond to external stimuli with switchable luminescence have attracted attention due to their applications in the construction of physical and chemical sensors, displays, and recording devices.[65-68] Organic and organometallic molecules with different solid-state packing modes have been widely used to construct such materials. Switching of luminescence is usually induced by stimuli such as light, mechanical grinding, temperature, shearing, pressure, and solvents, which can change the materials' intramolecular conformation[69-71] and intermolecular arrangement, resulting in the formation of excimers[72-75] or exciplexes,[76] amorphization,[77-80] and/or phase transitions.[81-84]

The first successful multicolored switch via controlling the crystallization of organic compound using mechanochemistry was introduced by Jia group in 2016.[69] Specifically, two structures **M-4-B** and **M-4** (**Scheme 3.1**) were examined. The latter exists as an amorphous powder and not form single crystals due to rotation of ethylene chain. By inserting boron-nitrogen moiety coordination, the molecular conformation was immobilized, resulting in crystallization of **M-4-B**. Subsequently, single crystals of **M-4-B** showed the emission

switching from deep-blue to green and then to a reddish color by amplifying the level of grinding. Authors explained that the color change from deep-blue to bluish-green originated from the tetraphenylethylene (TPE) phase change between crystalline and amorphous state while further grinding resulted in conformational planarization, causing the red-shift in emission.[69] However, the crystals collapse after grinding, showing the downside of this method.

Scheme 3.1. Structure of **M-4-B** and **M-4**.

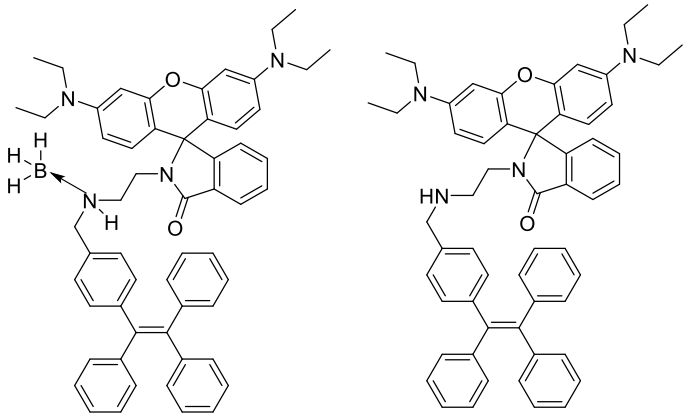

Solvent-based switching of solid-state luminescence shows advantages in recording, as the liquid state of solvents allows easy control of the stimuli position—analogous to writing ink.[76,85] Additionally, it can be utilized to detect volatile organic compounds (VOCs).[86-90]

There are different ways for solvents to inluence luminescence. In organometallic materials, solvent molecules can change luminescence by (a) directly coordinating to a metal cation,[86-89] (b) changing their position or occupancy number in the void space of crystals,[91-95] or (c) simple fuming without the net uptake of solvent molecules.[91] However, traditional organic fluorophores often suffer from aggregation-caused quenching problems, limiting their use in the development of organic solid-state luminescent emitters.[96-98] The emerging classes

of organic compounds showing aggregation-induced emission (AIE) can overcome such limitations.[99,100]

For organic materials with solid-state luminescence, the emission color switching by fuming an amorphous material was reported,[101,102] but the use of crystal solvation as a strategy to switch the solid-state emission in organics was only recently reported by Yin.[103] Considering the importance of solvents in the behavior of stimuli-responsive materials, more details on their role in building the basic units with organic fluorophores are acutely needed. Here, we report two crystal types of a new organic fluorophore (**Scheme 3.2**) with different solvation modes of DMF solvent. One of them shows solid-state fluorescence which switches from blue to green upon drying (and vice versa), while the other shows a constant cyan fluorescence. This difference is explained by the different roles of DMF molecules in the intermolecular packing.

Scheme 3.2. Structure of new organic fluorophore.

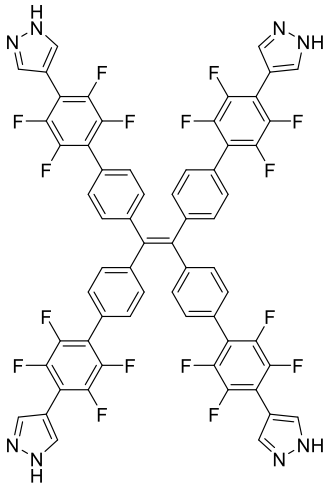

3.2 Results and Discussion

3.2.1 Ligand Synthesis

The synthesis of new organic fluorophore is described in **Scheme 3.3**. The procedure commences with bromination of tetraphenylethylene (TPE) using bromine in CH_2Cl_2 at room

temperature, affording tetra(p-bromophenyl)ethylene in good yield.[104] The brominated compound was reacted with **12** in the presence of copper (I) iodide, 1,10-phenanthroline, and potassium phosphate in DMF at 140 °C to yield product **31** in nearly quantitative yield. The last step in the procedure is protecting group exchange. Trifluoroacetic acid was used to remove trityl protecting group, generating unprotected intermediate. This intermediate was then dispersed and sonicated in chloroform before the Boc protecting group was added, affording product **32** in 61% yield. After preparing **32**, it was sent to Dr. Zhang in Dr. Miljanic group for crystals growth.

Scheme 3.3. Synthesis of tetraphenylethylene-based compound.

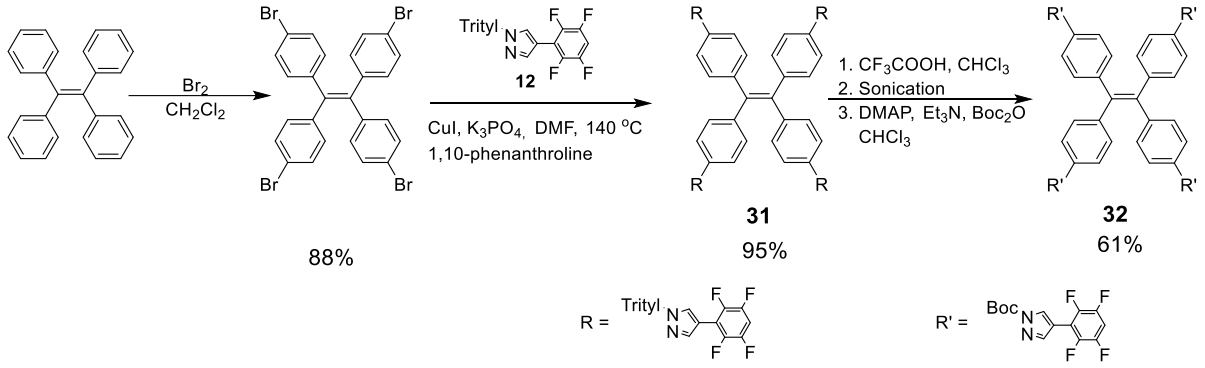

3.2.2 The Crystal Growth and "Wet/Dry" Testing. This work was performed by Dr. Zhang

By heating compound **32** in DMF/methanol mixture to 80 °C in the oven for one day, the crystals of **33** were obtained in 85% yield (**Scheme 3.4**). Interestingly, depending on further treatment of **33**, there were two different crystals observed. They are denoted as crystals **33-A** and **33-B**.

Scheme 3.4. Synthesis of crystal **33**.

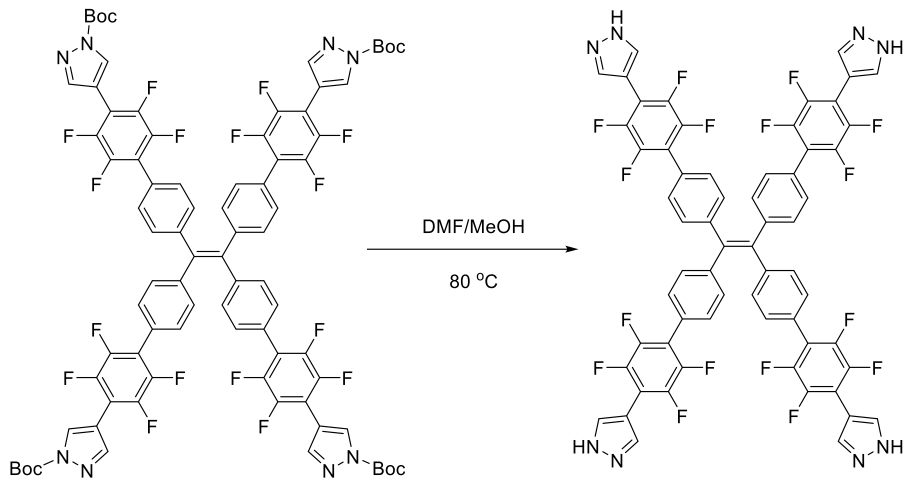

Specifically, crystals of **33-A** were produced by the slow evaporation of the solution obtained after a solvothermal reaction (80 °C, 24 h) of **32** (2.1 mg mL^{-1}) in a mixed solvent of DMF/MeOH. The crystals **33-A** are long, straight, and rod-like. They are colorless under white light and show an emission peak (λ_{em}) at 446 nm with visible blue color under UV irradiation (**Figure 3.1** a and c, labelled as ‘‘**wet 1**’’). Surprisingly, when crystals of **33-A** were filtered and air-dried, they became yellow. Such sensitive color changes prompted exploration of **33-A**’s emission under dry conditions as well. To do so, the mother liquor of the wet **33-A** was first absorbed using a Kimwipe and then the crystals were dried in *vacuo* at room temperature for 10 min. After the first drying, the crystals remained long, straight, and rod-shaped but became opaque and small cracks appeared on their surfaces. They showed λ_{em} at 503 nm with visible green fluorescence under UV irradiation (**Figure 3.1** a and c, ‘‘**dry 2**’’). Re-wetting the sample using 1–2 drops of DMF recovered its original emission spectrum with blue emission color (**Figure 3.1** a, ‘‘**wet 3**’’). The alternation of wet and dry conditions resulted in the reversible switching of the emission color from blue to green over six wetting–drying cycles.

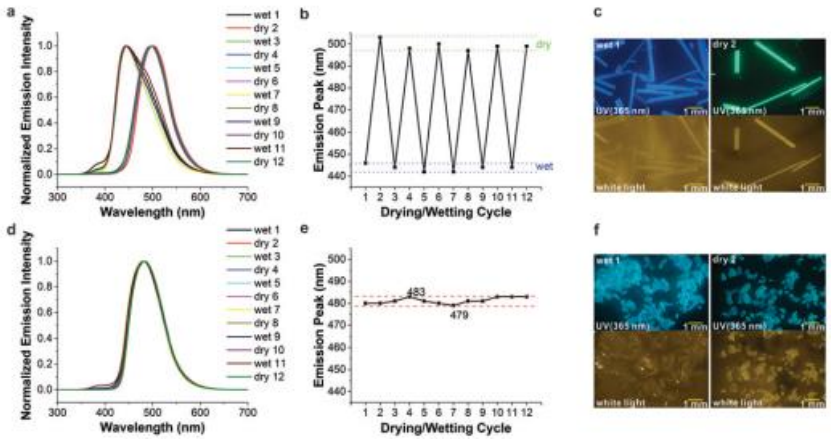

Figure 3.1. The behavior of crystals **33-A** (a–c) and **33-B** (d–f) during wetting and drying cycles.

On the other hand, recrystallization of the hot DMF solution of compound **33** (10 mg mL^{-1}) generated crystals of **33-B**, which are yellow and block-like, showing λ_{em} at 480 nm with visible cyan emission under UV light (**Figure 3.1** d and f, ‘‘**wet 1**’’). Subjected to the same drying and wetting cycles as those for **33-A**, the crystals of **33-B** changed λ_{em} only within a very narrow range (479–483 nm) and retained their cyan fluorescence over six wetting–drying cycles (**Figure 3.1** d–f). The excitation spectra were also recorded for crystals **33-A** and **33-B** which show that a new peak around 430 nm appeared after crystals of **33-A** were dried. However, the excitation spectra of **33-B** almost overlapped at the long wavelength side. All these emission and excitation spectra under the wet and dry conditions indicate that **33-A** is stimuli-responsive to DMF solvent, but **33-B** is not.

In summary, by utilizing copper catalyzed C – C bond formation, we found a short and convenient pathway to prepare a new tetraphenylethylene based material **33**. Additionally, depending on crystal growth conditions, the resulted products show difference in their emission behavior.

3.2 Experimental Section

The ^{1}H, ^{13}C, and ^{19}F NMR spectra were obtained on JEOL ECA-600, ECA-500 spectrometers, with working frequencies of 600, 500 MHz, respectively (for ^{1}H nuclei), and using the peaks of residual solvent as standards. Mass spectra of unknown compounds were obtained by The University of Texas at Austin Mass Spectrometry Facility. Infrared spectra were obtained on a Nicolet iS10 FT-IR spectrometer. The absorption, emission, and excitation spectra were measured by using a PerkinElmer LAMBDA 25 UV/VIS spectrometer and a PerkinElmer LS 55 Fluorescence spectrometer. All the calculations were carried out by Gaussian 16 program package. All pictures and video were taken by Canon EOS Rebel T3i. A microscope of Nikon SMZ-U with an external light source of a Leica KL 1500 LCD Fiber Optic Illuminator and an UVLS-28 UV lamp was used for the microscope photos.

All reactions were performed under nitrogen atmosphere in oven-dried glassware. The following starting materials and solvents were obtained from the respective commercial sources and used without further purification: 4-iodopyrazole, triethylamine (Et_3N), Boc_2O, hydroxylamine hydrochloride, 1,10-phenanthroline, tetraphenylethylene, trifluoroacetic acid (TFA), CH_2Cl_2, $CHCl_3$, $MgSO_4$, $NaHCO_3$, K_3PO_4, NH_4Cl, 4-dimethylaminopyridine (DMAP), Br_2, silica gel, hexane, ethyl acetate, EtOH (Sigma Aldrich), triphenylchloromethane (TrCl, AK Scientific), N,N-dimethyl formaldehyde (DMF, Sigma Aldrich and spectrometric grade of J. T. Baker), CuI (Strem), MeOH(Sigma Aldrich), tetrahydrofuran (THF, spectrometric grade, Macron Fine Chemicals), and H_2O (spectrometric grade, Macron Fine Chemicals), K_3PO_4 was activated at 150 °C under nitrogen atmosphere for 1 day before using.

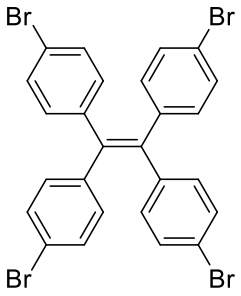

Tetra(p-bromophenyl)ethylene

This compound was obtained following a literature procedure.[104] Tetraphenylethylene (3.32 g, 10 mmol) was dissolved in CH_2Cl_2 (100 mL) in a round-bottom flask, followed by the dropwise addition of Br_2 (4 mL) in CH_2Cl_2 (20 mL) via syringe. The mixture was stirred at room temperature for 12 h, and then quenched with a saturated aqueous solution of hydroxylamine hydrochloride (100 mL). The aqueous solution was then extracted with an equal volume of CH_2Cl_2. The organic layer was dried over MgSO4, filtered, and evaporated. The solid was washed with EtOH (50 mL) to yield 5.7 g of a white powder (87 %).

^{1}H NMR (600 MHz, CD_2Cl_2) δ 7.26 (d, J = 6.0 Hz, 8H), 6.85 (d, J = 6.0 Hz, 8H).

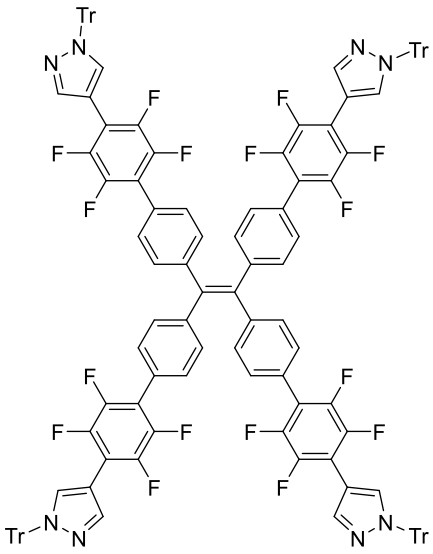

Compound 31

To a 150 mL pressure vessel, **12** (24.7 g, 54 mmol) and tetra(p-bromophenyl)ethylene (7.8 g, 12 mmol) were added at room temperature. The vessel was then placed in glove box. After that, CuI (1.15 g, 6.0 mmol), 1,10-phenanthroline (1.1 g, 6.0 mmol), K_3PO_4 (13.1 g, 62 mmol), and DMF (48 mL) were added to the pressure vessel. The vessel was sealed and taken out of the glove box followed by placing in oil bath at 140 °C for 36 h. Subsequently, the reaction mixture was

diluted with $CHCl_3$ (1.5 L) and filtered through Buchner filter. The solid was then washed with $CHCl_3$ (3 × 100 mL). The combined filtrate was washed with concentrated aqueous NH_4Cl (3 × 1 L) followed by drying over $MgSO_4$, filtration, and evaporation. The product was purified using silica gel chromatography (dry loading) with hexane/ethyl acetate (95/5) then $CHCl_3$/ethyl acetate (9/1) eluent. Yield 24.6 g (98 %) of a light-yellow solid, R_f = 0.85 (SiO_2, $CHCl_3$/ethyl acetate = 9/1), melting at 197–212 °C with decomposition.

^{1}H NMR (600 MHz, CD_2Cl_2) δ 8.10 (s, 4H), 7.91 (s, 4H), 7.33–7.29 (m, 44H), 7.23 (d, J = 8.2 Hz, 8H), 7.17–7.15 (m, 24H) ppm. ^{19}F NMR (565 MHz, CD_2Cl_2) δ −142.27 to −142.33 (m, 8F), −145.72 to −145.78 (m, 8F) ppm. HRMS (ESI) calcd. for $C_{138}H_{84}F_{16}N_8$ $[M+2Na]^{2+}$: 1101.8190; found: 1101.8219. FT-IR (neat, cm^{-1}) υ 3057, 3033, 1651, 1597, 1563, 1516, 1480, 1445, 1115. Anal. Calc'd for $C_{138}H_{84}F_{16}N_8$: C, 76.80; H, 3.92; N, 5.19. Found: C, 76.59; H, 3.96; N, 5.27

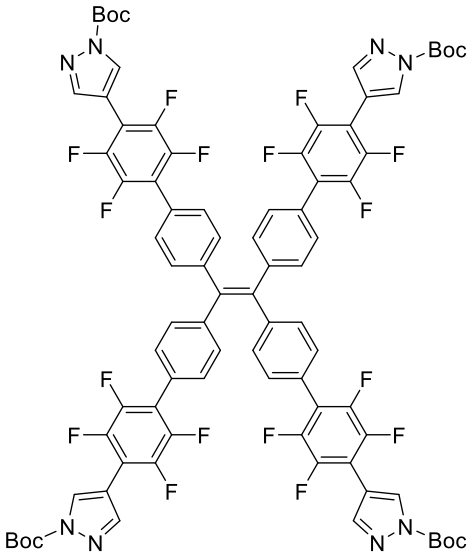

Compound 32

To a flame-dried round bottom flask was added compound **31** (25.4 g, 11.8 mmol) followed by $CHCl_3$ (300 mL). TFA (18.1 mL, 236 mmol) was added in one portion. The flask was sealed with a septum and the mixture was stirred at room temperature for one day. After that, the mixture was diluted with hexanes (300 mL) and stirred for 15 minutes. Precipitate was formed and filtered followed by washing with $CHCl_3$ (3 × 50 mL) and hexane (3 × 100 mL). After that, collected precipitate was dried under nitrogen atmosphere and vacuum for one day. The solid

was then suspended in $CHCl_3$ (250 mL) and sonicated overnight. This step removes trityl groups, and the obtained product is very insoluble.

To a flame-dried Schlenk flask containing $CHCl_3$ (1 L) was added the crude product obtained in previous step. Triethylamine (60 mL) was added in one portion and the suspension was stirred for 15 minutes followed by adding DMAP (11.6 g, 95 mmol) and Boc_2O (40.0 g, 183 mmol). The suspension was stirred until clear solution was formed, followed by evaporation of volatiles. Purification by silica gel chromatography (dry loading) with $CHCl_3$/ethyl acetate (9/1) eluent gave 11.5 g (61%) of a light-yellow solid, R_f = 0.75 (SiO_2, chloroform/ethyl acetate = 9/1, melting at 408–417 °C with decomposition.

^{1}H NMR (600 MHz, CD_2Cl_2) δ 8.57 (s, 4H), 8.15 (s, 4H), 7.35 (d, J = 8.2 Hz, 8H), 7.28 (d, J = 8.2 Hz, 8H), 1.64 (s, 9H) ppm. ^{19}F NMR (470 MHz, CD_2Cl_2) δ −141.53 to −141.60 (m, 8F), −144.88 to −144.95 (m, 8F). HRMS (ESI) calcd. for $C_{82}H_{60}F_{16}N_8O_8$ $[M+2Na]^{2+}$: 817.2032; found: 817.2018. FT-IR (neat, cm^{-1}) υ 3057, 2981, 2935, 1758, 1738, 1686, 1570, 1519, 1479, 1449, 1249, 1150, 1112. Anal. Calc'd for $C_{82}H_{60}F_{16}N_8O_8$: C, 61.97; H, 3.81; N, 7.05. Found: C, 61.94; H, 3.74; N, 7.16

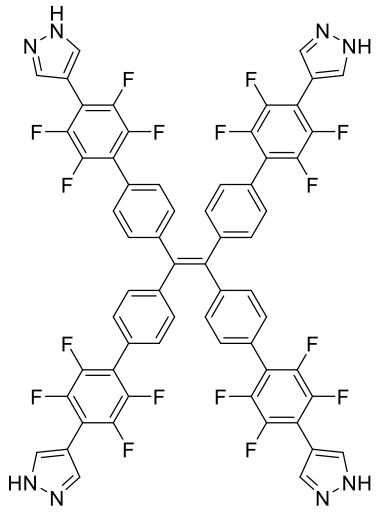

Compound 33

Compound **32** (300 mg, 0.19 mmol) was added to a 500 mL bottle. Solvents DMF (30 mL) and MeOH (270 mL) were added into the bottle and the bottle was capped, mixed for 10 min by a vortex mixer, and sonicated for 10 min, and then placed in an oven (80 °C) for 24 h. After cooling down to room temperature, the precipitate was filtered, washed with MeOH, and dried in the air. Yield 191 mg (85%) of yellow solid, melting at 377–386 °C with decomposition.

^{1}H NMR (600 MHz, DMSO-d6) δ 13.46 (s, 4H), 8.28 (s, 4H), 7.95 (s, 4H), 7.40 (d, J = 8.1 Hz, 8H), 7.25 (d, J = 8.1 Hz, 8H) ppm. ^{19}F NMR (565 MHz, DMSO-d6) δ −141.82 to −141.88 (m, 8F), −144.91 to −144.97 (m, 8F) ppm. HRMS (ESI) calcd. for $C_{62}H_{28}F_{16}N_8$ $[M+H]^+$: 1189.2254; found: 1189.2253. FT-IR (neat, cm−1) υ 3465, 3146, 3072, 1652, 1569, 1517, 1467, 1264, 1222, 1147, 1049. Anal. Calc'd for $C_{62}H_{28}F_{16}N_8 \cdot 2H_2O$: C, 60.79; H, 2.63; N, 9.15. Found: C, 60.56; H, 2.48; N, 8.83.

Synthesis of Crystals of 33-A and 33-B

Crystals 33-A

Compound **32** (400 mg, 0.25 mmol) was added to a 500 mL bottle. Solvents DMF (160 mL) and MeOH (27 mL) were added into the bottle and the bottle was capped, mixed for 10 min by a vortex mixer, and sonicated for 10 min, and then placed in an oven (80 °C) for 24 h to generate a yellow solution. After the solution was cooled down to room temperature, each 0.7 mL portion was placed in a new vial (1 dram) capped by aluminum foil, which was penetrated with 5 pores by a needle. After air evaporation (about two weeks), long, straight, rod-like, transparent, and colorless crystals were obtained.

Crystals 33-B

Compound **33** (111 mg, 0.09 mmol) was dissolved in DMF (11.1 mL) with heating. After cooling to room temperature, the mixture was filtered to produce clear yellow solution. Each 1 mL solution was placed in a new vial (2 dram) sealed with a cap, which generated yellow, block-like crystals after one day.

Pictures Under Wetting/Drying Cycles

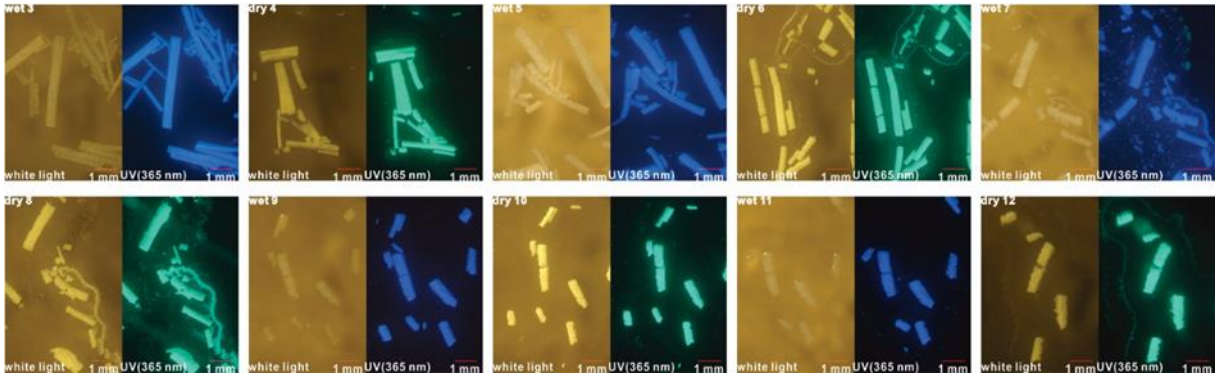

Figure 3.2. The digital microscope pictures under white light and UV (365 nm) for continued alternation of wet and dry conditions (from "wet 3" to "dry 12") of crystal **33-A**.

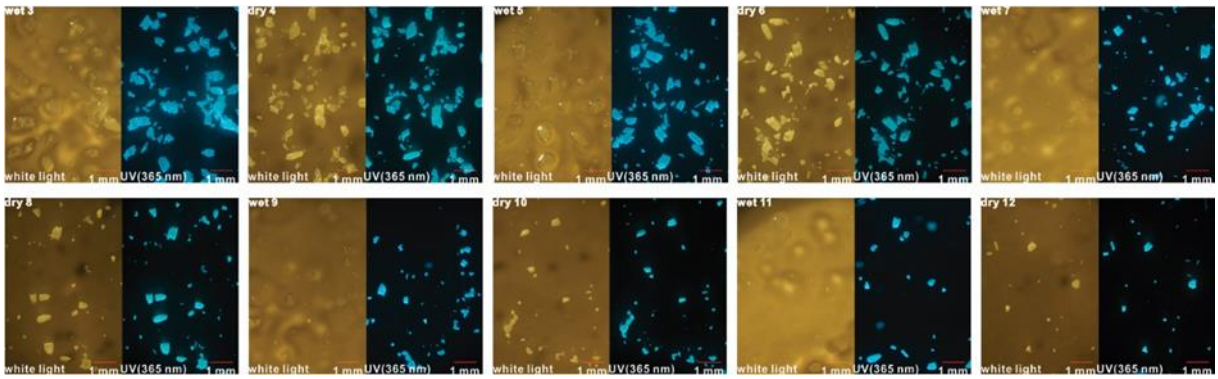

Figure 3.3. The digital microscope pictures under white light and UV (365 nm) for continued alternation of wet and dry conditions (from "wet 3" to "dry 12") of crystal **33-B**.

Single and Powder X-ray Diffusion Analysis

Table 3.1. Crystal data and structure refinement for **33-A** in wet condition

Identification code	P108D_XW143_sq
Empirical formula	$C_{68}H_{42}F_{16}N_{10}O_2$
Formula weight	1335.11
Temperature/K	123(2)
Crystal system	monoclinic
Space group	C2/c
a/Å	27.5164(10)
b/Å	29.4938(10)
c/Å	10.7214(4)
α/°	90
β/°	99.147(2)
γ/°	90
Volume/Å^3	8590.4(5)
Z	4
ρ_{calc}g/cm^3	1.032
μ/mm^{-1}	0.766
F(000)	2720.0
Crystal size/mm^3	0.500 × 0.120 × 0.010
Radiation	CuKα (λ = 1.54178)

Table 3.1 continued

2Θ range for data collection/°	4.422 to 133.572
Index ranges	$-32 \leq h \leq 31$, $-34 \leq k \leq 35$, $-12 \leq l \leq 12$
Reflections collected	32028
Independent reflections	7570 [R_{int} = 0.0420, R_{sigma} = 0.0333]
Data/restraints/parameters	7570/0/436
Goodness-of-fit on F^2	1.026
Final R indexes [I>=2σ (I)]	R_1 = 0.0548, wR_2 = 0.1631
Final R indexes [all data]	R_1 = 0.0637, wR_2 = 0.1735
Largest diff. peak/hole / e $Å^{-3}$	0.42/-0.28

Table 3.2. Crystal data and structure refinement for **33-B** in wet condition

Identification code	P8-6_XW147
Empirical formula	$C_{74}H_{56}F_{16}N_{12}O_4$
Formula weight	1481.30
Temperature/K	123(2)
Crystal system	triclinic
Space group	P-1
a/Å	17.4361(3)
b/Å	20.2383(4)
c/Å	21.2515(4)
α/°	88.9760(10)

Table 3.2 continued

β/°	72.8050(10)
γ/°	70.2550(10)
Volume/Å^3	6714.7(2)
Z	4
ρ_{calc}g/cm^3	1.465
μ/mm^{-1}	1.069
F(000)	3040.0
Crystal size/mm^3	0.380 × 0.310 × 0.010
Radiation	CuKα (λ = 1.54178)
2Θ range for data collection/°	4.37 to 133.334
Index ranges	$-20 \leq h \leq 20$, $-24 \leq k \leq 24$, $-25 \leq l \leq 25$
Reflections collected	60699
Independent reflections	60699 [R_{int} = 0.0476, R_{sigma} = 0.0641]
Data/restraints/parameters	60699/1507/2135
Goodness-of-fit on F^2	1.033
Final R indexes [I>=2σ (I)]	R_1 = 0.0669, wR_2 = 0.1771
Final R indexes [all data]	R_1 = 0.0917, wR_2 = 0.1994
Largest diff. peak/hole / e Å^{-3}	0.89/-0.40

Chapter 4: Synthesis of Fluorinated Tetraphenylethylenes and Their Reactivity in Photocyclization

4.1 Introduction

Tetraphenylethylene (TPE) and its derivatives have received significant interest in both theory and experiment.[105-107] Additionally, TPE is also a classic example of a molecule exhibiting aggregation-induced emission (AIE)[96,108,109] and has been widely used to develop responsive fluorescent materials in physical, chemical, and biological settings.[110-112] The AIE behavior of TPE analogue is mainly attributed to the rotational/torsional motions of phenyl and phenylvinyl groups in solution and solid state. Specifically, in solution, the intramolecular C-C bond rotation deactivates the excited state of these molecules, resulting in weak to no emission. In aggregated state, the free rotation is immobilized by multiple intermolecular C-H$\cdots\pi$ as well as other interactions. As a consequence, the radiative relaxation channel is activated, giving a strong emission in solid state.

Beside aggregation, there are some possible methods that can be used to inhibit the internal rotation and torsion of these molecules. For example, Fox and co-workers[113] reported that by inserting short hydrocarbon tethers within the TPE, the rigidity of framework was incrementally increased; as a result, the fluorescence behavior was improved significantly. In addition, Vyas and Rathore[114] and Wang and co-workers[115] independently explored the inhibition of rotation and torsion in TPE analogues by enhancing steric hindrance using bulky pentaphenylphenyl substitution on each of the phenyl rings of TPE. In 2012, Zhang and co-workers used dendrimers, as regularly branched, 3D architectures, to prevent TPE from rotating or distorting (**Sheme 4.1**).[116] Generally, it is believed that dendron-capped fluorophores show

strong emissions corresponding to the incremental increase of the generation number of dendron. Indeed, authors showed that there was weak or no emission observed in case of **34**, **34-A**, and **34-B**, while **34-C** and **34-D** became strongly emissive in solution. Presumably, the higher number of dendrons was generated in TPE, the higher energy barrier for internal rotation/torsion of TPE was observed. Authors also observed the photocyclization of TPE core into the respective 9.10-diphenylphenanthrene when subjected to UV light in solution (**Scheme 4.2**). This transformation is known as Mallory reaction.[117] Interestingly, the photochemical cyclization elimination reactivity also increased, followed by the number of dendron chain, in the order: **34-A** < **34-B** < **34-C** < **34-D**.[116]

Scheme 4.1. Synthesis of compounds **34**, **34-A**, **34-B**, **34-C**, and **34-D**.

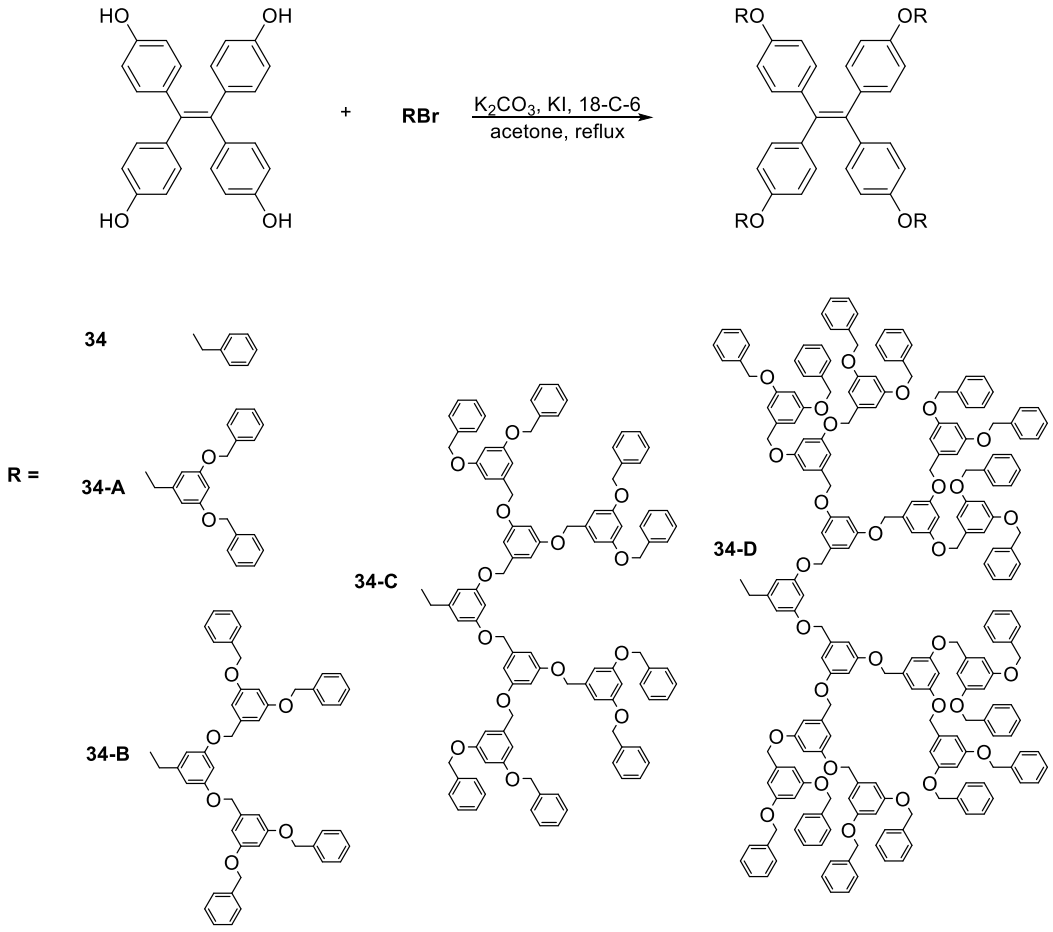

Scheme 4.2. Photocyclization products.

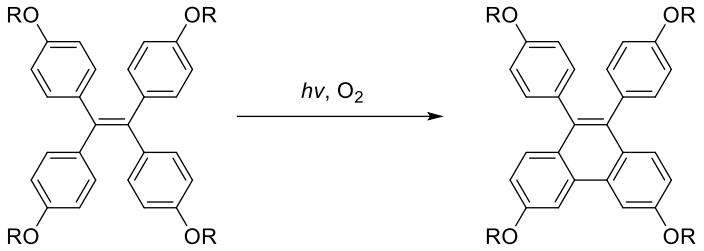

34	$R = CH_3$	**34'**	$R = CH_3$
34-A	$R = CH_2Ph$	**34'-A**	$R = CH_2Ph$
34 -B to 34-D	R = dendron unit	**34' -B to 34'-D**	R = dendron unit

TPE rigidity can be improved by insertion of fluorine atoms. Thus, fluorination of functional organic molecules and materials has often been used to modulate their physical and chemical characteristics.[118] Due to the unique properties of fluorine atom, such as small atomic radius and greatest electronegativity,[119,120] fluorinated materials generally possess lower HOMOs and LUMOs energy levels compared to non-fluorinated counterparts, resulting in enhancement in oxidative stability. Furthermore, fluorine atom is also involved in intra- or intermolecular interactions which determine the spectroscopic properties of fluorinated materials. Partial fluorination of TPE structural motif was reported to increase the fluorescence quantum yields[121,122] in crystals in addition to simplifying the separation of isomers on account of strong dipole-dipole intermolecular interactions.[123]

However, the fluorinated TPEs studied thus far have been ornamented with one, two, or three fluorine atoms at different positions on their aromatic rings, and they still maintain AIE behavior. Presumably, owing to complicated synthesis, no report has explored the effects of one, two, or three pentafluorobenzene rings (**Scheme 4.3**) on crystal structures and optical properties as well as photochemical cyclization elimination behavior of resulting TPEs. This work deals with synthesis and properties of pentafluoro-substituted PTEs.

Scheme 4.3. Fluorinated PTEs.

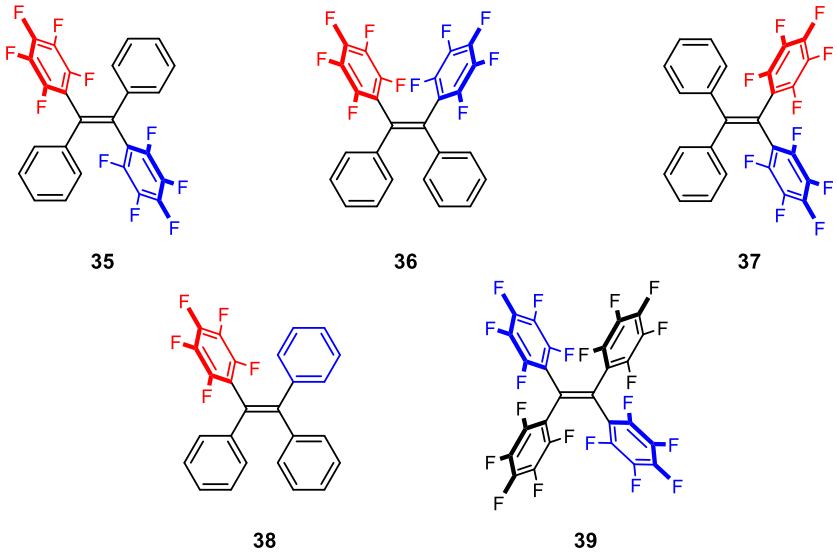

4.2 Results and Discussion

4.2.1 Synthesis Series of Perfluoroaryl Substituted PTEs

The synthesis of (E) – 1,2 – bis(pentafluorophenyl)stilbene **35** is described in **Scheme 4.4**. The procedure commences with bromination of diphenyl acetylene using bromine solution in CH_2Cl_2, giving (E) – 1,2 – dibromo stilbene in 42% yield. This method gave a clean product with no need to use column chromatography for purification. Subsequently, this dibromo product was coupled with pentafluoro benzene. Initially, we used our method published in 2008,[33] in which copper (I) iodide, potassium phosphate, and 1,10-phenanthroline in DMF were used to conduct the coupling between (E) – 1,2 – dibromo stilbene and pentafluorobenzene. However, based on the GC-MS results, product **35** was not generated. Instead, the dibromo compound was reduced to diphenylacetylene. This transformation has been reported in 1988.[124] All the efforts to conduct halogen exchange of vinyl bromides using metal iodides, were unsuccessful, presumably due to the inertness of vinyl halides.[124] Also, in this work, the authors

showed that using diglyme or DMF solvent the halogen exchange rate was remarkably reduced, leading to the formation of elimination by-products. This idea encouraged us to choose an appropriate solvent in order to inhibit the elimination rate. Among all the solvents were examined, m-xylene gave the best outcome. However, only mono coupling product was obtained as a major product, and only a small amount of biscoupling product **35** was formed. After this step, the crude mixture was used for further coupling using palladium (II) catalyst with organotin reagent, $C_6F_5SnBu_3$, giving compound **35** in 23% yield over two steps. Stille coupling reaction between dibromo compound and organotin reagent, $C_6F_5SnBu_3$, also gave **35** but only in low yield based on GC-MS observation. The isolation and purification was inefficient.

Scheme 4.4. The synthesis of (E) – 1,2 – bis(pentafluorophenyl)stilbene **35**.

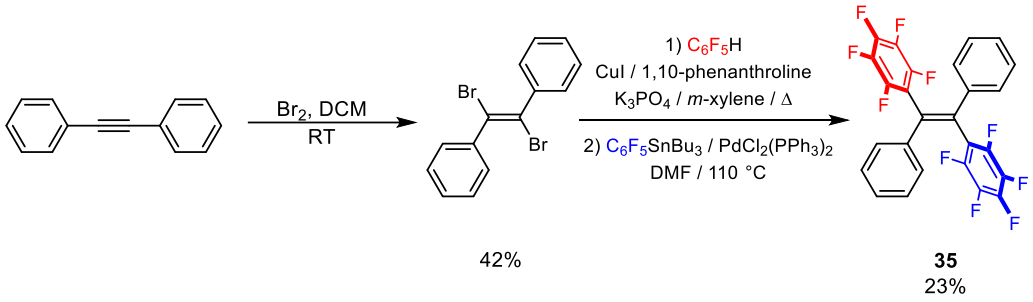

The preparation of Z isomer **36**, is described in **Scheme 4.5**. (Z) – 1,2 – dibromostilbene was synthesized by a known literature method.[125] Initially, the Suzuki coupling reaction between diphenylactylene and bis(pinacolato)diboron using platinum (0) catalyst in DMF provided exclusively Z – 1,2-bis(boropinacol)stilbene in good yield. This intermediate compound was treated with potasium hydrogen fluoride to form a potassium organotrifluoroborate. It is believed that potasium organotrifluoroborates are more reactive than respective pinacolborates in the reaction with tetrabutylamonium tribromide (TBATB). After

three consecutive steps, the pure (Z) – 1,2 – dibromostilbene was obtained in 54% yield. Subsequently, this compound was treated with pentafluorobenzene in the presence of copper (I) iodide, 1,10 – phenanthroline, and potassium phosphate in m-xylene at 125 °C. Interestingly, in contrast to E isomer **35**, only monocoupling was observed in this step, presumably due to the fact that E isomer favors elimination over direct coupling Finally, the Stille coupling reaction using palladium (II) catalyst provided product **36** in 47% yield over two steps. Again, we tested one step reaction between (Z) – 1,2 – dibromostilbene and $C_6F_5SnBu_3$ using a palladium (II) catalyst. However, the reaction was low yielding. Noticeably, the compound **36** is thermally unstable, and partially isomerizes to more stable (E) conformation under more forcing conditions.

Scheme 4.5. The synthesis of (Z) – 1,2 – bis(pentafluorophenyl)stilbene **36**.

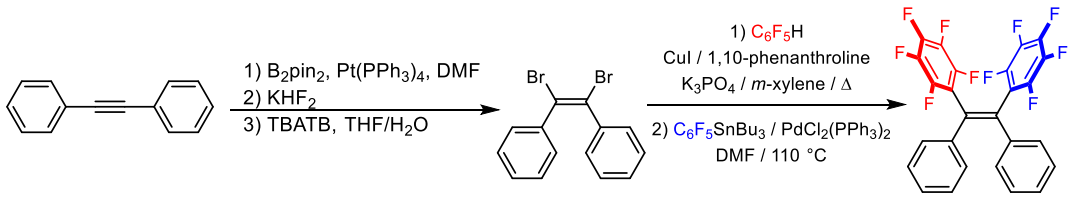

The synthesis of compound **37** is illustrated in **Scheme 4.6**. The 1,1 – dibromo – 2,2 – diphenylethylene was obtained using Corey-Fuchs reaction.[126] Treating benzophenone with CBr_4 and triphenyl phosphine in toluene under reflux gave 1,1 – dibromo – 2,2 – diphenylethylene in 26% yield. Similarly to above procedures, this dibromo intermediate was then coupled with pentafluorobenzene using copper (I) catalyst in m-xylene at 100 °C to provide mono-coupling product in quantitative yield. Subsequently, the mono-coupling product was

reacted with organotin reagent, $C_6F_5SnBu_3$, using palladium (II) catalyst to afford the final product **37** in 41% yield over two steps.

Scheme 4.6. The synthesis of 1,1 – bis(pentafluorophenyl) – 2,2 – diphenylethylene **37**.

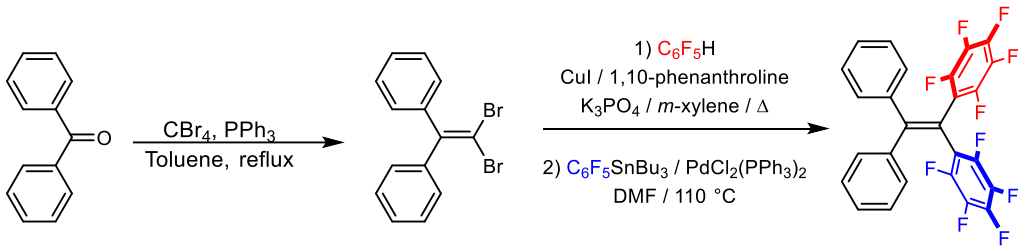

26%

37
41%

Compound **38** can be synthesized by using (E) or (Z) – 1,2 – dibromo stilbene or 1,1 – dibromo – 2,2 – diphenylethylene. However the use of (E) – 1,2 – dibromo stilbene starting material was problematic due to incomplete reaction. The synthetic route to **38** consists of two steps (**Scheme 4.7**). First, copper – catalyzed functionalization of (Z) – 1,2 – dibromo stilbene and pentafluorobenzene provides mono-coupling intermediate in quantitative yield. Then, Stille coupling between the intermediate and tetrabutyl(phenyl)stannane gave **38** in 42% over two steps.

Scheme 4.7. The synthesis of 1 – pentafluorophenyl – 1,2,2 – triphenylethylene **38**.

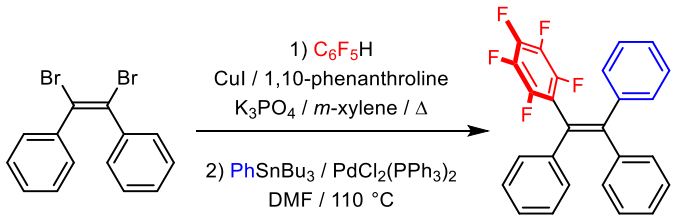

38
42%

Attempted preparation of perfluoro tetraphenylethylene **39** begin with arylation of bis(trimethylsilyl)acetylene with iodopentafluorobenzene in the presence of palladium (0) tetrakis(triphenyl)phosphine, copper (I) chloride, and diisopropylamine (DIPA) in DMF, giving decafluoro diphenylacetylene in 45% yield. This reaction follows a literature procedure.[127] Subsequently, this intermediate was treated with bromine in CH_2Cl_2 to give (E) – 1,2 – dibromo – 1,2 – pentafluorophenyl ethylene in 30% yield. The bromination offers a clean reaction and isomerically pure E product was obtained. To synthesize **39**, a copper catalyzed C – H functionalization was used; yet, all the starting materials were converted to decafluoro diphenylacetylene even when using m-xylene solvent. Presumably, highly electron deficient starting material, (E) – 1,2 – dibromo – 1,2 – pentafluorophenyl ethylene, increased the driving force of elimination reaction, inducing the formation of elimination by-product. However, Stille coupling reaction using palladium catalysts gave promising results. Specifically, treating (E) – 1,2 – dibromo – 1,2 – pentafluorophenyl ethylene with an organotin reagent, $C_6F_5SnBu_3$, in the presence of palladium (II) catalyst gave mono coupling intermediate **39-A** and compound **40** in 25% and 49% yields, respectively. On the other hand, the palladium (0) catalyst afforded both **39** and **40** based on GC-MS analysis. However, **39** was rapidly degraded or converted to **40** in purification step. Since degradation of **39** was unavoidable, compound **40** was used for further investigation. The general procedure for the synthesis of compound **40** is described in **Scheme 4.8**.

Scheme 4.8. The Synthesis of Tri(pentafluorophenyl)ethylene **40**.

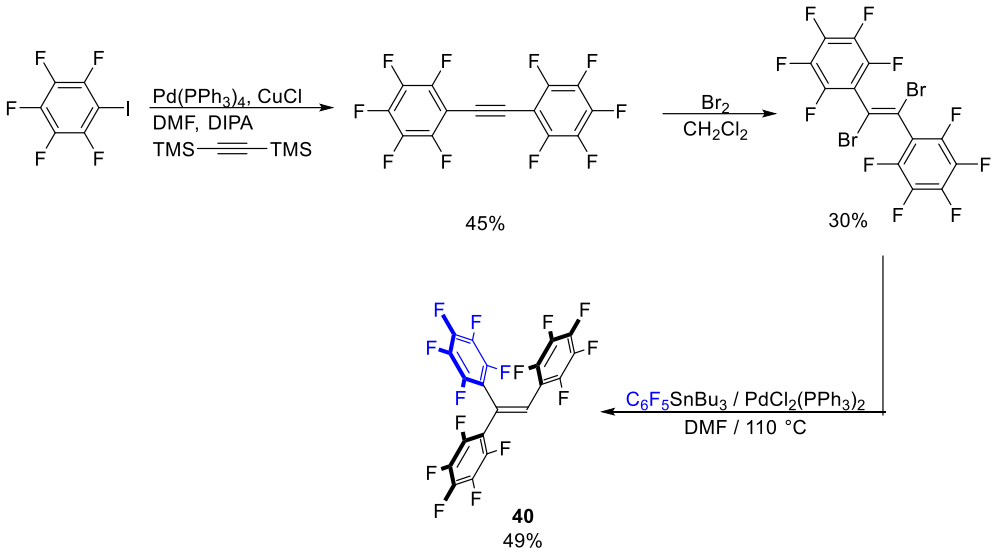

All the compounds synthesized above were then sent to Dr. Miljanic group for crystal growth and physicochemical property testing. These results described in next chapter were obtained by Dr. Zhang.

4.2.2 Photocyclization Experiments (Dr. Zhang's work)

Diffraction-quality single crystals of compounds **35**, **37**, and **40** were obtained by slow evaporation of their solutions (1 mg mL^{-1}) in MeOH; preliminary crystal structure of **36** was also obtained, but the data was of insufficient quality to allow full refinement. These crystal structures are shown in **Figure 4.1**. Noticeable is the significant twisting of aromatic rings in all four systems. This deplanarization effectively prevents face-to-face [π···π] stacking despite the presence of electronically complementary fluorinated and non-fluorinated aromatic motifs.

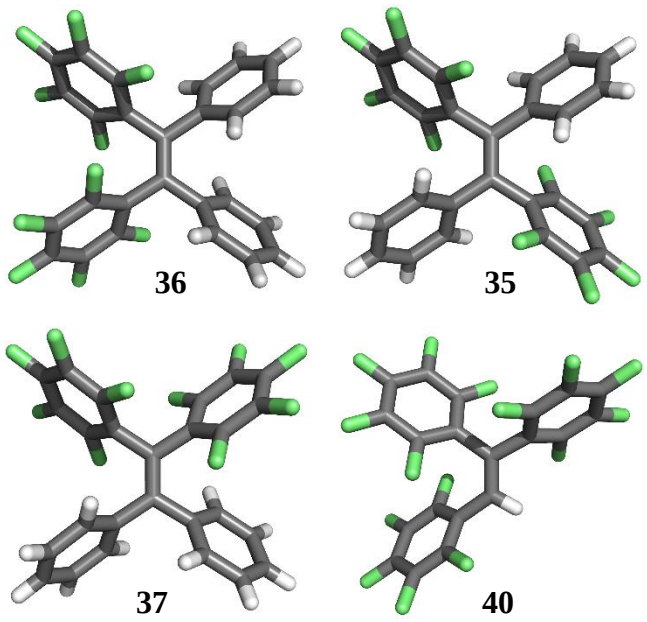

Figure 4.1. Crystal structures of **35 - 37** and **40**.

Element colors: C—gray, H—white, F—lime. Crystal structure of **36** is preliminary and shown only to illustrate connectivity; only one of the eight unique molecules in its unit cell is shown.

The solid-state fluorescence of crystals of **35 – 38** and **40**, as well as their chemical similarity to TPE led us to expect that these new fluorinated TPEs should be AIE active. However, the intensity of their emission decreases under solvent conditions promoting aggregation (H_2O:THF = 99.3:0.7) to only 20% (**38**), 43% (**35**), and 31% (**40**) of the original emission intensity in pure THF solutions, respectively. Under the same aggregation-inducing solvent conditions, the emission intensity of **37** increases by about 65% compared to that in pure THF solution. In contrast, the aggregation of TPE under the same conditions increases its emission 13.5 times. This phenomenon indicated that the fluorinated TPEs unfortunately do not exhibit aggregation-induced emission, in contrast to tetraphenylethylene (TPE).

Scheme 4.9. Photocyclization of compounds **35 – 38** to phenanthrenes **41 – 44**.

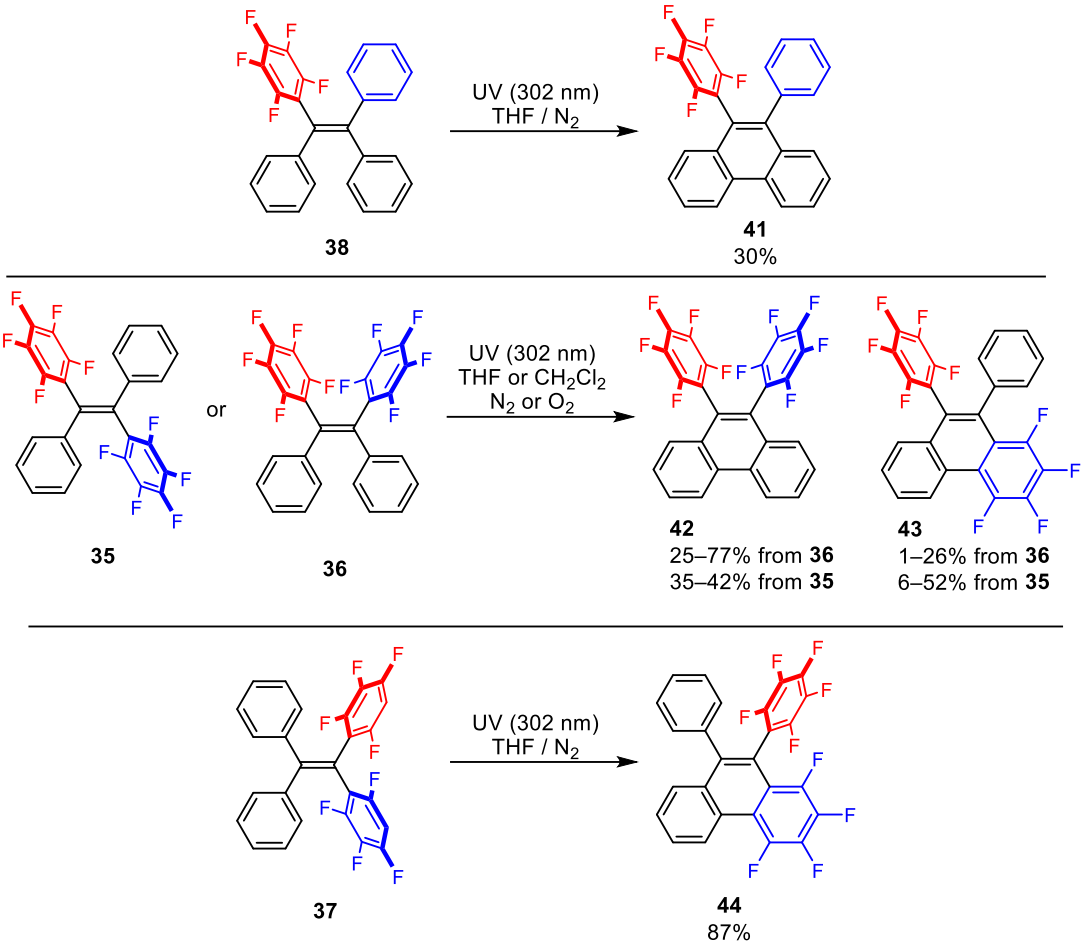

During UV/Vis absorption studies, Dr. Zhang noticed that fluorinated TPEs are photosensitive in solution. The THF solutions of **38** and **36** changed color from colorless to yellow upon UV irradiation. Additionally, NMR spectroscopy and crystallographic analysis conclusively demonstrated that the UV irradiation at 302 nm of THF solutions of **35 – 38** generated phenanthrenes **41 – 44** (**Scheme 4.9**) through either oxidative or redox-neutral photocyclizations. No photocyclization was observed in the case of **40**. Despite extensive experimentation, we were unable to obtain **41** in its pure form. Mechanistically, this type of reaction is known as Mallory reaction, in which the substrates, stilbene analogues, are

photocyclized into trans-4a,4b-dihydrophenanthrene under UV irradiation, and then rapidly oxidized to produce phenanthrene.[117]

Both the Z-**36** and its E-isomer **35** generated a mixture of phenanthrenes **42** and **43**, suggesting that the rates of Z/E photoisomerization and photocyclization are comparable. Since the formation of **42** requires an oxidant and that of **43** does not, Dr. Zhang tested the effects of oxygen exclusion on the ratio of **42** and **43**. The photoreactions of **36** and **35** were carried out under either O_2 or N_2 atmosphere, in CH_2Cl_2 and THF (**Table 4.1**). Although all solvents were degassed by the freeze-pump-thaw method, the reactions performed under N_2 atmosphere still generated significant yields of oxidized **42**. Previous reports suggest that trace amounts of O_2 could facilitate oxidative photocyclization.[117,128] Reactions run in CH_2Cl_2 as the solvent gave higher **42**:**43** ratios than their counterparts performed in THF; in the case of **36** as the starting material, **42** was obtained as essentially the only product. Dr. Zhang tentatively attributed this solvent-dependent selectivity to the lower solubility of HF in CH_2Cl_2 than in THF, which was reported to trap the acid side product in the photocyclization of cis-stilbene.[129] Photocyclizations of **38** into **41** and **37** into **44** only generated one product.

Table 4.1. Photocyclizations of **35** and **36**[a]

Reaction	Starting compound	Solvent	Atmosphere	Yield of **42**	Yield of **43**
1	**36**	THF	O_2	42%	13%
2	**36**	THF	N_2	25%	26%
3	**36**	CH_2Cl_2	O_2	73%	1%
4	**36**	CH_2Cl_2	N_2	77%	2%

Table 4.1. continued

5	**35**	THF	O_2	39%	52%
6	**35**	THF	N_2	36%	34%
7	**35**	CH_2Cl_2	O_2	35%	10%
8	**35**	CH_2Cl_2	N_2	42%	6%

[a] General reaction conditions: the starting material **36** or **35** were dissolved in THF or CH_2Cl_2 (~2 mg/mL). Then, the solution was degassed by freeze-pump-thaw method and either O_2 or N_2 were bubbled through it. All reactions were carried out at room temperature with UV (302 nm) irradiation for 15 h. Each reaction was repeated three times; the reported yields are averages, determined by ^{1}H or ^{19}F NMR with 1,2,4,5-tetrafluorobenzene as the internal standard.

In summary, five TPE derivatives functionalized with pentafluorophenyl groups were synthesized using palladium and copper catalyzed C – C bond formation. While fluorescent in the solid state, they do not exhibit aggregation-induced emission, in contrast to the TPE parent system. Instead, their UV irradiation leads to rapid photocyclization resulting in phenanthrenes formation.

4.3 Experimental Section

All syntheses were performed in standard oven-dried glassware. Column chromatography was performed on 60 Å silica gel (Dynamic Adsorbents Inc.). ^{1}H NMR, ^{13}C NMR, and ^{19}F NMR spectra were recorded on JEOL ECA-400 or ECA-500 spectrometers using the peaks of tetramethylsilane or the residual solvent as standards. Infrared spectra were collected on a Perkin Elmer Spectrum 100 FT-IR or Nicolet iS10 FT-IR spectrometers. Mass spectra were collected by the Mass Spectrometry Facility (MSF) at University of Texas-Austin. Elemental analyses were conducted at Atlantic Microlab, Norcross, GA. Analytical thin layer chromatography was performed on silica gel plates. All procedures were performed under argon unless otherwise noted.

The following starting materials and solvents were obtained from Sigma Aldrich and used without further purification: CBr_4, Br_2, CuI, K_3PO_4, KHF_2, $MgSO_4$, CH_2Cl_2, DMF, hexane, m-xylene, tetraphenylethylene, pentafluorobenzene, 1,10-phenanthroline, bis(triphenylphosphine)palladium dichloride, bis(pinacolato)diboron, $PdCl_2(PPh_3)_2$, tetrabutylammonium tribromide, and pentafluoro-iodobenzene.

Solvents used for absorption and emission spectra measurements were THF and H_2O of spectrophotometric grade. Absorption spectra were recorded using a PerkinElmer LAMBDA 25 UV/VIS spectrometer, and the steady-state emission spectra were measured by a PerkinElmer LS 55 fluorimeter. Dynamic light scattering measurements were carried out by a Zetasizer Nano Malvern. An UVLMS-38 UV lamp was used as the UV source for all photoreactions and samples' photos under irradiation. Preparative thin-layer chromatography plates were obtained from Miles Scientific.

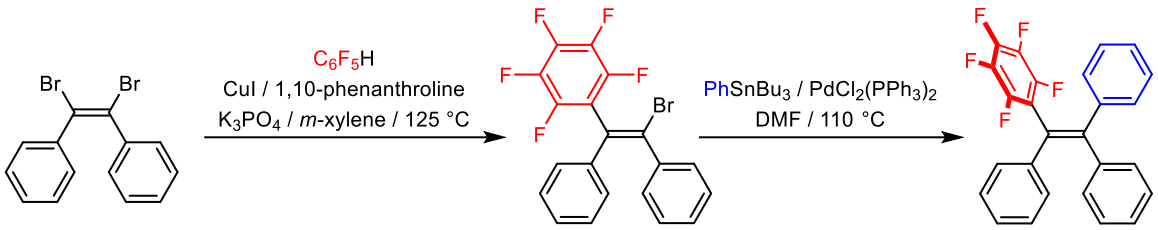

36' **38**

(*Z*)-1-Bromo-2-pentafluorophenyl-1,2-diphenylethene (36′)

A two-dram vial with a screw cap (PTFE liner) was charged with (Z) – 1,2 – dibromo stillbene (0.17 g, 0.50 mmol), and placed in a glove box. After that, CuI (4.78 mg, 0.03 mmol), 1,10-phenanthroline (4.5 mg, 0.03 mmol), K_3PO_4 (0.73 g, 3.44 mmol), pentafluorobenzene (0.44 mL, 4.0 mmol), and *m*-xylene (1.0 mL) were added to the vial. The vial was sealed, taken out of the glove box, and placed in a reaction block on a hot plate stirrer, where it was heated at 125 °C for 36 h. After cooling, the reaction mixture was diluted with CH_2Cl_2 (15 mL), and washed with H_2O (3×10 mL). The organic phase was then dried over anhydrous $MgSO_4$, filtered, and evaporated. The product **36′** was purified by column chromatography on silica gel with hexane as the eluent. Compound **36′** was obtained as a white solid (R_f=0.45, 190 mg, 90%), and used in the subsequent step without further purification.

36′: mp 93–96 °C (hexane). ^{1}H NMR (400 MHz, CD_2Cl_2) δ 7.38 – 7.26 (m, 2H), 7.26 – 7.18 (m, 3H), 7.18 – 7.07 (m, 3H), 7.07 – 6.98 (m, 2H). ^{19}F NMR (376 MHz, CD_2Cl_2) δ -141.2 to -141.3 (m, 2F), -155.4 to -155.8 (m, 1F), -162.3 to -162.4 (m, 2F). FT-IR (neat) $\bar{\nu}$ 1652, 1489, 983, 696 cm^{-1}.

1 – Pentafluorophenyl – 1,2,2 – triphenylethylene 38.

A two-dram vial with a screw cap (PTFE liner) was charged with **36′** (0.21 g, 0.50 mmol) and placed in a glove box. After that, $PdCl_2(PPh_3)_2$ (35 mg, 0.05 mmol),

tributylphenylstannane (0.28 g, 0.76 mmol), and DMF (1.0 mL) were added to the vial. The vial was sealed, taken out of the glove box, and placed in a reaction block on a hot plate stirrer, where it was heated at 110 °C for 36 h. After cooling, reaction mixture was diluted with CH_2Cl_2 (15 mL), and then washed with a saturated aqueous NH_4Cl solution (3×10 mL). The organic phase was dried over anhydrous $MgSO_4$, filtered, and evaporated. The crude product was purified using column chromatography on silica gel with hexane as the eluent. Compound **38** was obtained as a white solid (R_f=0.45, 88.5 mg, 47%).

38: mp 103–107 °C (hexane). ^{1}H NMR (400 MHz, CD_2Cl_2) δ 7.20 – 7 .10 (m, 9H), 7.10 – 7.02 (m, 6H). ^{19}F NMR (376 MHz, CD_2Cl_2) δ -140.5 to -140.6 (m, 2F), -156.4 to -156.5 (m, 1F), -163.2 to -163.3 (m, 2F). HRMS (ESI) calcd. for $C_{26}H_{15}F_5$ $[M]^+$: 422.1094; found: 422.1099. FT-IR (neat) $\bar{\nu}$ 1652, 1490, 982, 696 cm^{-1}. Anal. calcd (%) for $C_{26}H_{15}F_5$: C 73.93, H 3.58; found: C 74.01, H 3.76.

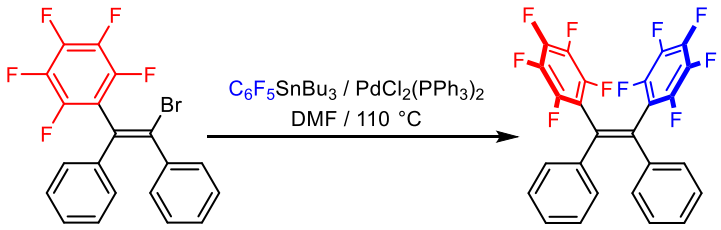

36' **36**

(Z) – 1,2 – bis(Pentafluorophenyl)stillbene 36.

A two-dram vial with a screw cap (PTFE liner) was charged with **36′** (0.21 g, 0.5 mmol), and placed in a glove box. After that, $PdCl_2(PPh_3)_2$ (35 mg, 0.05 mmol), tributyl(pentafluorophenyl) stannane (0.34 g, 0.74 mmol, and DMF (1.0 mL) were added to the vial. The vial was sealed, taken out of the glove box, and placed in a reaction block on a hot plate stirrer, where it was heated at 110 °C for 36 h. After cooling, the reaction mixture was

diluted with CH_2Cl_2 (15 mL) and washed with a saturated aqueous NH_4Cl solution (3×10 mL). The organic phase was dried over anhydrous $MgSO_4$, filtered, and evaporated. The crude product was purified by column chromatography on silica gel with hexane as the eluent. Compound **36** was isolated as a white solid (R_f=0.45, 0.12 g, 52%)

36: mp 145–146 °C (hexane). ^{1}H NMR (400 MHz, CD_2Cl_2) δ 7.22 – 7.14 (m, 6H), 7.05 (d, *J*=7.2 Hz, 4H). ^{19}F NMR (376 MHz, CD_2Cl_2) δ -139.9 to -140.4 (m, 2F), -154.0 to -154.1 (m, 1F), -161.7 to -161.8 (m, 2F). ^{13}C{^{1}H} NMR (151 MHz, CD_2Cl_2) δ 145.1 – 143.3 (m), 142.1 – 140.3 (m), 138.4 – 136.7 (m), 137.9, 132.5, 129.7, 128.3, 116.2 – 115.9 (m), 112.7. HRMS (ESI) calcd. for $C_{26}H_{10}F_{10}$ $[M]^+$: 512.0623; found: 512.0623. FT-IR (neat) $\bar{\nu}$ 1651, 1489, 982, 696 cm^{-1}. Anal. calcd (%) for $C_{26}H_{10}F_{10}$: C 60.95, H 1.97; found: C 60.31, H 2.05.

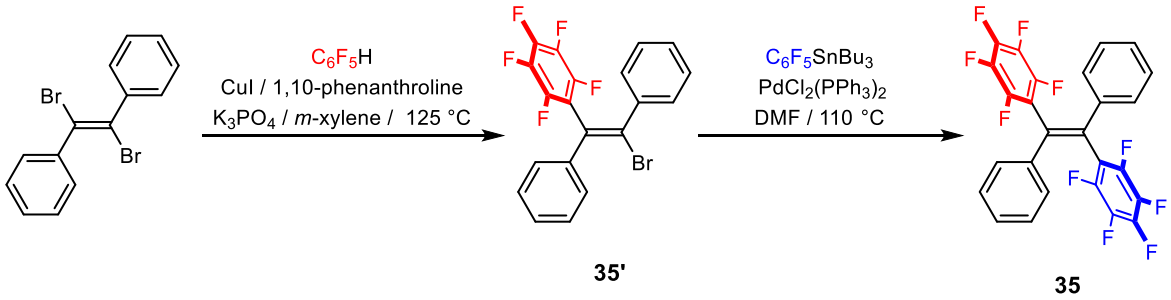

(E) – 1,2 – bis(Pentafluorophenyl)stillbene 35.

A two-dram vial with a screw cap (PTFE liner) was charged with (E) – 1,2 – dibromo stilbene (0.17 g, 0.50 mmol) and placed in a glove box. After that, CuI (4.78 mg, 0.03 mmol), 1,10-phenanthroline (4.5 mg, 0.03 mmol), K_3PO_4 (0.73 g, 3.44 mmol), pentafluorobenzene (0.44 mL, 4.0 mmol), and *m*-xylene (1.0 mL) were added to the vial. The vial was sealed, taken out of the glove box, and placed in a reaction block on a hot plate stirrer, where it was heated at 125 °C for 36 h. Subsequently, the reaction mixture was cooled, diluted with CH_2Cl_2 (15 mL) and washed with water (3×10 mL). The organic phase was dried over anhydrous $MgSO_4$,

filtered, and evaporated. The product was purified using column chromatography on silica gel with hexane as the eluent. After column chromatography, **35' (**R_f=0.45) was still impure, containing elimination byproduct and disubstituted product. The crude product was used in the next step without further purification.

A two-dram vial with a screw cap (PTFE liner) was charged with crude product **35′** (ca. 0.5 mmol, all of the material obtained in the previous step) and placed in a glove box. After that, $PdCl_2(PPh_3)_2$ (35 mg, 0.05 mmol), tributyl(pentafluorophenyl)stannane (0.34 g, 0.74 mmol), and DMF (1.0 mL) were added to the vial. The vial was sealed, taken out of the glove box, and placed in a reaction block on a hot plate stirrer, where it was heated at 110 °C for 36 h. Subsequently, the reaction mixture was cooled and then diluted with CH_2Cl_2 (15 mL), and washed with a saturated aqueous NH_4Cl solution (3×10 mL). The organic phase was dried over anhydrous $MgSO_4$, filtered, and evaporated. The crude product was purified by column chromatography on silica gel with hexane as the eluent, to give **35** as a white solid (R_f=0.45, 59 mg, 23%).

35: mp 167–169 °C (hexane). ^{1}H NMR (400 MHz, CD_2Cl_2) δ 7.26 – 7.18 (m, 6H), 7.14 – 7.08 (m, 4H). ^{19}F NMR (376 MHz, CD_2Cl_2) δ -139.5 to -139.8 (m, 2F), -154.7 to -154.8 (m, 1F), -162.4 to -162.5 (m, 2F). ^{13}C{^{1}H} NMR (151 MHz, CD_2Cl_2) δ 144.9 – 143.2 (m), 142.0 – 140.3 (m), 138.7, 138.5 – 136.8 (m), 132.8, 128.7, 128.5, 128.1, 116.2 – 115.8 (m). HRMS (ESI) calcd. for $C_{26}H_{10}F_{10}$ $[M]^+$: 512.0623; found: 512.0620. FT-IR (neat) $\bar{\nu}$ 1651, 1489, 981, 696 cm^{-1}. Anal. calcd (%) for $C_{26}H_{10}F_{10}$: C 60.95, H 1.97; found: C 61.06, H 1.90.

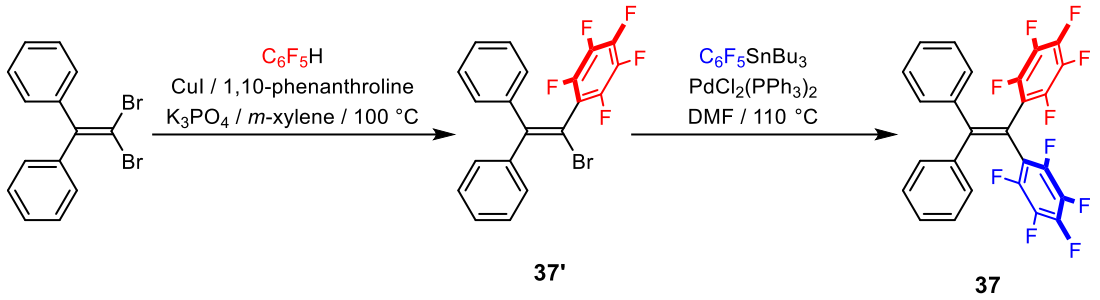

1-Bromo-1-pentafluorophenyl-2,2-diphenylethene (37′)

A two-dram vial with a screw cap (PTFE liner) was charged with 1,1-dibromo-2,2-diphenylethene (0.17 g, 0.50 mmol), and placed in a glove box. After that, CuI (4.78 mg, 0.03 mmol), 1,10-phenanthroline (4.5 mg, 0.03 mmol), K_3PO_4 (0.73 g, 3.44 mmol), pentafluorobenzene (0.44 mL, 4.0 mmol), and *m*-xylene (1.0 mL) were added to the vial. The vial was sealed, taken out of the glove box, and placed in a reaction block on a hot plate stirrer, where it was heated at 100 °C for 36 h. After cooling, the reaction mixture was diluted with CH_2Cl_2 (15 mL) and then washed with H_2O (3×10 mL). The organic phase was dried over anhydrous $MgSO_4$, filtered, and evaporated. The crude product was purified using column chromatography on silica gel with hexane as the eluent, yielding compound **37′** as a white solid (R_f=0.45, 200 mg, 95%).

37′: mp 96–99 °C (hexane). ^{1}H NMR (400 MHz, CD_2Cl_2) δ 7.43 – 7.31 (m, 8H), 7.20 – 7.14 (m, 4H), 7.08 – 7.01 (m, 3H). ^{19}F NMR (376 MHz, CD_2Cl_2) δ -139.3 to -139.5 (m, 2F), -153.8 to -154.0 (m, 1F), -162.2 to -162.3 (m, 2F). FT-IR (neat) $\bar{\nu}$ 1654, 1488, 982, 696 cm^{-1}.

1,1 – bis(Pentafluorophenyl) – 2,2 – diphenylethylene 37.

A two-dram vial with a screw cap (PTFE liner) was charged with **37′** (0.21 g, 0.5 mmol) and placed in a glove box. After that, $PdCl_2(PPh_3)_2$ (35 mg, 0.05 mmol), tributyl(pentafluorophenyl)-stannane (0.34 g, 0.74 mmol), and DMF (1.0 mL) were added to

the vial. The vial was sealed, taken out of the glove box, and placed in a reaction block on a hot plate stirrer, where it was heated at 110 °C for 36 h. After cooling, the reaction mixture was diluted with CH_2Cl_2 (15 mL) and then washed with a saturated aqueous NH_4Cl solution (3×10 mL). The organic phase was then dried over anhydrous $MgSO_4$, filtered, and evaporated. The crude product was purified using column chromatography on silica gel with hexane as the eluent, to yield **37** as a white solid (R_f=0.45, 105 mg, 41%)

37: mp 134–137 °C (hexane). ^{1}H NMR (400 MHz, CD_2Cl_2) δ 7.28 – 7.15 (m, 3H), 7.07 (d, *J* = 8.0 Hz, 2H). ^{19}F NMR (376 MHz, CD_2Cl_2) δ -140.0 to -140.2 (m, 2F), -154.8 to -154.9 (m, 1F), -162.7 to -162.9 (m, 2F). ^{13}C{^{1}H} NMR (100 MHz, CD_2Cl_2) δ 156.4, 145.8 – 143.4 (m), 142.5 – 139.8 (m), 139.9, 138.8 – 136.3 (m), 129.3, 128.9, 128.3, 114.7 – 114.9 (m). HRMS (ESI) calcd. for $C_{26}H_{10}F_{10}$ $[M]^+$: 512.0623; found: 512.0620. FT-IR (neat) $\bar{\nu}$ 1652, 1489, 981, 696 cm^{-1}. Anal. calcd (%) for $C_{26}H_{10}F_{10}$: C 60.95, H 1.97; found: C 60.65, H 1.87.

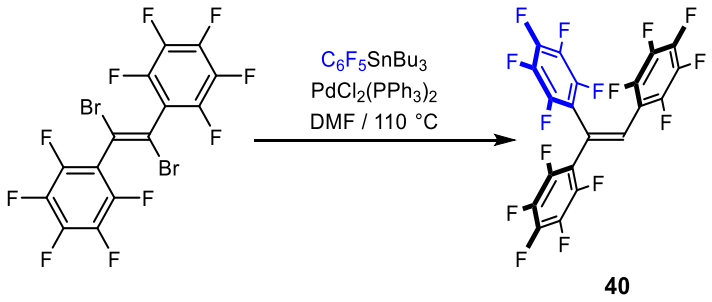

40

Tris(pentafluorophenyl)ethylene 40.

A two-dram vial with a screw cap (PTFE liner) was charged with (E)-1,2-dibromo-1,2-di(pentafluorophenyl)ethylene (0.26 g, 0.50 mmol). The vial was then placed in a glove box and $PdCl_2(PPh_3)_2$ (70 mg, 0.10 mmol), tributyl(pentafluorophenyl)stannane (0.80 g, 1.75 mmol), and DMF (1.0 mL) were added to the vial. The vial was sealed, taken out of the glove box, and placed in a reaction block on a hot plate stirrer, where it was heated at 110 °C for 36

h. After cooling, reaction mixture was diluted with CH_2Cl_2 (15 mL) and washed with a saturated aqueous NH_4Cl solution (3×10 mL). The organic phase was then dried over anhydrous $MgSO_4$, filtered, and evaporated. The crude product was purified using dry-silica chromatography with hexane as the eluent, to yield **40** as a white solid (R_f=0.30, 105 mg, 40%).

40: mp 125–126 °C (hexane). ^{1}H NMR (400 MHz, CD_2Cl_2) δ 7.06 (s, 1H). ^{19}F NMR (376 MHz, CD_2Cl_2) δ -139.3 to -139.4 (m, 1F), -140.3 to -140.4 (m, 1F), -141.7 to -141.8 (m, 1F), -152.0 to -152.1 (m, 1F), -152.2 to -152.3 (m, 1F), -152.7 to -152.8 (m, 1F), -161.1 to -161.2 (m, 1F), -161.3 to -161.4 (m, 1F), -161.7 to -161.8 (m, 1F). ^{13}C{^{1}H} NMR (101 MHz, CD_2Cl_2) δ 145.9 – 143.5 (m), 145.2 – 142.7 (m), 143.2 – 140.7 (m), 143.0 – 140.3 (m), 139.1 – 136.6 (m), 139.0 – 136.5 (m), 127.7, 121.3, 113.8 – 113.6 (m), 112.1 – 111.6 (m), 109.9 – 109.6 (m). HRMS (ESI) calcd. for $C_{20}HF_{15}$ $[M]^+$: 525.9839; found: 525.9827. FT-IR (neat) $\bar{\nu}$ 1653, 1489, 982, 696 cm^{-1}. Anal. calcd (%) for $C_{20}HF_{15}$: C 45.65, H 0.19; found: C 45.67, H 0.10.

General Procedure for Photocyclizations (performed by Dr. Zhang)

A 5 mL round-bottom flask was charged with either THF or CH_2Cl_2 (2.5 mL), a fluorinated TPE derivative of interest (**35 – 38**, 5 mg), and a magnetic stir bar. The flask was then filled with either N_2 or O_2 and irradiated by UV light at 302 nm for 15 h at room temperature. The THF and CH_2Cl_2 solvents were degassed by freeze-pump-thaw method with molecular sieves (4 Å), and either N_2 or O_2 were bubbled through the solution. The mixture was then separated on a preparative thin-layer chromatography plate, eluting with hexane/CH_2Cl_2 (3/1, v/v) for **41** and pure hexane for **42 – 44**.

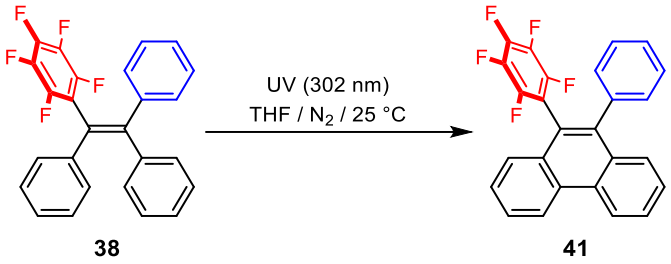

38 41

9-Pentafluorophenyl-10-phenylphenanthrene (41)

Despite extensive experimentation, this compound could not be obtained in its pure form, and the yield of ~30% is an estimate.

41: ^{1}H NMR (500 MHz, DMSO-d_6): δ 9.02 (d, J=8.0 Hz, 2H), 7.79 (m, 2H), 7.65–7.55 (m, 3H), 7.42–7.36 (m, 4H), 7.19–7.13 (m, 2H) ppm. ^{19}F NMR (470 MHz, DMSO-d_6): −138.84 (m, 2F), −154.58 (t, J=22.1 Hz, 1F), −162.44 (m, 2F) ppm.

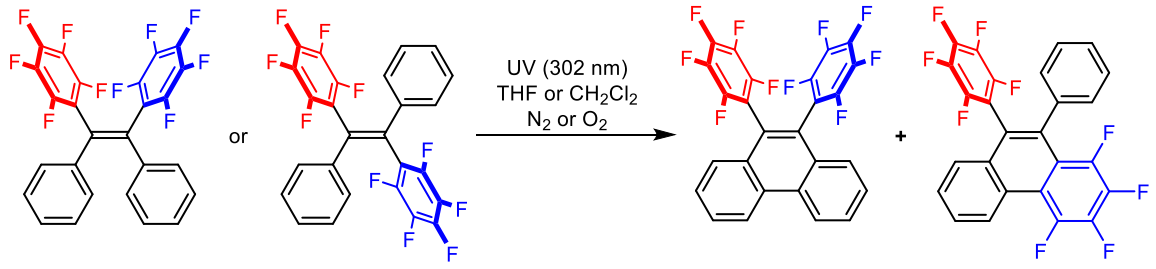

36 35 42 43

9,10-Di(pentafluorophenyl)phenanthrene (42)

42: ^{1}H NMR (500 MHz, $CDCl_3$): δ 8.87 (d, J=8.0 Hz, 2H), 7.81 (t, J=7.8 Hz, 2H), 7.63 (t, J=7.3 Hz, 2H), 7.43 (d, J=8.0 Hz, 2H) ppm. ^{19}F NMR (470 MHz, $CDCl_3$): δ −137.79 to −137.71 (m, 4F), −151.74 (t, J=20.9 Hz, 2F), −160.35 (dd, J=20.9, 14.8 Hz, 4F) ppm. ^{13}C{^{1}H} NMR (126 MHz, $CDCl_3$): δ 145.6 (m), 143.5 (m), 142.5 (m), 140.4 (m), 138.6 (m), 136.6 (m), 131.2, 129.7, 128.6, 128.0, 126.0, 125.6, 123.3, 112.4 (m). HRMS (APPI) calcd. for $C_{26}H_8F_{10}$ [M^+]: 510.0461; found: 510.0470. FT-IR (neat) $\bar{\nu}$ 3073, 1653, 1560, 1519, 1486, 1448, 1433, 1389,

1330, 1307, 1213, 1164, 1121, 1051, 1025, 985, 967, 895, 855, 805, 785, 740, 719, 714, 634, 617, 578, 543, 483, 467, 436, 424, 413, 404 cm^{-1}.

1,2,3,4-Tetrafluoro-9-(pentafluorophenyl)phenanthrene (43)

43: ^{1}H NMR (500 MHz, $CDCl_3$): δ 9.18 (d, *J*=9.0 Hz, 1H), 7.79 (t, *J*=7.5 Hz, 1H), 7.65 (t, *J*=7.8 Hz, 1H), 7.39 (d, *J*=8.5 Hz, 1H), 7.28 (m, 3H), 7.20 (m, 2H) ppm. ^{19}F NMR (470 MHz, $CDCl_3$) δ −133.41 (dd, *J*=20.7, 13.6 Hz, 1F), −137.57 (dd, *J*=23.0, 7.5 Hz, 2F), −137.85 (t, *J*=16.7 Hz, 1F), −153.02 (t, *J*=21.2 Hz, 1F), −154.79 (t, J=20.0 Hz, 1F), −156.30 to −156.20 (m, 1F), −161.56 (td, J=21.9, 7.7 Hz, 2F) ppm. $^{13}C\{^{1}H\}$ NMR (126 MHz, $CDCl_3$): δ 147.1 (m), 144.9 (m), 142.9 (m), 140.0 (m), 138.4 (m), 136.4 (m), 135.4 (m), 130.6, 128.9, 128.7, 127.9 (m), 127.7, 127.5 (m), 127.2 (m), 126.0 (m), 125.8, 117.6 (m) ppm. HRMS (APPI) calcd. For $C_{26}H_9F_9$ [M^+] 492.0555; found: 492.0543. FT-IR (neat) $\bar{\nu}$ 3066, 1647, 1596, 1541, 1524, 1509, 1495, 1471, 1443, 1427, 1382, 1339, 1316, 1276, 1232, 1189, 1158, 1134, 1106, 1067, 1042, 1032, 983, 922, 883, 841, 814, 781, 753, 736, 702, 695, 680, 658, 639, 625, 612, 584, 578, 535, 481, 442, 434, 419, 409, 403 cm^{-1}.

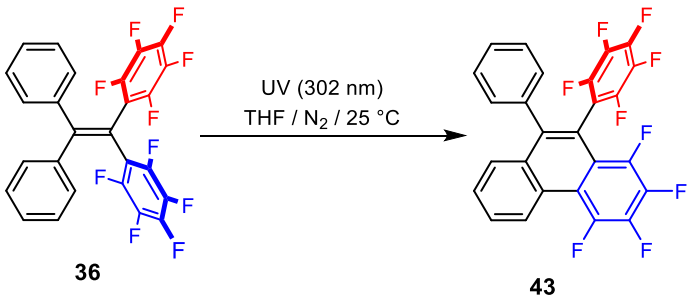

36 43

1,2,3,4-Tetrafluoro-10-(pentafluorophenyl)phenanthrene (44)

44: Yield: 87%. ^{1}H NMR (500 MHz, $CDCl_3$): δ 9.16 (dd, *J*=8.8, 2.3 Hz, 1H), 7.79 (t, *J*=7.8 Hz, 1 H), 7.60 (t, *J*=7.5 Hz, 1H); 7.51 (d, *J*=8.0 Hz, 1H), 7.34 (t, *J*=3.3 Hz, 3H), 7.18 (s, 2H) ppm. ^{19}F NMR (470 MHz, $CDCl_3$): δ −137.28 (t, *J*=16.0 Hz, 1F), −139.11 (dd, *J*=23.5, 7.5 Hz, 2F),

−142.72 (dd, *J*=20.0, 13.4 Hz, 1F), −154.43 (t, *J*=20.7 Hz, 1F), −155.83 (t, *J*=20.0 Hz, 1F), −156.03 (td, *J*=20.7, 4.3 Hz, 1F), −162.94 (td, *J*=22.1, 7.7 Hz, 2F) ppm. $^{13}C\{^{1}H\}$ NMR (126 MHz, $CDCl_3$) δ 144.30, 137.35, 131.93, 129.18, 128.79, 128.64, 128.40, 127.29, 127.06 ppm. HRMS calcd. For $C_{26}H_9F_9$ [M^+] 492.0561; found: 492.0558. FT-IR (neat) $\bar{\nu}$ 1521, 1496, 1471, 1443, 1336, 1024, 984, 939, 768, 724, 704, 697 cm^{-1}.

Single Crystal Structures and Analyses

Crystals of **35 – 37** and **40** were obtained by air evaporation of their MeOH solution (1 mg mL^{-1}). The quality of crystals of **35**, **37**, and **40** was high enough to allow full refinement of their single crystal structures. Diffraction data was also obtained for the crystals of **36**, but was of insufficient quality to allow full refinement. Crystals of **42** and **43** were obtained by air evaporation of their $CDCl_3$ solutions, while those of **44** resulted from air evaporation of its CH_2Cl_2 solution.

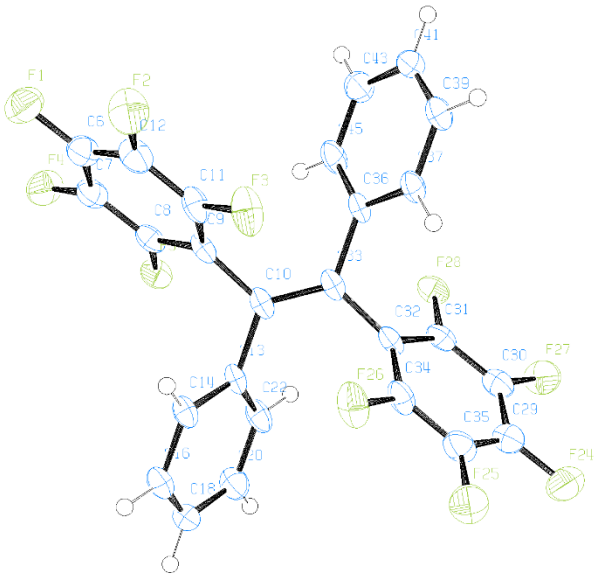

Figure 4.2. ORTEP plot of the crystal structure of **35**. Thermal ellipsoids shown at 50% probability.

Table 4.2. Crystal data and structure refinement for **35**

Identification code	P141-4B_XW214C
Empirical formula	$C_{26}H_{10}F_{10}$
Formula weight	512.34
Temperature / K	123(2)
Wavelength / Å	0.71073
Crystal system	Orthorhombic
Space group	*F*dd2
a / Å	18.4539(18)
b / Å	39.622(4)
c / Å	5.9123(6)
α / °	90
β / °	90
γ / °	90
Volume / Å^3	4322.9(7)
Z	8
ρ_{calc} / Mg/m^3	1.574
Absorption coefficient/mm^{-1}	0.152
F(000)	2048
Crystal size / mm^3	0.44 × 0.26 × 0.01

Table 4.2. continued

Theta range for data collection	2.435 to 28.329°
Index ranges	$-24 \leq h \leq 24$, $-52 \leq k \leq 52$, $-7 \leq l \leq 7$
Reflections collected	14502
Independent reflections	2674 [R_{int}=0.0328]
Completeness to theta=25.242°	99.60%
Absorption correction	Empirical
Max. and min. transmission	0.7457 and 0.6004
Refinement method	Full-matrix least-squares on F^2
Data / restraints / parameters	2674 / 1 / 164
Goodness-of-fit on F^2	1.063
Final R indexes [I>2 σ (I)]	R_1=0.0398, wR_2=0.1082
R indexes (all data)	R_1=0.0430, wR_2=0.1111
Absolute structure parameter	0.4(9)
Largest diff. peak / hole / e Å^{-3}	0.291 / −0.196

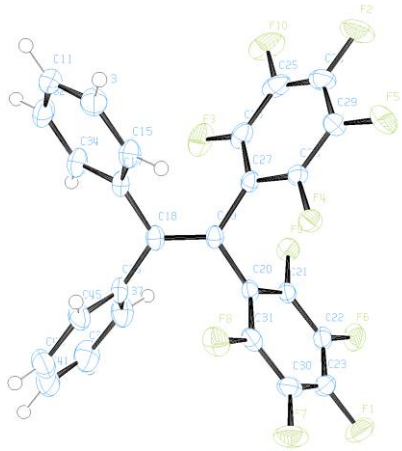

Figure 4.3. ORTEP plot of the crystal structure of **37**. Thermal ellipsoids shown at 50% probability.

Table 4.3. Crystal data and structure refinement for **37**

Identification code	P141-2A_XW212
Empirical formula	$C_{26}H_{10}F_{10}$
Formula weight	512.34
Temperature / K	123(2)
Wavelength / Å	0.71073
Crystal system	Monoclinic
Space group	*C*2/c
a / Å	40.7724(12)
b / Å	6.0040(2)
c / Å	19.6291(6)
α / °	0
β / °	115.8920(10)

Table 4.3. continued

γ / °	90
Volume / Å^3	4322.8(2)
Z	8
ρ_{calc} / Mg/m^3	1.574
Absorption coefficient/mm^{-1}	0.152
F(000)	2048
Crystal size / mm^3	0.40 × 0.21 × 0.19
Theta range for data collection	2.966 to 28.292°.
Index ranges	$-54 \leq h \leq 41, -6 \leq k \leq 8, -26 \leq l \leq 26$
Reflections collected	12847
Independent reflections	5252 [R(int)=0.0233]
Completeness to theta=25.242°	97.70%
Absorption correction	Empirical
Max. and min. transmission	0.7457 and 0.6736
Refinement method	Full-matrix least-squares on F^2
Data / restraints / parameters	5252 / 0 / 325

Table 4.3. continued

Goodness-of-fit on F^2	1.03
Final R indexes [I>2 σ (I)]	R_1=0.0419, wR_2=0.1119
R indexes (all data)	R_1=0.0486, wR_2=0.1178
Largest diff. peak / hole / e Å^{-3}	0.396 / −0.362

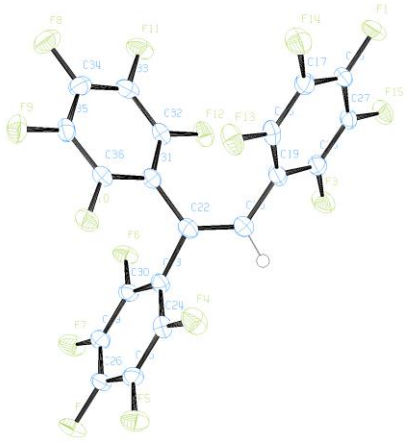

Figure 4.4. ORTEP plot of the crystal structure of **40**. Thermal ellipsoids shown at 50% probability.

Table 4.4. Crystal data and structure refinement for **40**

Identification code	127-7_XW215
Empirical formula	$C_{20}HF_{15}$
Formula weight	526.21
Temperature / K	123(2)
Wavelength / Å	1.54178
Crystal system	Triclinic

Table 4.4. continued

Space group	$P\bar{1}$
a / Å	5.7320(2)
b / Å	13.8425(6)
c / Å	23.4407(10)
α / °	72.946(2)
β / °	85.1640(10)
γ / °	85.8890(10)
Volume / Å^3	1769.64(13)
Z	4
ρ_{calc} / Mg/m^3	1.975
Absorption coefficient/mm^{-1}	2.095
F(000)	1024
Crystal size / mm^3	0.38 × 0.04 × 0.03
Theta range for data collection	1.976 to 67.957°.
Index ranges	$-6 \leq h \leq 6$, $-16 \leq k \leq 16$, $-27 \leq l \leq 27$
Reflections collected	24515
Independent reflections	6198 [R_{int}=0.0262]

Table 4.4. continued

Completeness to theta=67.679°	96.70%
Absorption correction	Empirical
Max. and min. transmission	0.7530 and 0.5972
Refinement method	Full-matrix least-squares on F^2
Data / restraints / parameters	6198 / 0 / 631
Goodness-of-fit on F^2	1.028
Final R indexes [I>2 σ (I)]	R_1=0.0371, wR_2=0.0940
R indexes (all data)	R_1=0.0403, wR_2=0.0973
Largest diff. peak / hole / e Å^{-3}	0.378 / −0.236

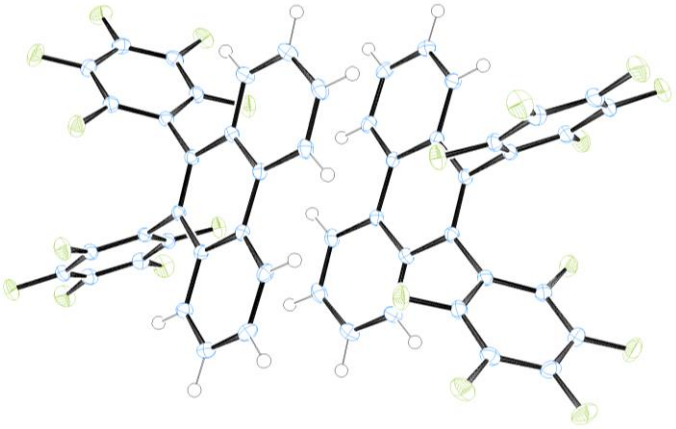

Figure 4.5. ORTEP plot of the crystal structure of **42**. Thermal ellipsoids shown at 50% probability.

Table 4.5. Crystal data and structure refinement for **42**

Identification code	P43R1O2-2_XW270B
Empirical formula	$C_{26}F_{10}H_8$
Formula weight	510.32
Temperature/K	123(2)
Crystal system	triclinic
Space group	$P\bar{1}$
a / Å	7.6133(6)
b / Å	9.2673(8)
c / Å	14.2415(12)
α / °	97.7530(10)
β / °	90.3640(10)
γ / °	105.9340(10)
Volume / Å^3	956.37(14)
Z	2
ρ_{calc}/g/cm^3	1.772
μ/mm^{-1}	0.171
F(000)	508.0
Crystal size / mm^3	0.49 × 0.10 × 0.07
Radiation	MoKα (λ=0.71073)

Table 4.5. continued

2Θ range for data collection / °	4.618 to 61.32
Index ranges	$-10 \leq h \leq 10$, $-13 \leq k \leq 13$, $-20 \leq l \leq 20$
Reflections collected	24054
Independent reflections	5778 [R_{int}=0.0100, R_{sigma}=0.0080]
Data / restraints / parameters	5778 / 0 / 325
Goodness-of-fit on F^2	1.042
Final R indexes [$I \geq 2\sigma(I)$]	R_1=0.0333, wR_2=0.0980
Final R indexes (all data)	R_1=0.0362, wR_2=0.1010
Largest diff. peak / hole /e Å^{-3}	0.49 / −0.20

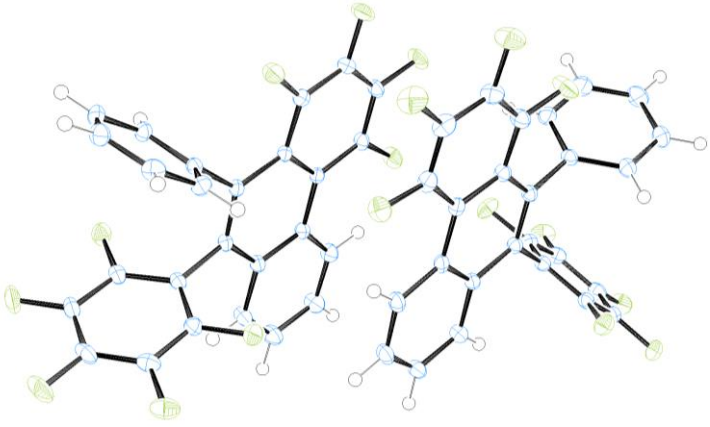

Figure 4.6. ORTEP plot of the crystal structure of **43**. Thermal ellipsoids shown at 50% probability.

Table 4.6. Crystal data and structure refinement for **43**

Identification code	P43R1O2_XW270
Empirical formula	$C_{26}F_9H_9$
Formula weight	492.33
Temperature / K	123(2)
Crystal system	triclinic
Space group	$P\bar{1}$
a / Å	10.6975(8)
b / Å	13.8503(11)
c / Å	14.4787(11)
α / °	64.2670(10)
β / °	89.4680(10)
γ / °	83.1000(10)
Volume / Å^3	1916.3(3)
Z	4
ρ_{calc} / g/cm^3	1.707
μ / mm^{-1}	0.160
F(000)	984.0
Crystal size / mm^3	0.43 × 0.12 × 0.09
Radiation	MoKα (λ=0.71073)
2Θ range for data collection / °	3.292 to 59.086

Table 4.6. continued

Index ranges	$-14 \leq h \leq 14$, $-19 \leq k \leq 19$, $-20 \leq l \leq 20$
Reflections collected	53860
Independent reflections	10652 [R_{int}=0.0123, R_{sigma}=0.0081]
Data / restraints / parameters	10652 / 0 / 631
Goodness-of-fit on F^2	1.022
Final R indexes [$I \geq 2\sigma(I)$]	R_1=0.0327, wR_2=0.1003
Final R indexes [all data]	R_1=0.0360, wR_2=0.1042
Largest diff. peak / hole / e Å^{-3}	0.44 / −0.23

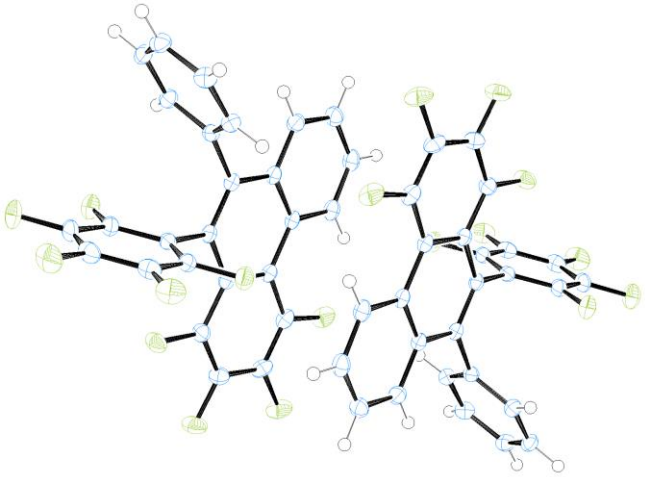

Figure 4.7. ORTEP plot of the crystal structure of **44**. Thermal ellipsoids shown at 50% probability.

Table 4.7. Crystal data and structure refinement for **44**

Identification code	P72_XW280
Empirical formula	$C_{26}F_9H_9$
Formula weight	492.33
Temperature / K	123(2)
Crystal system	triclinic
Space group	$P\bar{1}$
a / Å	10.7734(6)
b / Å	12.8066(8)
c / Å	14.0039(8)
α / °	87.8190(10)
β / °	82.9010(10)
γ / °	86.6180(10)
Volume / Å^3	1913.05(19)
Z	4
ρ_{calc} / g/cm^3	1.709
μ / mm^{-1}	0.161
F(000)	984
Crystal size / mm^3	0.39 × 0.09 × 0.06
Radiation	MoKα (λ=0.71073)
2Θ range for data collection / °	3.816 to 56.636

Table 4.7. continued

Index ranges	$-14 \leq h \leq 14$, $-17 \leq k \leq 17$, $-18 \leq l \leq 18$
Reflections collected	45212
Independent reflections	9481 [R_{int}=0.0151, R_{sigma}=0.0119]
Data / restraints / parameters	9481 / 0 / 631
Goodness-of-fit on F^2	1.036
Final R indexes [$I \geq 2\sigma(I)$]	R_1=0.0320, wR_2=0.0921
Final R indexes [all data]	R_1=0.0381, wR_2=0.0966
Largest diff. peak/hole / e Å^{-3}	0.40 / −0.21

Chapter 5: Ligands for Transition Metal – Catalyzed Asymmetric Transformations

5.1 C_3-Symmetric Sulfur Containing Ligands and Their Complexes with Group VIII/IX/XI Transition Metals.

5.1.1. Introduction.

The intimate relationship between transition metals and ligands has a deep effect on the outcome of catalytic reactions.[130] Many transition metal-catalyzed C – H bond functionalizations have been successfully accomplished by palladium complexed with phosphine or amine-based ligands.[131] Meanwhile, cyclopentadienyl (Cp) – metal complexes and their derivatives have been extensively used in C – H functionalization due to the fact that the reactions proceed under mild conditions, and tolerate broad variety of functional groups.[130]

After ferrocene was synthesized in 1951,[132] the cyclopentadienyl anion (Cp) has become a principal type of ancillary ligands for a wide range of transition metals.[133-136] Possessing 6-π electrons in aromatic ring, Cp moiety is known as a good σ- and π-donor ligand, coordinating to transition metals in η^5-fashion, inducing high stability of the Cp metal complexes (CpM).[137,138] This allows chemical reactions at metal center to proceed without modifying the Cp ligand. Additionally, the stereoelectronic properties of metal center are adjustable via introduction of substituents on cyclopentadiene.[139-141] In particular, the replacement of hydrogen atoms on Cp ring by methyl groups giving Cp* ligand, results in the increase in σ-donating ability, leading to higher ligand-metal dissociation energy.[142,143] Presumably, the first reactions that can be deemed "C – H activation" via (Cp*)Rh(L) or (Cp*)Ir(L) fragments were published by Bergman[144] and Jones[145] in 1982. Brookhart subsequently showed that enamines

can be synthesized by employing (Cp*)Co(bis-olefin) catalyst via hydrogen transfer in protected amines.[146] Furthermore, modification in electronic and steric nature of Cp* ligand may lead to significant improvements in selectivity as well as reactivity. For example, in 2011, Rovis and coworkers reported that by changing the steric character of Cp* ligand, they could significantly increase the selectivity of alkyne insertion for the synthesis of pyridones.[147] Specifically, precatalyst rhodium (III) complex bearing a 1,3-di-*tert*-butylcyclopentadienyl group (Cp^t) showed a remarkable improvement in coupling regioselectivity (14:1) (**Scheme 5.1**). Moreover, various substitutions on acrylamide were well tolerated and the pyridines were obtained in high yields and good regioselectivity. Extensive investigation uncovered that unsymmetrical alkynes with an alkyl and an aryl group produced higher selectivity when using Cp^t ligand, compared to that with Cp*.

Scheme 5.1. Regioselectivity in the coupling of acrylamides with alkynes.

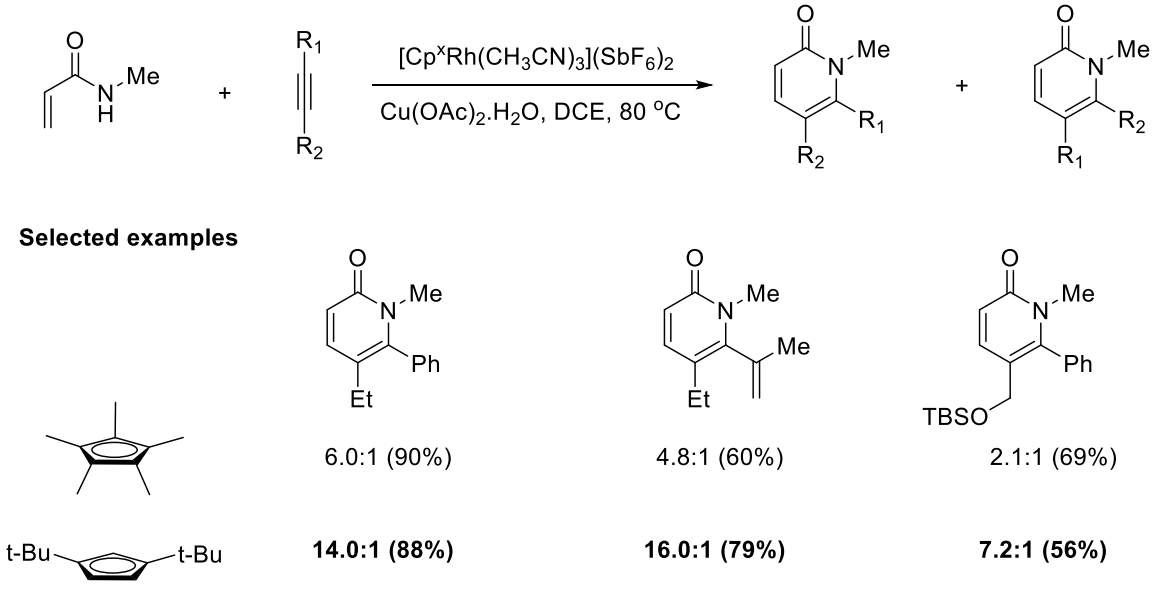

Another example from the same group showed that by tuning the electronic porperties of Cp* ligand bound to rhodium, the rate of 2,3-dihydropyridine formation was significantly

increased.[148] The insertion of hindered alkenes into α,β-unsaturated oximes to deliver 2,3-dihydropyridine could proceed in 74% conversion in 10 hours when cationic Cp*Rh(III) catalyst was used (**Scheme 5.2**). However, by replacing one methyl group on Cp* ligand with trifluoromethyl group, resulting in Cp^{*CF3} ligand, or in other words, by increasing electronegative character of Cp* ligand, full conversion was obtained only after 2 h and desired product was isolated in 84% yield. Interestingly, this ligand was also compatible with broad scope of substituents on oxime to access diversely substituted 2,3-dihydropyridine rings.

Scheme 5.2. Coupling of α,β-unsaturated oximes with 1,1-disubstituted alkenes: synthesis of 2,3-dihydropyridines.

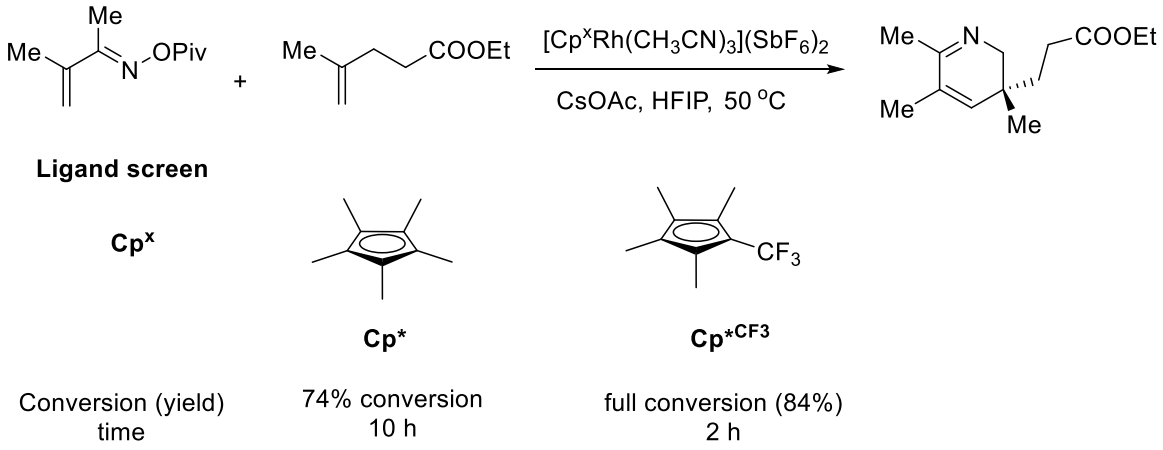

Asymmetric catalysis with transition metal complexes is one of the most powerful tools to achieve highly enantioselective transformations.[149] Besides well-known chiral ligands such as **TADDOL**, **BOX**, **BINAP**, **BINOL**, **SALEN**, and **NHC** (**Figure 5.1**),[150,151] modified cyclopentadienyl anions (**Cp^x**) are also good candidates for asymmetric catalysis.[152,153]

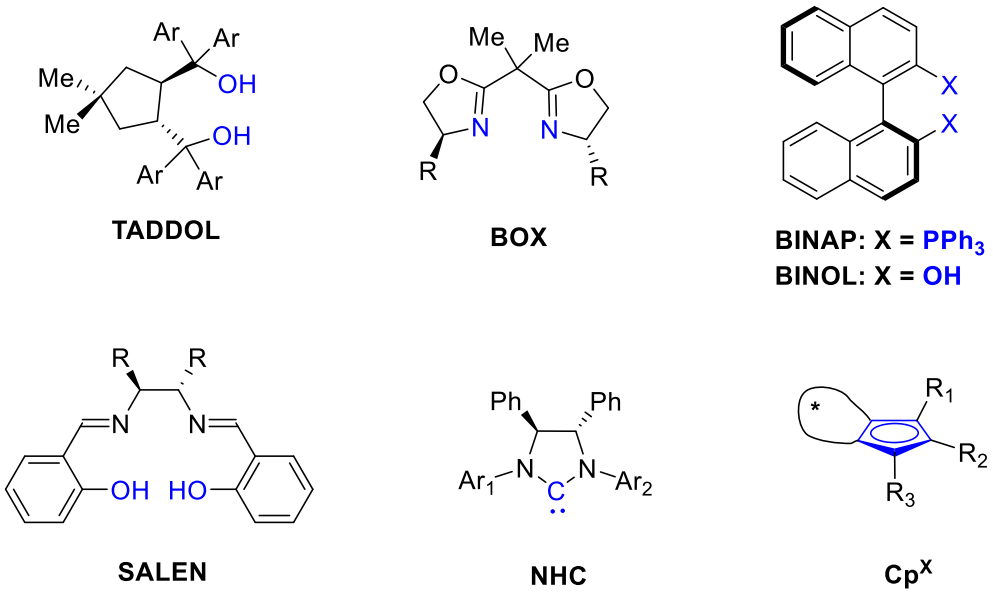

Figure 5.1. Selected privileged chiral ligands for asymmetric catalysis.

There are several types of chiral Cp ligands that have been utilized in enantioselective transformations, depending on number of available coordination sites at the metal center (**Figure 5.2**). For example, owing to saturated coordination sites, planar chiral metallocenes (**45**) are used as chemically inert backbones for heteroatom-coordinating ligands, such as ferrocenyl diphosphine ligands, Josiphos.[150,154] For *ansa*-metallocenes **46**,[155] Cp unit **48** with external bidentate chiral ligands,[156-158] or chiral ligands tethered to Cp unit **48-A**,[159,160] metals possess one or two available coordination sites, preventing their usage in many transformations. Meanwhile, analogues of **47** bearing one Cp ligand, are called "half sandwich" or "piano stool" complexes where chirality originates from the Cp ligand. In addition, possessing three available coordination sites, those complexes have been employed in various enantioselective reactions.[161]

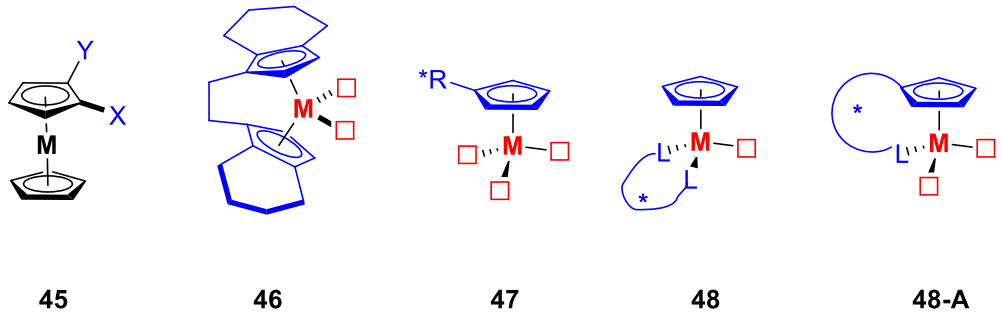

Figure 5.2. Chiral metal complexes bearing the Cp ligand and their available coordination sites.

The idea of utilizing chiral Cp ligands for asymmetric catalysis can be traced back to 1978 when Kruger and co-workers introduced the synthesis of (–)-menthol-derived cyclopentadiene, complexed with different metal centers including titanium and zirconium.[162,163] Later on, two chiral Cp ligands, where chirality originates from natural sources such as (+)-tartaric acid,[164] or (+)-camphor,[165] were obtained by Volhardt. Halterman succeeded in preparing a chiral ligand precursor containing an atropisomeric binaphthyl backbone (**Figure 5.3**).[166] However, those ligand were not able to induce highly enantioselective transformations.[162]

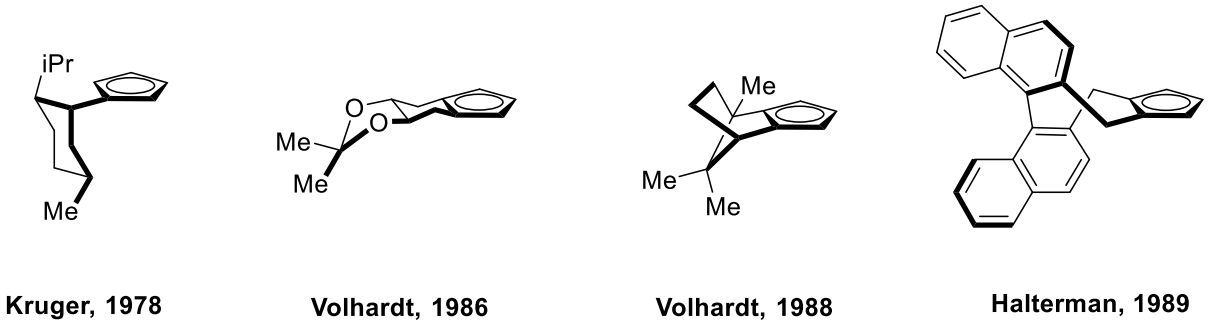

Figure 5.3. Selected first examples of chiral cyclopentadienes.

This chemistry was somewhat dormant for over two decades until the group of Cramer designed a new Cp ligand system in 2012. Generally, two new Cp ligands from Cramer group were developed based on their predecessors in 1986 and 1989. The ligands were named Mannitol-Cp[167] and BINOL-Cp[168] (**Figure 5.4**). The key factor, determining the efficiency of these ligands in asymmetric transformations, are two identical substituents on the flank of ligand backbone, acting as sidewall and a bulky group at the rear, known as backwall.[167] Additionally, it is crucial for Cp^x ligands to possess C_2 symmetry, with both faces of Cp ring being equivalent, in order to prevent the tedious separation of diastereomeric metal complexes.

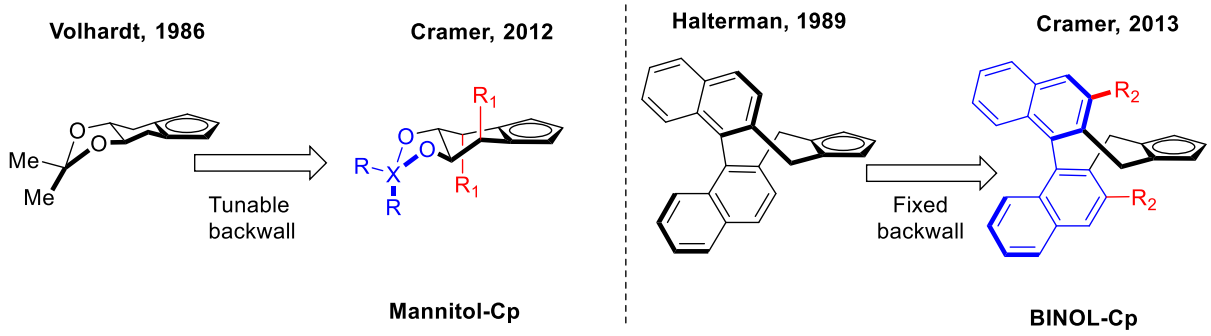

Figure 5.4. Improved Cpx ligands based on novel design principles.

After original work by Cramer group, many chiral cyclopentadienyl ligands have been investigated. They can be categorized into six different types depending on their scaffold (**Figure 5.5**).[169] In 2012, **Mannitol-Cp** was introduced by Cramer and co-workers.[167] The ligand was synthesized from D-mannitol in 8-9 steps. Total of seven derivatives for this ligand family were prepared and used in two Rh-catalyzed asymmetric reactions. In the same year, Ward and Rovis collaboratively reported an enzyme-based Cp ligand, **SavCp**, which was explored in Rh-catalysis.[170] However, due to the high sensitivity of enzymes as well as mutagenesis techniques requirement, the applications of these ligands have been limited. The

C_2-symmetric atropochiral BINOL-Cp, reported by Cramer group,[168] appears to be the most broadly applied in asymmetric catalysis with over 25 derivatives and 35 different enantioselective transformations explored. The ligands can coordinate with various transition metals including Rh, Ru, Ir, Co, as well as rare-earth metals such as Sc, Y, La, Sm, Gd, etc. Additionally, adding more substituents onto Cp ring may improve the complexes' reactivity as well as reaction selectivity.[171,172] In 2016, You and co-workers introduced a second C_2-symmetric ligand family based on spirocyclic backbone, named **SCp**. The single crystal structure analysis showed that the R substituents on **SCp** were closer to metal center, compared to **BINOL-Cp**, resulting in better stereocontrol.

In 2017, Antonchick and Waldmann prepared piperidine-fused **JasCp** ligands, containing four adjustable positions.[173] The straightforward synthesis resulted in over 30 derivatives constructed in short time. However, the lack of C_2-symmetry required additional efforts in their preparation as well as use, and only three applications in Rh-catalyzed asymmetric reactions were reported. More recently, Cramer group developed **cPent-Cp** ligands, bearing two aryl substituents on cyclopentane-fused ring; those groups can be easily tuned to adjust the electronic as well as steric characteristics of the system.[174] Interestingly, this class of chiral ligands could be obtained in convenient two-step synthesis, offering nearly enantiopure product with C_2 symmetry. However, there have been only two applications of this type of ligand in ruthenium (II) catalysis.[174,175] In 2020, Wang and co-workers reported the synthesis of an analogue of C_2-symmetric chiral ferrocene based Cp ligands, **FcCp** in 6-8 steps. Ligand is derived from ferrocene via amine chiral auxiliary.[176] Several transition metals such as Rh^{I}, Ir^{I}, and Ru^{II} were successfully coordinated to those ligands.

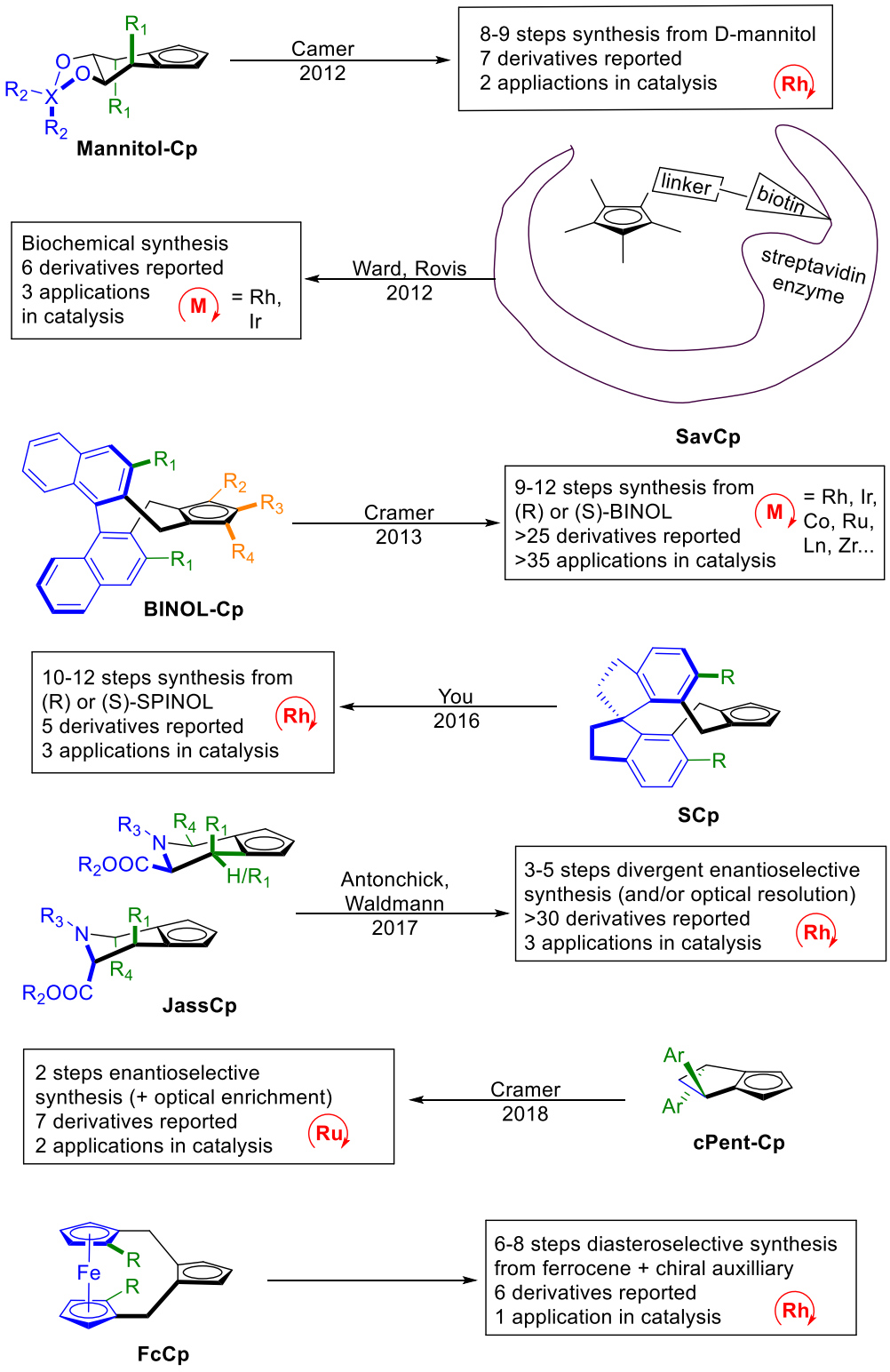

Figure 5.5. An overview of the current families of Cp^X ligands.[169]

The cyclopentadienyl ligands discussed above are powerful stereocontroling tools in asymmetric catalysis. However, they still possess some inherent drawbacks. First, the synthesis of most chiral Cp ligands requires five or more steps which increases required effort. The C_2-symmetric structure is essential in order to prevent complications in separation of diastereomeric mixture after metallation step. Additionally, the long distance between chirality and active metal center reduces the ligand influence in some reactions. Thus, design of a novel ligand family that overcomes problems noted above is essential. The subsequent chapter will describe synthesis and reactivity of C_3-symmetric tridentate sulfur containing ligands.

5.1.2 C_3-Symmetric Tridentate Sulfur Containing Ligand Design

To solve the drawbacks mentioned above, we chose C_3 – symmetric sulfide based ligands, which are easily accessible and where chirality should reside close to the metal center (**Figure 5.6**).

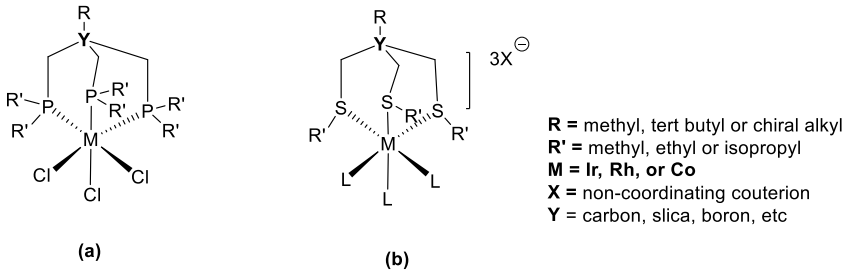

Figure 5.6. (a) Neutral TriPhos complexes (b) Cationic tridentate sulfur containing complexes.

The idea stems from the structure of TriPhos ligands family (**Figure 5.6 a**).[177] The triphos complexes share the same octahedral symmetry as Cp complexes. Hence, the catalytic activity as well as the substrate interactions within catalytic cycle would be somewhat similar. It has been suggested that C_2-symmetry is the key factor to maximize enantioselectivity in asymmetric synthesis.[178] However, it has been also accepted that further restriction in symmetry

from C_2 to C_3 might lower the number of degrees of freedom in substrate-catalyst complex, resulting in better outcome in terms of selectivity.[179-183]

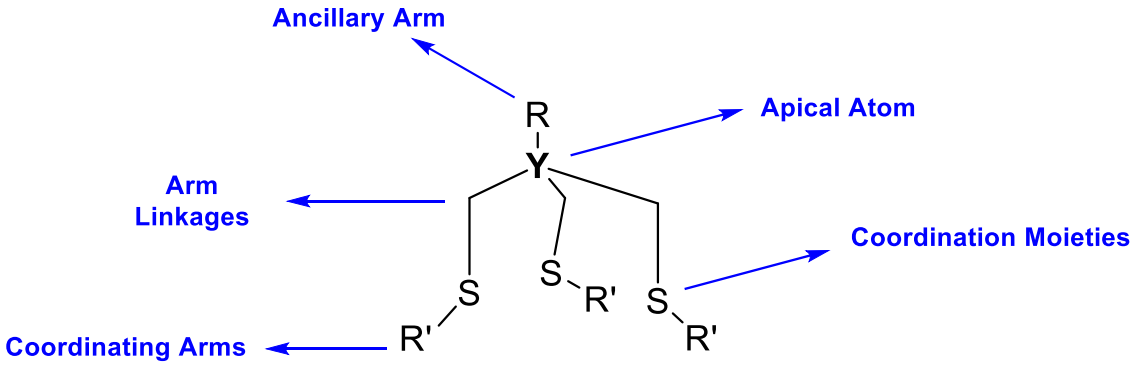

Figure 5.7. Possible variations of C_3-symmetric tridentate sulfur containing ligands.

In contrast to Cp ligands, the C_3-ligand type structure is more versatile with many possible positions for alternations including the ancillary arm, apical atom, arm linkages, coordination moieties, and coordinating arms (**Figure 5.7**). The first potential place that can generate chirality is ancillary arm. Indeed, several alkyl chain can be asymmetrically functionalized at this position.

In terms of apical atom, apart from carbon atom, many heteroatoms can be installed at that position. Examples used in TriPhos ligand family include boron,[184,185] nitrogen,[186,187] silicon,[188,189] tin,[189] or phosphrous.[190,191] Additionally, TriPhos bearing apical boron atom is by far the most well explored structure with general formula $R'B(CH_2PR_2)_3^-$ owing to formal ligand-based charge. These anionic ligands stabilize neutral metal complexes in their +1 oxidation state.[177]

There are various options for coordination moieties including phosphorous, nitrogen, oxygen, or sulfur atoms. Among them, sulfur was selected in this thesis due to its high

coordinative ability to most late transition metals. Furthermore. asymmetric sulfur ligands have been intensively investigated for enantioselective catalysis over last 30 years.[192] Additionally, sulfur-containing compounds are stable, resulting in convenient storage and use. Another interesting features of sulfur containing ligands in asymmetric synthesis is the possible generation of stereogenic center after coordination to metal. However, controlling the new chiral center might sometimes be difficult or impossible due to low inversion barrier (10 – 15 kcal mol $^{-1}$).[193]

Other possible chiral centers can be generated on the coordination arms. These substituents may act as not only chiral control agents in asymmetric transformations but also bulky groups enhancing regioselectivity.

To the best of our knowledge, preparation and exploration of enantioselective catalysis of complexes based on these chiral C_3-symmetric sulfur containing ligands has not been reported. In next section we will present preparation of tripod trisulfide ligands and their complexation to transition metals.

5.1.3 Results and Discussion

5.1.3.1 Functionalization on Ancillary Arm

The non-chiral ligand **49** was synthesized by a reported procedure.[194] Heating 1,1,1-tris(chloromethyl)ethane and sodium thiomethoxide in DMF with sodium iodide, the C_3-symmetric sulfur containing ligand **49** was obtained in nearly quantitative yield (**Scheme 5.3**). The ligand **49** was refluxed with rhodium (III) or iridium (III) salts to yield yellow solids. Unfortunately, these solids were insoluble in any common organic solvents, resulting in difficulties in characterization and use. By replacing methyl group with an ethyl group in the

ligand, we could obtain rhodium complex **52** and iridium complex **56** in 81% and 74% yields, respectively. The solubility of these complexes is still very poor. Subsequently, these complexes were treated with silver (I) hexafluoroantimonate in acetonitrile. Rhodium (III) complex **54** was obtained in 33% yield, while same method for iridium complex was unsuccessful. Additionally, *iso*-propyl substituted complexes **53** and **57** were obtained in 70% and 65% yields, respectively. The solubility of **53** and **57** were improved relative to **52** and **56**.

Scheme 5.3. Synthesis of C_3-symmetric rhodium and iridium complexes.

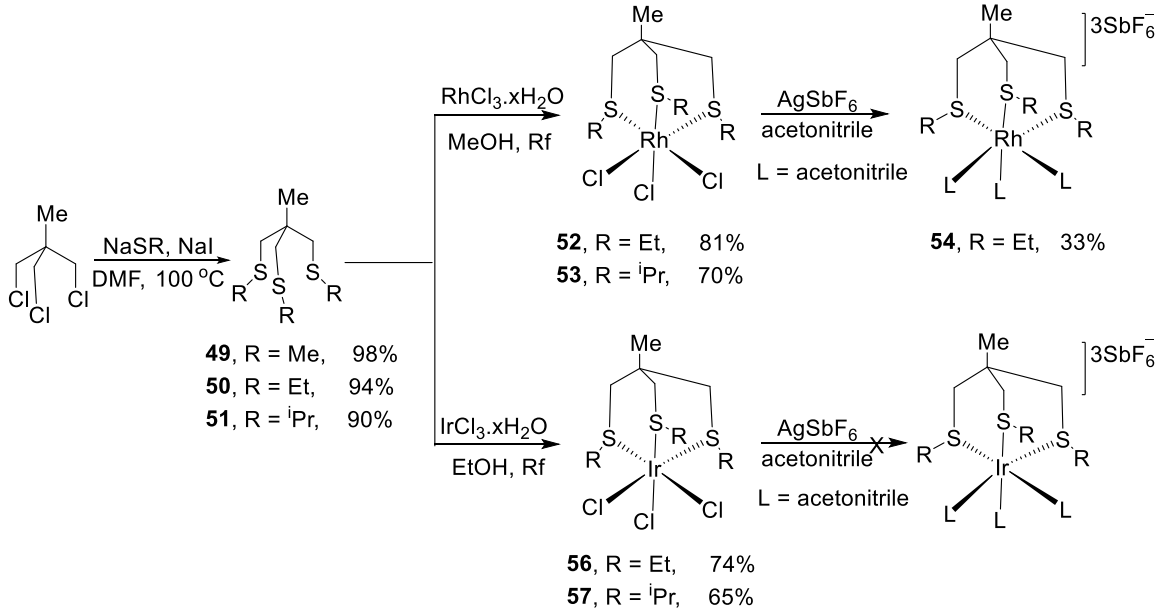

Hydrogen/deuterium exchange in 4-tert buyl benzoic acid and 2-ethylpyridine were used to test the reactivity of the new complexes (**Scheme 5.4**). The results showed that H/D exchange at ortho position of p-*tert* butyl benzoic acid occurred at 120 °C using **52** in the presence of silver hexafluoroantimonate in deuterated acetic acid. Notably, no reaction was observed without the silver salt. The sp^3 H/D exchange was also tested using aliphatic carboxylic acids, yet only trace amount of exchange was recorded. Meanwhile, 45 % deuterium

exchange at primary C – H bond of 2 – ethyl pyridine was observed. These results reveal that the new complex is competent in C – H activation of both sp^2 and sp^3 C – H bonds. Further experiments were directed at preparing chiral non-racemic catalysts.

Scheme 5.4. H/D exchange experiments.

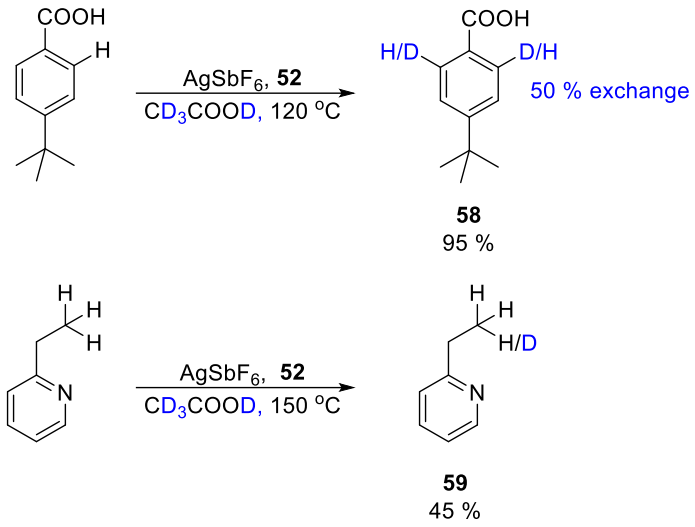

The bulkier tridentate sulfur containing ligand **62** was also examined (**Scheme 5.5**). Treating commercially available diethyl tert-butylmalonate with paraformaldehyde, using potassium carbonate and benzyltrimethylammonium chloride in DMSO at 80 °C, gave compound **60** in 32% yield. Reduction of compound **60** gave tri-alcohol **61** in 46% yield. The following steps were alcohol protection and nucleophilic substitution reaction, producing final ligand **62** in 90% yield. This ligand was then complexed with rhodium (III) salts in different solvents, yet the formation of corresponding complexes were not observed.

Scheme 5.5. Synthesis of ligand **62**.

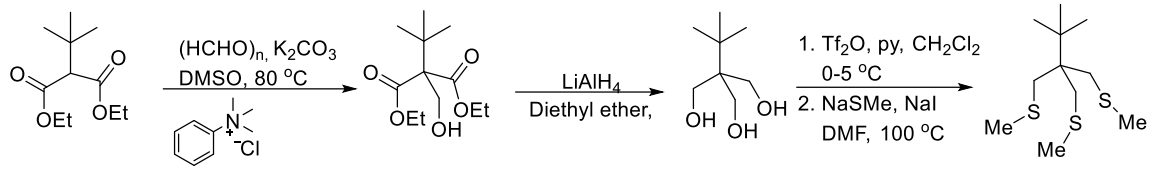

60 32% **61** 46% **62** 90%

For preparation of chiral ligand, the deprotonation of (S)-4-benzyl oxazolidinone, Evans auxiliary,[195] using nBuLi was followed by quenching with corresponding acid chloride to produce *N*-acyloxazolidinone **63** in 76% yield . Then, treating **63** with lithium diisopropylamide (LDA) followed by quenching with methyl iodide, gave intermediate **64** in 89% yield with diastereomeric ratio of 14:1. This ratio could be increased up to >20:1 by recrystallization from cyclohexane. Next, auxiliary removal by hydrolysis using lithium hydroxide and hydrogen peroxide mixture gave corresponding chiral carboxylic acid **65** in 83% yield. Subsequently, acid **65** was reduced using lithium aluminum hydride, to give chiral alcohol **66**. The alcohol protection gave **67** in 40% yield. Reaction of compound **67** with diethyl malonate did not occur under a number of conditions. Alternatingly, reaction of **67** with sodium iodide in DMF gave chiral halide **68** in 77%, followed by nucleophilic substitution reaction to form **69** in 20% yield.

Scheme 5.6. The synthesis of fragment **69**.

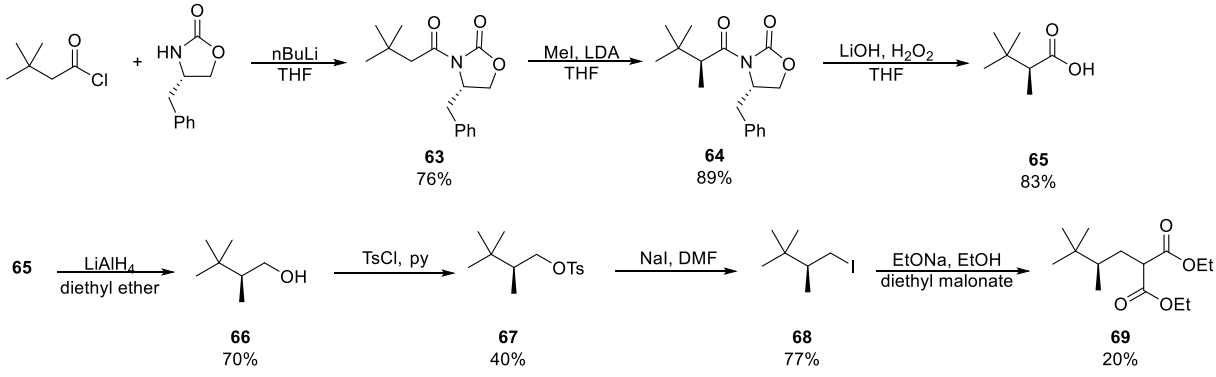

In order to increase the yield of **69**, Mitsunobu reaction was investigated. However, traditional Mitsunobu conditions using diethyl azodicarboxylate (DEAD) or diisopropyl azodicarboxylate (DIAD) with triphenyl phosphine at low temperature did not give the desired product **69** (**Scheme 5.7**). Reaction of diazo compound **70** with tributyl phosphine at 80 °C, gave **69** in 30 % yield. Same conditions were applied for chiral secondary alcohol, (R)-4,4-dimethylpentan-2-ol, yet only trace amount of product was observed. Next, substrate **69** was reacted with paraformaldehyde using potassium carbonate and benzyltrimethylammonium chloride in DMSO at 80 °C. However, only trace of **70** was obtained. The low yield of this step prevents the use of this synthetic route.

Scheme 5.7. The synthesis of fragment **71**.

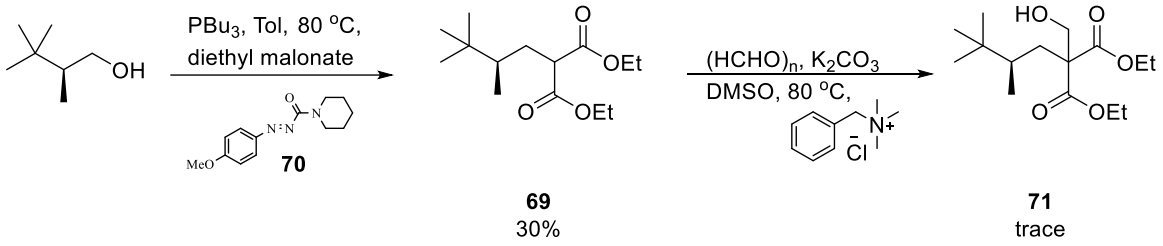

In summary, all efforts to generate chiral center at ancillary arm did not work. More investigations will be required to access chiral catalysts. In next part, we will present the preparation of chiral sulfur containing ligand in which chirality is attached to arm linkages.

5.1.3.2 Chiral Centers on Linkages

In 2012, Arnold and co-workers introduced the synthesis of C_3-symmetric chiral triphosphine **75-A** via asymmetric deprotonation pathway (**Scheme 5.8**).[196] Specifically, treating $PMe_2(t\text{-Bu})(BH_3)$ **73** with s-BuLi and (–)-sparteine **74** followed by quenching with $MeSiCl_3$, gave mixture of C_3 and C_1-symmetric phosphine-boranes **75-A** and **75-B** in a ratio of

2.1:1 (C_3/C_1). After recrystallization, the diasteromeric ratio increased to 30:1 C_3/C_1. The authors also prepared complexes of C_3 ligand with several transition metals, however their reactivity was not explored.

Scheme 5.8. Synthesis of C_3-symmetric-TriPhos ligand **75**. Note: the structure of **75-A** and **-B** are top view.

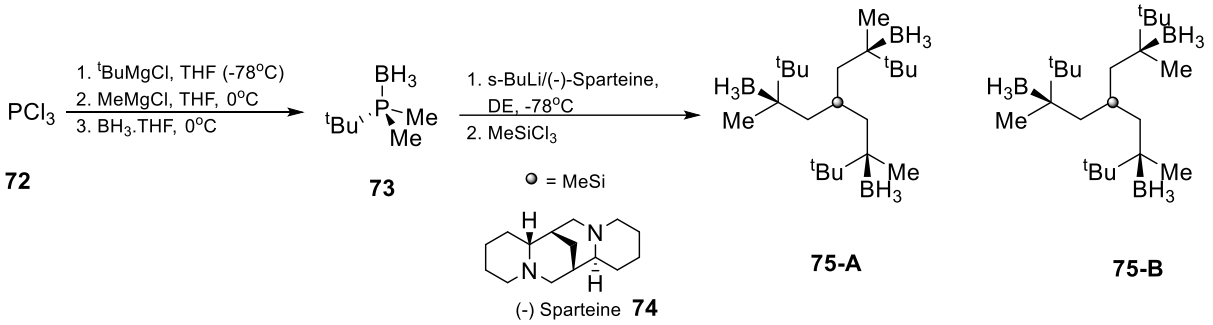

We attempted to use this method for preparation of chiral sulfur containing ligand. Thus, the reaction of benzyl methyl sulfide with methyltrichlorosilane using nBuLi and (+)-sparteine at -78 °C; however, desired product was not observed. Alternatively, increasing temperature to -30 °C allowed deprotonation step to proceed and after quenching with methyltrichlorosilane ligand **76** was found in 45% yield (**Scheme 5.9**) and 1:5 ratio of C_3/C_1 isomers.

Scheme 5.9. The synthesis of ligand **76**.

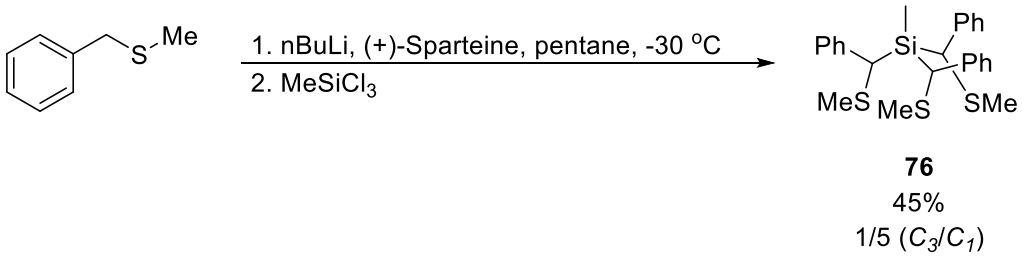

The crude mixture of C_3 and C_1 isomers was recrystallized in hot pentane. The first recrystallization gave totally pure C_1 isomer. Next, recrystallization of residue gave pure C_3

isomer. The pure C_3 was analyzed by HPLC and unfortunately only 10% ee of the product was observed. Extensive screening of reaction parameters did not give improved results.

Scheme 5.10. Synthesis of rhodium complex based ligand **76**.

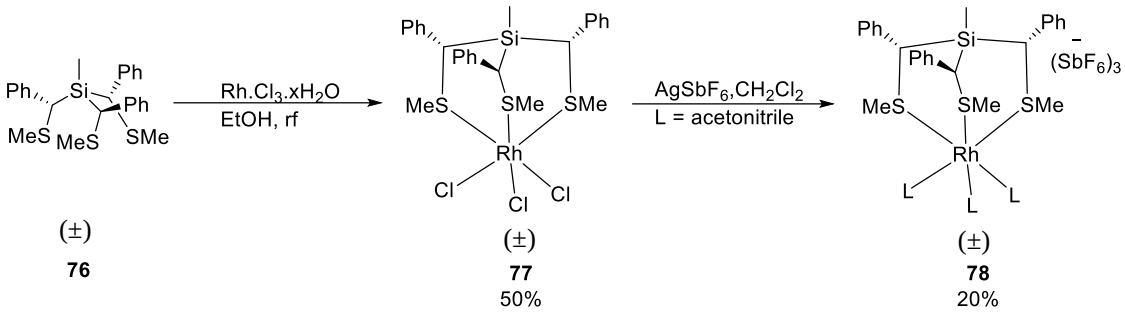

In terms of making complexes, refluxing the mixture of C_1-symmertic ligand **76** and rhodium (III) salt in ethanol (**Scheme 5.10**) gave C_1-symmetric rhodium complex **77** in 50% yield. In addition, **78** was also prepared by using silver hexafluoroantimonate in presence of CH_3CN, giving complex **78** in 20% yield. Then, complex **77** was used to investigate hydrogen/deuterium exchange experiment (**Scheme 5.11**). A 60% deuterium incorporation was observed, showing that complex **77** can activate C – H bonds.

Scheme 5.11. Hydrogen/deuterium exchange experiment of complex **77**.

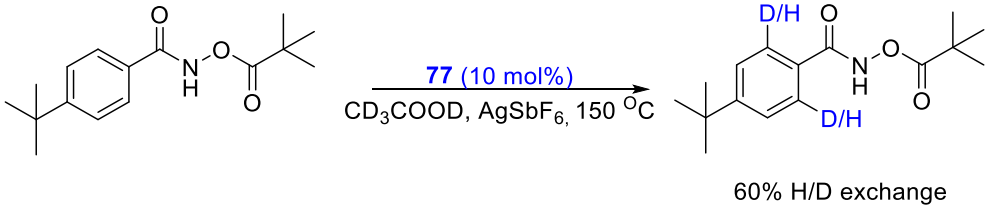

Other transition metals were used to prepare complexes with C_1-symmetric ligand **76** (**Scheme 5.12**). Heating ligand **76** with dichlorotetrakis(dimethylsulfoxide)-ruthenium(II), complex **79** was obtained in 50% yield. Alternatively, stirring ligand **76** with

tetrakis(acetonitrile)-copper(I) hexafluorophosphate in THF at room temperature, gave copper (I) complex **80** in 32% yield. In terms of activity, ruthenium (II) complex was used in nitrene insertion reaction between adamantane and tosyl azide in the presence of silver hexafluoroantimonate. A 16% yield of amination product at tertiary position on adamantane was produced. For copper (I) complex, a carbene insertion reaction was chosen to test reactivity (**Scheme 5.13**). The insertion of ethyl diazoacetate (EDA) in THF with 1 mol% of **80** gave **82** in 50% yield. Additionally, the catalyst also worked well with adamantane and diethyl ether but low yield was observed. With 1,4-dioxane, insert product was not observed.

Scheme 5.12. Synthesis of ruthenium (II) complex (**A**) and copper (I) complex (**B**).

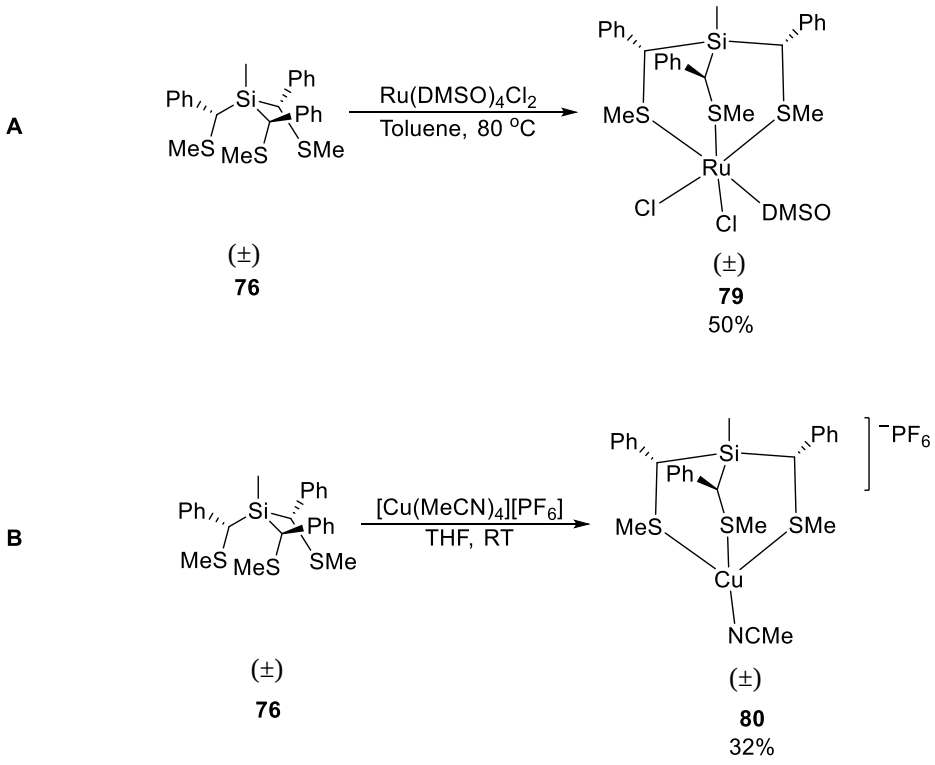

Scheme 5.13. Copper (I) complex **80** catalyzed C-H bond insertion reaction.

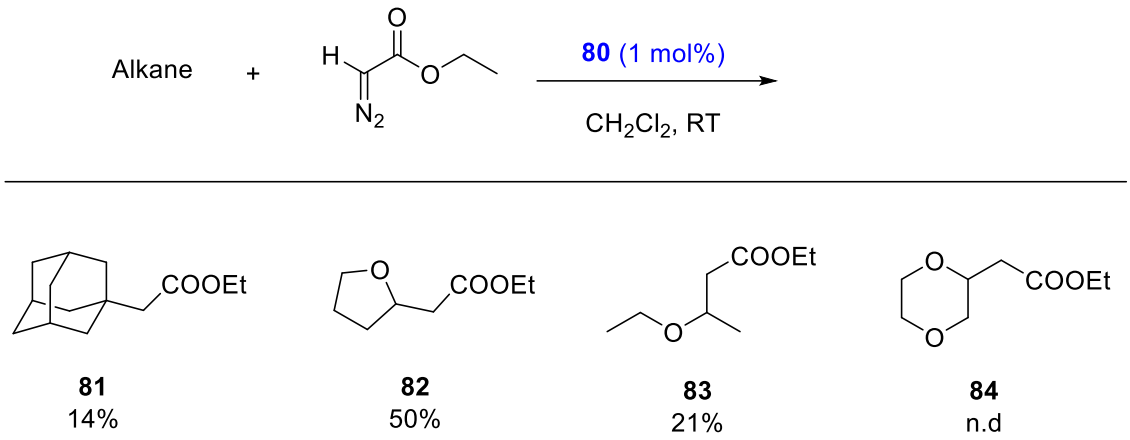

In summary, we successfully synthesized C_3-symmetric tridentate sulfur containing ligand and their complexes with some transition metals also showed promising results in C – H bond functionalization reactions. However, the ligand is formed with low enantioselectivity. More explorations to improve enantioselectivity of reaction is essential.

5.1.3.3 Chiral Centers Attached to End Groups.

There are two possible pathways to attach chiral moieties at end groups. 1,1,1-Tris(hydroxymethyl)ethane derivatives may react with a chiral thiol. Alternatively, treating 1,1,1-tris(sulfanylmethyl)ethane (trithiol) with chiral alcohol derivatives may afford the same product. The synthesis using trithiol is described in **Scheme 5.14**.

Scheme 5.14. Synthesis of chiral sulfur containing ligand **90**.

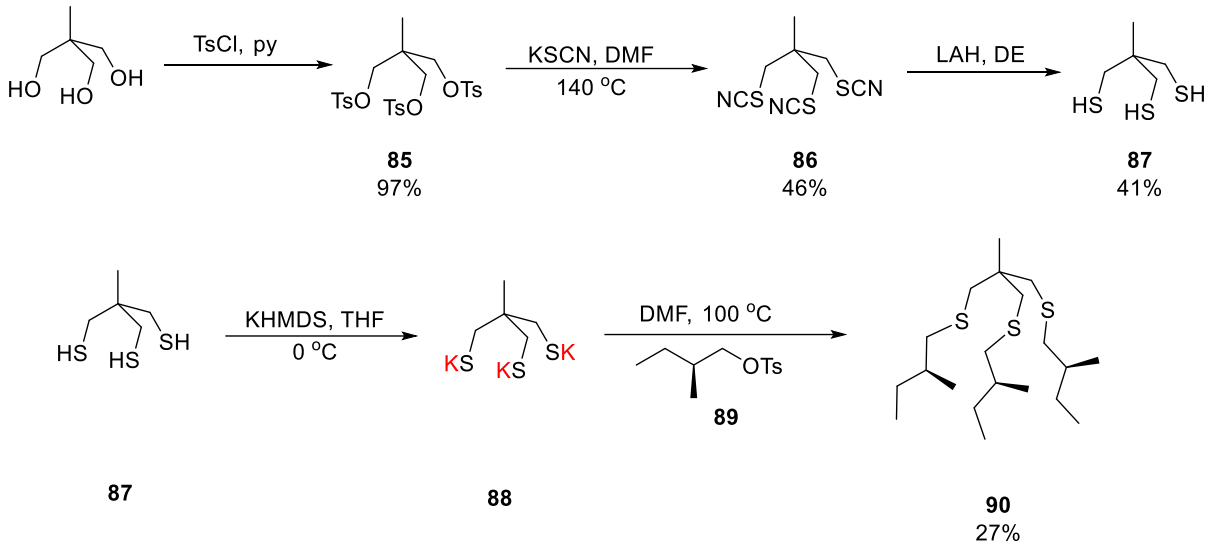

The procedure commences with protection of 1,1,1-tris(hydroxymethyl)ethane using tosyl chloride in pyridine at room temperature, giving compound **85** in quantitative yield. The nucleophilic substitution reaction between **85** and potassium thiocyanide in DMF produced **86** in 46% yield. Reduction with lithium aluminum hydride gave tri-thiol **87** in 41% yield. Compound **87** is not bench-stable and two thiol groups rapidly form disulfide when exposed to air. Although pKa of alkyl thiols are 10-11, the Mitsunobu reaction between tri-thiol **87** and (S)-butan-2-ol did not occur even at high temperature and by using different diazo compounds. Tri-thiol **87** was deprotonated using potassium bis(trimethylsilyl)amide (KHMDS) to form thiolate **88**. After that, nucleophilic substitution reaction of thiolate **88** and protected chiral alcohol **89** occurred in DMF at 100 °C to give ligand **90** in 27% yield. This approach may work with secondary alcohols, yet chirality on alcohol may be scrambled during synthesis. Another approach was used starting from triol and chiral thiolate (**Scheme 5.15**).

Scheme 5.15. Synthesis of ligand **92**.

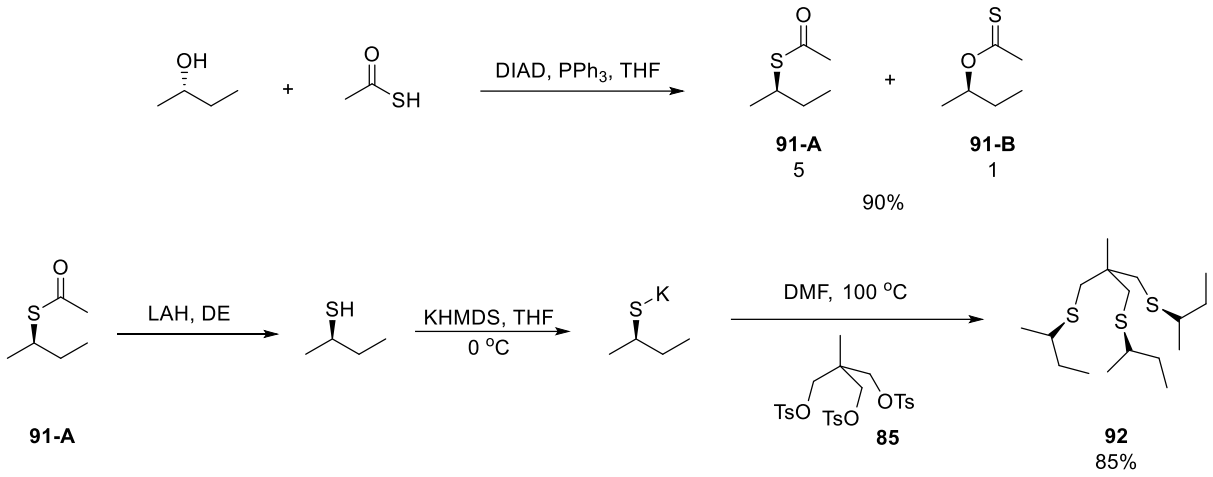

(S)-2-Butanol was treated with thioacetate using DIAD and triphenylphosphine in THF to give a mixture of isomers **91-A** and **91-B** in 90% yield with a ratio of 5:1. The mixture was then reduced with lithium aluminum hydride to produce (R)-butane-2-thiol, followed by deprotonation using KHMDS to give potassium (R)-butane-2-thiolate. The last step is nucleophilic substitution between **85** and potassium (R)-butane-2-thiolate in DMF, producing chiral ligand **92** in 85% yield on last step. The ligand was then used to make complexes with rhodium (III) and copper (I). Although resulted complexes were soluble in most common solvents, their NMR spectra are quite complicated. Mixture of diastereoisomers at sulfur formed during complexation may be a likely explanation.

In summary, two types of chiral ligands were successfully synthesized. However, the characterization of their metal complexes are difficult. Thus, more work need to be done to have better explanation for results and prepare new catalyst.

5.1.4. Experiment Section

General

Reactions were performed using standard glassware or were run in 2-dram vials with PTFE/Liner screw caps and 8-dram vials using w/polyseal screw caps. Column chromatography was performed on 60Å silica gel (Dynamic Adsorbents Inc.). ^{1}H, ^{13}C-NMR spectra were recorded on JEOL EC-400, JEOL EC-500, JEOL EC-600 spectrometers. Analytical thin layer chromatography was performed on silica gel IB-F (Baker-flex) by J. T. Baker. All procedures were performed under nitrogen unless otherwise noted. Reagents and starting materials were obtained from commercial sources and used without further purification unless otherwise noted.

Substrate synthesis

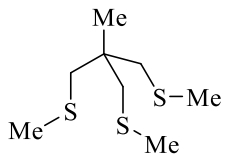

Ligand 49.

To a flame-dried Schlenk flask (250 mL) equipped with a magnetic stir bar was added 1,1,1-tris(chloromethyl)ethane (1.38 mL, 10 mmol), sodium thiomethoxide (4.2 g, 60 mmol), and sodium iodide (1.5 g, 10 mmol). The flask was refilled with nitrogen and then DMF (100 mL) was added. The mixture was placed in an oil bath preheated to 100 °C for 24 h. The crude mixture was diluted with ethyl acetate (200 mL), washed with NaOH/H_2O (3 x 300 mL, 1/1), combined organic phase was dried over $MgSO_4$, filtered, and concentrated, yielding 21.5 g of a colorless oil (98%). This compound is known.[194]

^{1}H NMR (400 MHz, $CDCl_3$) δ 2.65 (s, 6H), 2.14 (s, 9H), 1.10 (s, 3H). $^{13}C\{^{1}H\}$ NMR (400 MHz, $CDCl_3$) δ 44.4, 41.4, 23.9, 17.9.

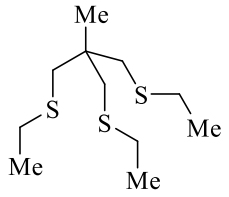

Ligand 50.

To a flame-dried Schlenk flask (250 mL) equipped with a magnetic stir bar was added 1,1,1-tris(chloromethyl)ethane (1.38 mL, 10 mmol), sodium ethanethiolate (5.1 g, 60 mmol), and sodium iodide (1.5 g, 10 mmol). The flask was refilled with nitrogen and then DMF (100 mL) was added. The mixture was placed in an oil bath preheated to 100 °C for 24 h. The crude mixture was diluted with ethyl acetate (200 mL), washed with $NaOH/H_2O$ (3 x 300 mL, 1/1), combined organic phase was dried over $MgSO_4$, filtered, and concentrated, yielding 23.7 g of a light yellow oil (94%). This compound is known.[197]

^{1}H NMR (600 MHz, $CDCl_3$) δ 2.65 (s, 6H), 2.54 (q, *J* = 7.8 Hz, 6H), 1.24 (t, *J* = 7.8 Hz, 9H), 1.10 (s, 3H). $^{13}C\{^{1}H\}$ NMR (600 MHz, $CDCl_3$) δ 40.1, 39.7, 36.6, 36.5, 23.8.

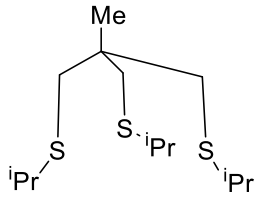

Ligand 51.

To a flame-dried Schlenk flask (250 mL) equipped with a magnetic stir bar was added 1,1,1-tris(chloromethyl)ethane (1.38 mL, 10 mmol), sodium 2-propanethiolate (5.9 g, 60 mmol), and sodium iodide (1.5 g, 10 mmol). The flask was refilled with nitrogen and then DMF (100 mL) was added. The mixture was placed in an oil bath preheated to 100 °C for 24 h. The crude mixture was diluted with ethyl acetate (200 mL), washed with $NaOH/H_2O$ (3 x 300 mL, 1/1), combined organic phase was dried over $MgSO_4$, filtered, and concentrated, yielding 26.5 g of a red oil (90%).

^1H NMR (600 MHz, $CDCl_3$) δ 2.87 – 2.80 (m, 3H), 2.59 (s, 6H), 1.20 (d, J = 6.6 Hz, 18H), 1.10 (s, 3H). $^{13}C\{^1H\}$ NMR (600 MHz, $CDCl_3$) δ 41.5, 40.4, 28.1, 23.9, 15.2.

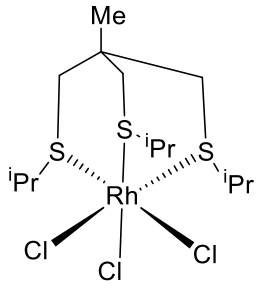

Rhodium (III) complex 53.

To a round bottom flask equipped with magnetic stir bar and reflux condenser was added compound **51** (0.29 g, 1.0 mmol), $RhCl_3.xH_2O$ (0.20 g, 0.95 mmol), and methanol (10 mL).

The flask was then placed in oil bath preheated at 90 °C overnight. After cooling to room temperature, the mixture was filtered through Buchner funnel size F. The solid was then washed with diethyl ether (3 x 30 mL) and dried under vacuum yielding 0.32 g of a dark yellow solid (70 %)

^{1}H NMR (600 MHz, CD_2Cl_2) δ 3.91 – 3.84 (m, 3H), 2.70 (d, *J* = 12.0 Hz, 3H), 2.30 (d, *J* = 12.0 Hz, 3H), 1.50 (d, *J* = 6.8 Hz, 18H), 1.33 (s, 3H). ^{13}C{^{1}H} NMR (400 MHz, CD_2Cl_2) δ 40.9, 35.6, 32.6, 22.5, 20.0.

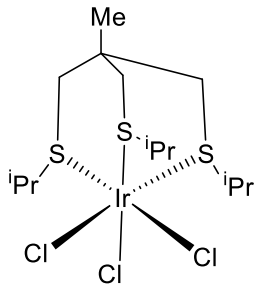

Iridium (III) complex 57.

To a round bottom flask equipped with magnetic stir bar and reflux condenser was added compound **51** (0.29 g, 1.0 mmol), $IrCl_3.xH_2O$ (0.33 g, 0.95 mmol), and methanol (10 mL). The flask was then placed in oil bath preheated at 90 °C overnight. After cooling to room temperature, the mixture was filtered through Buchner funnel size F. The solid was then washed with diethyl ether (3 x 30 mL) and dried under vacuum yielding 0.37 g of a dark yellow solid (65 %).

^{1}H NMR (400 MHz, CD_2Cl_2) δ 3.85 – 3.75 (m, 3H), 2.82 (d, *J* = 12.0 Hz, 3H), 2.28 (d, *J* = 12.0 Hz, 3H), 1.52 – 1.46 (m, 11H), 1.40 (d, J = 6.8 Hz, 7H), 1.30 (s, 3H).

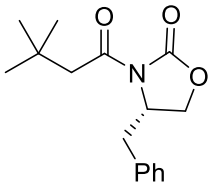

Compound 63.

In a flame-dried Schlenk flask (250 mL) equipped with a magnetic stir bar, (S)-4-benzyloxazolidin-2-one (2.48 g, 14 mmol) was dissolved in anhydrous THF (140 mL) and the mixture was cooled to -78 °C using EtOAc/N_2 bath. Then nBuLi (1.6 M in hexane, 10.5 mL, 16.8 mmol) was added in 5 minutes and reaction was kept at -78 °C for 1 hour. Subsequently, 3,3-dimethylbutanoyl chloride (2.14 mL, 14.4 mmol) was added to the mixture in 10 minutes. The solution was slowly warmed up to room temperature and kept stirring overnight. After that, silica was added and solvent was removed by rotovap. The product was purified using column chromatography with hexane/ethyl acetate (5/1), R_f = 0.5 (SiO2, Hexane/EtOAc = 5/1). Yield 2.93 g (76%) of white solid. This compound is known.[195]

^{1}H NMR (600 MHz, $CDCl_3$) δ 7.34 – 7.21 (m, 5H), 4.68 – 4.65 (m, 1H), 4.14 – 4.13 (m, 2H), 3.50 (d, *J* = 10.2 Hz, 1H), 2.99 (d, *J* = 15 Hz, 1H), 2.85 (d, *J* = 15 Hz, 1H), 2.70 (d, *J* = 10.2 Hz, 1H), 1.08 (s, 9H).

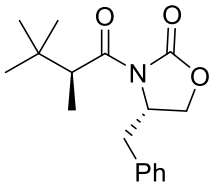

Compound 64.

In a flame-dried Schlenk flask (250 mL) equipped with a magnetic stir bar, di-*iso*-propyl amine (1.83 mL, 13 mmol) was dissolved in anhydrous THF (100 mL) and the mixture was cooled to -78 °C using EtOAc/N_2 bath. Then nBuLi (1.6 M in hexane, 7.5 mL, 12 mmol) was added in 5 minutes and reaction was warmed up to room temperature in 1 hour then cooled down to -78 °C again. To the mixture, a solution of compound **63** (2.75 g, 10 mmol) in THF (20 mL) was added dropwise in 10 minutes and mixture was stirred at -78 °C for another 1 hour. After that, methyl iodide (2.49 mL, 40 mmol) was added to the mixture in 5 minutes. Then the mixture was slowly warmed up and stirred overnight. After one night, silica was added and solvent was removed by rotovap. The product was purified using column chromatography with hexane/ethyl acetate (6/1), R_f = 0.46 (SiO_2, Hexane/EtOAc = 6/1). Yield 2.57 g (89%) of white solid. This compound is known.[195]

^{1}H NMR (400 MHz, $CDCl_3$) δ 7.41 – 7.22 (m, 5H), 4.68 – 4.65 (m, 1H), 4.14 – 4.13 (m, 2H), 3.90 – 3.85 (m, 1H), 3.27 (d, *J* = 13.2 Hz, 1H), 2.77 – 2.59 (m, 1H), 1.17 (d, *J* = 7.2 Hz, 3H), 1.06 (s, 9H).

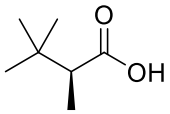

Chiral acid 65.

To the round bottom flask (250 mL) equipped with magnetic stir bar was added lithium hydroxide (0.74 g, 31 mmol), THF (50 mL), and H_2O (15 mL). The mixture was stirred until clear solution was obtained and then cooled to 0 °C using ice bath. To the mixture, a solution of **64** (2.54 g, 8.8 mmol) in 50 mL THF was added in one portion. The mixture was stirred for 5 minutes. After that, hydrogen peroxide on a 30% aqueous solution (4.0 g, 22 mmol) was added to the mixture, ice bath was removed, and the flask was stirred over night at room temperature. The mixture was extracted with CH_2Cl_2 (50 mL). The organic phase was discarded while HCl (conc. 5 mL) was added, followed by extraction with CH_2Cl_2 (3 x 50 mL). The combined organic phase was dried over $MgSO_4$, then filtered and concentrated to give pure chiral acid **63**. Yield 0.95 g (83%) of a colorless oil. This compound is known.[195]

^{1}H NMR (400 MHz, $CDCl_3$) δ 2.28 – 2.21 (m, 1H), 1.11 (d, *J* = 7.2 Hz, 3H), 0.97 (s, 9H).

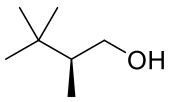

Chiral alcohol 66.

In the flame-dried Schlenk flask (250 mL) equipped with magnetic stir bar was added lithium aluminum hydride (0.67 g, 17.6 mmol), and anhydrous diethyl ether (100 mL). The flask was cooled to 0 °C using ice bath, then acid **65** (0.95 g, 7.3 mmol) was added dropwise in 10 minutes. The mixture was slowly warmed up to room temperature and stirred overnight.

After that, the mixture was cooled to 0 °C using ice bath and ice water was added in small portions until no bubbles were released. The ice bath was removed and mixture was extracted with HCl 1 M (30 mL) and then NaCl aq. (3 x 30 mL). The organic layer was dried over $MgSO_4$, filtered and solvent was removed, giving compound **66**. Yield 0.59 g (70%) of colorless oil. This compound is known.[195]

^{1}H NMR (400 MHz, $CDCl_3$) δ = 0.88 (s, 9H), 0.94 (d, J = 7.0 Hz, 3H), 1.37 − 1.45 (m, 1H), 3.28−3.38 (m, 1H), 3.82 (dd, J = 10.5, 4.0 Hz, 1H).

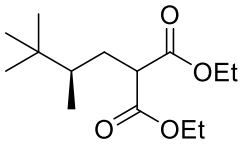

Compound 69.

In a flame-dried Schlenk flask (50 mL) equipped with magnetic stir bar was placed diazo compound **70** (2.1 g, 8.4 mmol) and toluene (20 mL). The mixture was stirred for 5 minutes then tri-butyl phosphine (2.1 mL, 8.4 mmol) was added dropwise in 5 minutes and mixture was stirred for additional 10 minutes. After that, chiral alcohol **66** (0.81 g, 7.0 mmol) and diethyl malonate (1.62 mL, 8.4 mmol) were added to the mixture. Subsequently, the flask was placed in preheated oil bath at 80 °C and stirred overnight. The oil bath was removed and the flask was cooled to room temperature before silica was added. Solvent was removed by rotovap and product was purified using column chromatography with hexane/EtOAc (10/1), R_f = 0.7 (SiO2, hexane/EtOAc = 10/1). Yield 0.55 g (17%) of a yellow oil.

^{1}H NMR (400 MHz, $CDCl_3$) δ 4.21 – 4.14 (m, 4H), δ 3.43 – 3.84 (m, 1H), δ 1.97 – 1.89 (m, 1H), δ 1.69 – 1.59 (m, 1H), δ 1.40 – 1.29 (m, 2H), δ 1.29 – 1.20 (m, 6H), δ 1.19 – 1.10 (m, 1H),

δ 0.9 – 0.8 (m, 6H). $^{13}C\{^{1}H\}$ NMR (400 MHz, $CDCl_3$) 170.0 169.8, 61.3, 50.2, 35.5, 32.5, 29.3, 18.8, 14.2, 11.2.

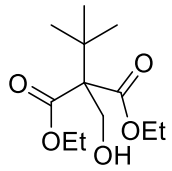

Compound 60.

A 20 dram vial equipped with magnetic stir bar, was charged diethyl *tert* butyl malonate (0.43 g, 1.99 mmol), paraformaldehyde (0.37 g, 12.3 mmol), potassium carbonate (72 mg, 0.52 mmol), benzyltrimethylammonium chloride (5 mg, 1.5 mol%), and DMSO (3 mL). The vial was sealed and placed in a preheated oil bath at 80 °C and stirred overnight. After indicated time, the vial was cooled to room temperature and mixture was diluted with EtOAc (30 mL). The mixture was then extracted with NaCl aq (3 x 20 mL) and the combined organic layer was dried over $MgSO_4$, filtered and concentrated. Product was purified using column chromatography with hexane/EtOAc (9/1) then EtOAc/MeOH (4/1), R_f = 0.8 (SiO2, EtOAc/MeOH = 4/1). Yield 0.16 g (32%) of a colorless oil.

^{1}H NMR (400 MHz, $CDCl_3$) δ 4.27 – 4.21 (m, 4H), 4.10 (d, *J* = 7.6H, 2H), 3.01 (t, J = 7.6 Hz, 1H), δ 1.31 – 1.20 (m, 6H), δ 1.11 (s, 9H). $^{13}C\{^{1}H\}$ NMR (400 MHz, $CDCl_3$) δ 171.5, 66.4, 64.6, 61.3, 35.7, 27.5, 14.1.

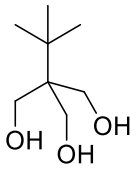

Compound 61.

A flame-dried Schlenk flask (50 mL) equipped with magnetic stir bar was charged lithium aluminum hydride (73 mg, 1.92 mmol) and anhydrous diethyl ether (10 mL). The flask was cooled to 0 °C using ice bath, then a solution of **72** (0.16 g, 0.64 mmol) in diethyl ether (5 mL) was added dropwise in 10 minutes. The flask was then connected to a condenser and ice bath was replaced by an oil bath. The system was refluxed under nitrogen atmosphere for 36 hours. After that, the mixture was cooled to 0 °C using ice bath and ice water was added in small portions until no bubbles were released. The ice bath was removed and mixture was extracted with HCl 1 M (30 mL) then NaCl aq. (3 x 30 mL). The organic layer was dried over $MgSO_4$, filtered and solvent was removed, giving compound **61**. Yield 47 mg (46%) of a white solid.

^{1}H NMR (400 MHz, $CDCl_3$) δ 3.86 (s, 6H), 3.44 (s, 3H), 0.89 (s, 9H).

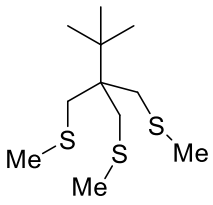

Compound 62.

To the round bottom flask (50 mL) equipped with a magnetic stir bar was added with **61** (66 mg, 0.4 mmol) and CH_2Cl_2 (10 mL). The flask was cooled to 0 °C using ice bath. To the

mixture, pyridine (0.16 mL, 1.4 mmol) and trifluoromethanesulfonic anhydride (0.34 mL, 1.4 mmol) were added. The mixture was slowly warmed up to room temperature and stirred overnight. After indicated time, the mixture was diluted with CH_2Cl_2 (20 mL) and washed with NaCl aq (3 x 40 mL) then dried over $MgSO_4$, filtered and concentrated. The product was used for next step without further purification.

To a flame-dried Schlenk flask (50 mL) equipped with a magnetic stir bar was added intermediate from procedure above, sodium methylthiolate (0.17 g, 2.4 mmol), and sodium iodide (0.6 g, 0.4 mmol). The flask was refilled with nitrogen and then DMF (10 mL) was added. The mixture was placed in an oil bath preheated to 100 °C for 24 h. The crude mixture was diluted with ethyl acetate (20 mL), washed with $NaOH/H_2O$ (3 x 30 mL, 1/1), combined organic phase was dried over $MgSO_4$, filtered, and concentrated, yielding 0.91 g of a colorless oil (90%).

^1H NMR (500 MHz, $CDCl_3$) δ 3.40 (s, 9H), 2.08 (s, 6H), 1.65 (s, 9H). $^{13}C\{^1H\}$ NMR (500 MHz, $CDCl_3$), δ 34.2, 39.0, 26.6, 26.0, 15.6.

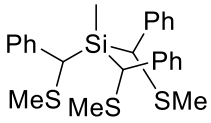

Compound 76.

A flame-dried Schlenk flask (100 mL) equipped with stir bar was charged with (+)-sparteine (0.91 mL, 4.0 mmol), pentane (20 mL), and benzyl methyl sulfide (0.55 g, 4.0 mmol). The flask was then cooled down to -30 °C using $MeOH/H_2O$ (3/2) and dry ice. To the mixture, nBuLi (2.5M in hexane, 1.60 mL, 4.0 mmol) was added dropwise in 10 minutes and the solution

was stirred at -30 °C. After indicated time, a solution of methyltrichlorosilane (0.13 mL, 1.1 mmol) in pentane (2 mL) was added dropwise in 5 minutes. Subsequently, the flask was slowly warmed up to room temperature and stirred overnight. The mixture was diluted with diethyl ether (20 mL) and washed with HCl 1M (15 mL) followed by H_2O (2 x 20 mL). After drying over $MgSO_4$, the solvent was removed to obtain white solid isomer mixture. Yield 0.69 g (45%) of a white solid.

Isomer mixture was then dissolved in minimal amount of hot pentane and cooled to room temperature before keeping in the fridge overnight. After indicated time, white crystals were filtered and washed with cool pentane (3 x 10 mL). Yield 0.35 g (23%) of white crystals (*C_1* isomer). The combined organic solution was concentrated and residue was recrystallized from pentane. Yield 0.15 g (10%) of white crystals (*C_3* isomer).

***C_1* isomer**.

^{1}H NMR (400 MHz, $CDCl_3$) δ 7.36 – 7.08 (m, 15H), 3.54 (s, 1H), 3.33 (s, 1H), 2.92 (s, 1H), 1.96 (s, 3H), 1.87 (s, 3H), 1.75 (s, 3H), -0.11 (s, 3H).

***C_3* isomer**.

^{1}H NMR (400 MHz, $CDCl_3$) δ 7.17 – 7.08 (m, 9H), 7.21 – 6.50 (m, 6H), 3.55 (s, 3H), 1.98 (s, 9H), -0.16 (s, 3H).

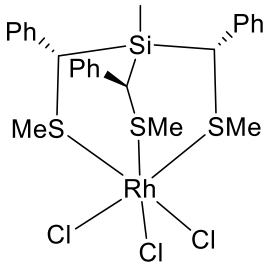

Rhodium (III) complex 77.

A round bottom flask (100 mL) equipped with magnetic stir bar was charged with *C*$_1$-symmetric **76** (69 mg, 97 μmol), $RhCl_3.xH_2O$ (25.6 mg, 97 μmol), and ethanol (20 mL). The flask was connected with a condenser and placed in preheated oil bath to reflux under ambient atmosphere overnight. The oil bath and condenser were removed and the flask was cooled to room temperature. The mixture was filtered and solid was washed with pentane (3 x 20 mL) and dried under vacuum. Yield 32 mg (50%) of a yellow solid.

^{1}H NMR (600 MHz, $CDCl_3$) δ 7.48 – 7.34 (m, 10H), 7.11 – 7.08 (m, 1H), 6.99 – 6.97 (m, 2H), 6.29 – 6.25 (m, 2H), 3.95 – 3.86 (m, 3H), 2.64 (s, 3H), 2.45 (s, 3H), 2.33 (s, 3H), -0.45 (s, 3H).

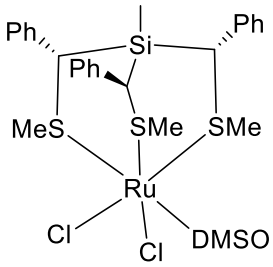

Ruthenium (II) complex 79.

A 10 dram vial equipped with a magnetic stir bar war charged with $Ru(DMSO)_4Cl_2$ (36.3 mg, 75 μmol), *C*$_1$-symmetric **76** (34 mg, 75 μmol), and toluene (5 mL). The vial was sealed and placed in oil bath preheated at 80 °C for two days. After indicated time, the solution

was filtered and solid was washed with pentane (3 x 20 mL) then dried under vacuum for 1 day. Yield 26 mg (50%) of a dark-yellow solid.

^{1}H NMR (400 MHz, $CDCl_3$) δ 7.47 – 7.36 (m, 8H), 7.33 – 7.27 (m, 2H), 7.04 – 6.92 (m, 3H), 6.57 – 6.51 (m, 2H), 4.06 (s, 1H), 3.52 – 3.49 (m, 4H), 3.42 (s, 3H), 3.37 (s, 1H), 2.75 (s, 3H), 2.50 (s, 3H), 2.29 (s, 3H), -0.64 (s, 3H).

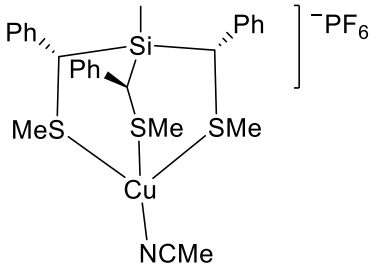

C**opper (I) complex 80**.

A flame-dried Schlenk flask (50 mL) equipped with magnetic stir bar was charged with $[Cu(NCMe)_3][PF_6]$ (0.25 g, 0.67 mmol) and dry THF (10 mL). The mixture was stirred for 10 minutes. To the mixture, a solution of *C*$_1$-symmetric **76** (0.31 g, 0.67 mmol) in 5 mL of dry THF was added. The flask was stirred at room temperature overnight. After indicated time, the solvent was removed under vacuum. Dry diethyl ether (20 mL) was added and mixture was filtered under vacuum. White solid was washed with pentane (3 x 20mL) then dried under vacuum and kept in glovebox. Yield 0.15 g (32%) of a white solid.

^{1}H NMR (400 MHz, $CDCl_3$) δ 7.38 – 7.21 (m, 10H), 7.10 – 6.95 (m, 3H), 6.66 – 6.65 (m, 2H), 3.67 (s, 1H), 3.53 (s, 1H), 2.73 (s, 1H), 2.16 (s, 3H), 1.95 – 1.92 (m, 6H), 1.62 (s, 3H), -0.01 (s, 3H).

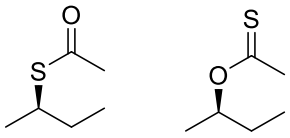

Compound 91.

A flame-dried Schlenk flask (100 mL) equipped with magnetic stir bar was charged with triphenyl phosphine (2.65 g, 10.1 mmol), DAID (2.05 mL, 10.1 mmol), and THF (50 ml). The flask was cooled to 0 °C using ice bath and stirred for 30 minutes. To the mixture, a solution of (S)-2-butanol (0.61 mL, 6.7 mmol) and thioacetic acid (0.72 mL, 10.1 mmol) in 5 mL of THF was added. The ice bath was removed and the flask was stirred at room temperature overnight. After that, the mixture was diluted with diethyl ether (50 mL) then washed with water (3 x 30 mL) and dried over $MgSO_4$, filtered and concentrated. The product was purified using column chromatography with hexane/EtOAc (10%), R_f = 0.45 (SiO_2, hexane/EtOAc = 10%). Yield 0.80 g (90%) of colorless oil as a mixture of two isomer (dr = 5/1). This compound is known.[198]

^{1}H NMR (600 MHz, $CDCl_3$) δ 3.48 (s, 3H), 2.29 (s, 3H), 1.57 – 1.55 (m, 2H), 1.26 (s, 3H), 0.93 – 0.86 (m, 3H). (major product)

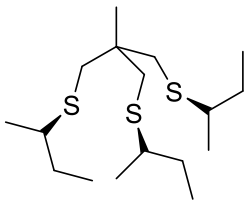

Compound 92.

A flame-dried Schlenk flask (50 mL) equipped with magnetic stir bar was charged with lithium aluminum hydride (0.38 g, 22.4 mmol) and diethyl ether (10 mL). The flask was cooled to 0 °C then a solution of **91** (0.88 g, 6.7 mmol) in 10 mL of diethyl ether was slowly added. The flask was stirred at room temperature overnight. After that, it was cooled to 0 °C then HCl 1M (10 mL) was added dropwise to the mixture. Organic layer was transferred to another Schlenk flask and kept under nitrogen atmosphere.

To a flame-dried Schlenk flask (50 mL) equipped with magnetic stir bar was added KHMDS (1.0 g, 5.0 mmol) and THF (20 mL). The mixture was cooled to 0 °C using ice bath. To the mixture, a solution of chiral thiol in diethyl ether from above transformation was added via cannula. Precipitate was formed after addition and the mixture was stirred at room temperature overnight. After that, solvent was removed under reduced vacuum to dryness. To the solid, solution of **85** (0.29 g, 0.5 mmol) in 15 mL of DMF was added. The flask was then placed in oil bath and heated at 100 °C overnight under nitrogen atmosphere. Subsequently, the mixture was cooled to room temperature, diluted with diethyl ether (40 mL), and washed with aqueous NaOH 1N (20 mL), then NaCl aq. (2 x 30 mL). The organic layer was dried over $MgSO_4$, filtered and concentrated. The product was purified using column chromatography with hexane/EtOAc (5%), R_f = 0.6 (SiO_2, hexane/EtOAc = 10/1). Yield 0.14 g (85%) of a yellow oil.

^{1}H NMR (400 MHz, $CDCl_3$) δ 2.73 – 2.62 (m, 9H), 1.68 – 1.45 (m, 6H), 1.24 (d, *J* = 7.6 Hz, 9H), 1.08 (s, 3H), 0.96 (t, *J* = 7.6 Hz, 9H).

5.2. Chiral 1,3-Dikentone Cobalt Complexes in Asymmetric Synthesis of Isoquinolones Derivatives.

5.2.1. Introduction

The C – C bond formation is a powerful tool in organic synthesis and has gained significant attention.[199] Early development in this field generally focused on the use of organometallic compounds[200] or metathesis and cross-coupling reactions.[201] However, these methodologies generate stoichiometric amount of waste. Additionally, difficulty in handling of many organometallic compounds and atom economy issues present obvious problems. To this end, well-established C – H bond functionalization strategies may provide more efficient methods for construction of C – C bonds, minimizing the amount of byproducts and decreasing number of synthetic steps to product.

In 2005, our group introduced bidentate directing groups (DGs). Two new bidentate directing moieties, quinolinamide and picolinamide, were explored for palladium-catalyzed arylation of *ortho*-C(sp^2) – H and C(sp^3) – H bonds.[202] Many other bidentate DGs have also been successfully used for C – C bond construction subsequently.[203-206]

Aliphatic C – H bonds are the most abundant bonds in nature. Due to high bond energy dissociation, low acidity, and weak coordination to transition metal centers, their reactivities are generally low. Among them, palladium (II) – catalyzed intermolecular C(sp^3) – H functionalization reactions with assistance of monodentate or bidentate directing groups are most widely used.

In terms of reactivity, it is generally agreed that bidentate DGs possess higher C – H functionalization reactivity relative to monodentate DGs.[204,206] However, metal complexes

ligated by bidentate DGs contain only one vacant coordination site, often preventing the participation of ligand in catalytic cycle. Most enantioselective transformations using transition metals require assistance of chiral ligands. Consequently, use of bidentate DGs in asymmetric synthesis has been rare. The only success in this field was the use of chiral BINOL-based phosphoric acid for palladium (II) catalyzed enantioselective arylation of a C(sp^3) – H bond.[207-209]

In 2014, our group developed a method for cobalt-catalyzed aminoqunioline-directed reaction of C(sp^2) – H bonds with alkenes (**Scheme 5.16**).[210] The reaction works well at room temperature and tolerates a broad substrate range including aliphatic alkenes and styrenes. Additionally, Dr. Grigorjeva found that bulky 1,3-diketone was chelated to cobalt in catalytic cycle while acetylacetone ligand was dissociated (**Scheme 5.16**). This result suggests that chiral center on a bulky 1,3-diketone ligand may give rise to enantioselective reaction. This is main purpose for the work described this section.

Scheme 5.16. The plausible mechanism of cobalt-catalyzed C(sp^2) – H bond functionalization.

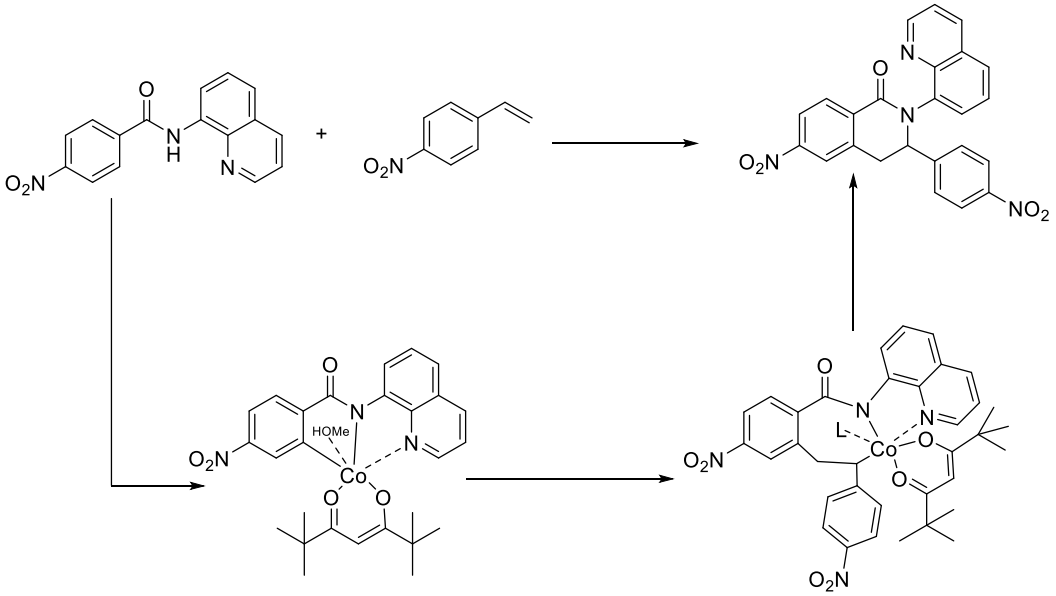

5.2.2. Results and Discussion

5.2.2.1. Chiral 1,3-Diketone Ligand and Cobalt Complex Synthesis

Scheme 5.17. Synthesis of chiral 1,3-diketone derivatives.

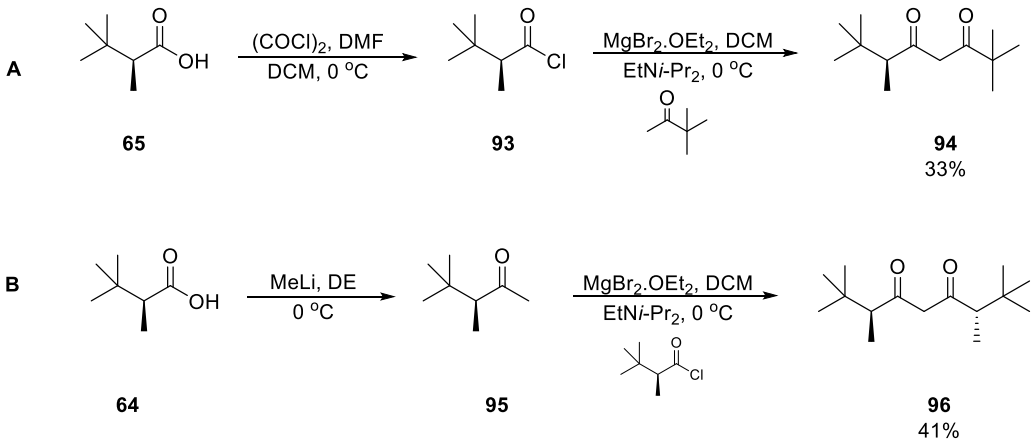

Chiral acid **65** was prepared as described in section **5.1.3.1**. **Scheme 5.17** illustrates the synthesis of chiral 1,3-diketones **94** and **96**. Specifically, chiral acid chloride **93** was obtained by treating (S)-2,3,3-trimethylbutanoic acid **64** with oxalyl chloride and catalytic amount of DMF in CH_2Cl_2. The preparation of 1,3-diketone followed precedent in literature.[211] Thus, soft enolization conditions afforded chiral 1,3-diketone **94** from chiral acid chloride **93** and pinacolone in 33% yield. The advantage of this method is that it proceeds at low temperature which suppresses racemization. Next, chiral ketone **95** was synthesized from **65** using methyl lithium affording chiral symmetric 1,3-diketone **96**. Using same enolization conditions, compound **96** was produced in 41% yield. Subsequently, substrates **94** and **96** were deprotonated using sodium hydroxide, followed by coordination to cobalt to give corresponding complexes **97** and **98** in 82% and 63% yields, respectively (**Scheme 5.18**).

Scheme 5.18. Synthesis of chiral cobalt complexes.

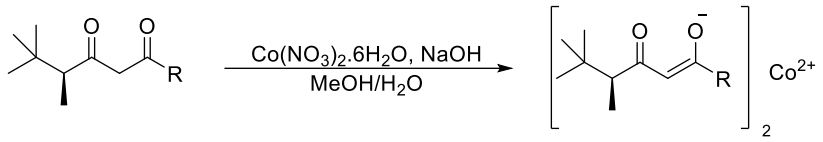

94, R = ^{t}Bu
96, R = 2,2-dimethyl-*sec*-butyl

97, R = ^{t}Bu 82%
98, R = 2,2-dimethyl-*sec*-butyl 63%

These compounds were tested in C – H functionalization, leading to the synthesis of isoquinolone derivatives.[210] The preliminarily results (**Table 5.1**) show that in terms of alkene insertion reaction between **99** and styrene, the combination of cobalt salt and ligand **94** or **96** was inefficient, providing low yield and ee of product **100**. Interestingly, when using complex **98** as catalyst, the enantiomeric excess of **100** was increased significantly up to 41% while the yield was still low at 10%. Although, the results are not get acceptable, they show that bulky diketone ligand influences reaction enantioselectivity. Thus, further investigation was clearly warranted.

Table 5.1. Preliminary results

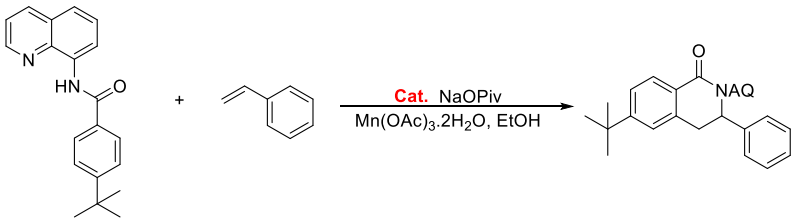

99 **100**

Entry	Catalyst	Yield (%)	ee (%)
1	$Co(NO_3)_2.6H_2O$, and **94**, RT	10	7
2	$Co(NO_3)_2.6H_2O$, and **96**, 40 °C	15	7
3	Complex **98**, 60 °C	10	41

5.2.2.2. Optimization and Reaction Scope.

The first essential issue was to improve reaction yield. A structurally similar diketone, dipivaloylmethane, which is commercially available, was used to optimize reaction conditions. Using the same method, the cobalt complex **101** was generated in 65% yield (**Scheme 5.19**).

Scheme 5.19. Synthesis of non-chiral cobalt complex **101**.

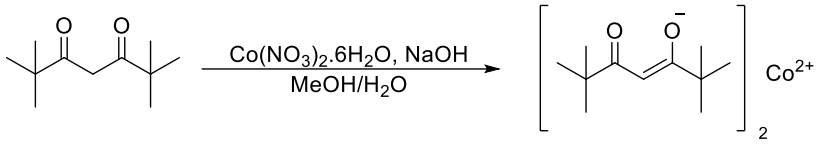

101
65%

With **101** in hand, we screened reaction under different conditions and results are summarized in **Table 5.2**. The influence of solvent on reaction outcome was examined first and variety of solvents were tested including methanol, ethanol, isopropanol, and hexafluoro-*iso*-propanol (HFIP). Interestingly, using 20 mol% of **101**, with manganese (III) acetate and sodium pivalate additives, the reaction between substrate **99** and styrene in methanol at 60 °C afforded product **100** in 57% yield. Meanwhile, only 40% yield of product was obtained using ethanol solvent. Alternatively, the reaction could proceed even at room temperature, giving **100** in 51% yield in methanol solvent. The increase in water level did not help to improve reaction yield (**Entry 6, 7, 8. Table 5.2**). When oxygen was used as external oxidant, the yield increased to 61%. In contrast, reducing the amount of manganese (III) acetate resulted in significant decrease in reaction yield to 25%. Furthermore, manganese (II) acetate additive was inefficient, giving low yield of **100**. Different bases were also investigated and among them, cesium acetate gave the best outcome, offering product **100** in 71% yield.

Table 5.2. Investigation of optimal conditions

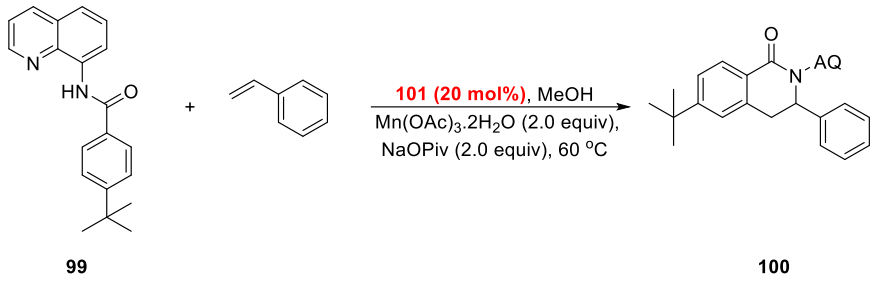

99 100

Entry	Change from Conditions	Yield (%)[a]
1	None	57
2	EtOH was used	40
3	IPA was used	Trace
4	HFIP was used	Trace
5	Room temperature	51
6	5 wt.% of water added	41
7	10 wt.% of water added	48
8	20 wt.% of water added	34
9	0.5 equivalent of $Mn(OAc)_3.2H_2O$ was used	25
10	$Mn(OAc)_2$ used instead of $Mn(OAc)_3.2H_2O$	12
11	Oxygen atmosphere,	61
12	CsOPiv, oxygen atmosphere	64
13	Cs_2CO_3, oxygen atmosphere	33
14	CsTFA, oxygen atmosphere	57
15	CsOAc, oxygen atmosphere	71

[a]Isolated yield. Abbreviations: IPA = isopropyl alcohol; HFIP = 1,1,1,3,3,3-hexafluoroisopropanol; CsOPiv = cesium pivalate; CsTFA = cesium trifluoroacetate.

Various substrates were tested using both chiral and non-chiral cobalt complexes (**Scheme 5.20**). Specifically, under same conditions, chiral catalyst **98** gave product **100** in lower yield, compared to non-chiral catalyst. A 52% yield of 100 with 26% ee was obtained. Interestingly, both electron withdrawing and electron donating groups on styrene accelerated reaction, giving higher yields of products **102** and **103**. However, lower ee was observed in case of **102**, with 16% ee. Additionally, racemic **103** could not be resolved on any chiral stationary phase (CSP) columns. Reactions with alphatic alkenes were also explored. Specifically, 1-hexene gave 81% of **104** with 16% ee. In contrast, vinylcylclohexane and 1-cyclohexne produced product **105** and **106** in lower yield but slightly higher ee.

Scheme 5.20. Substrate scopes.

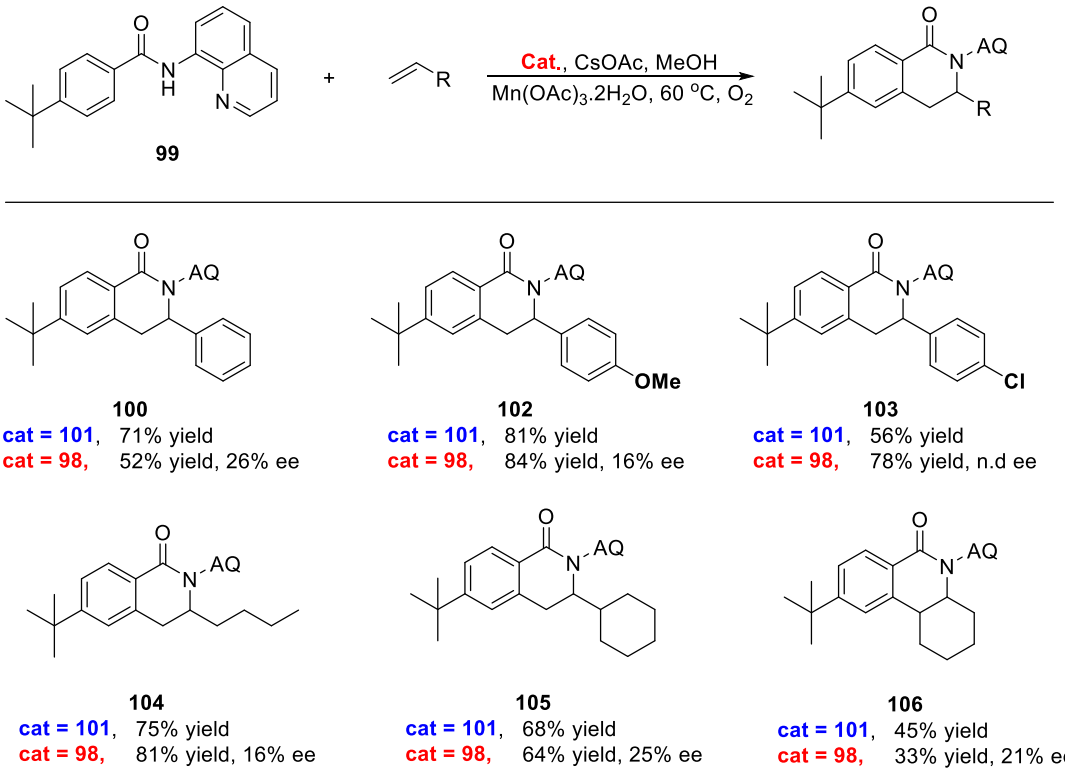

Next, a series of experiments at room temperature were conducted to enhance reaction enantioselectivity (**Scheme 5.21**). The enantiomeric excess of **105** and **102** slightly increased to 31% and 20% when lowering temperature from 60 °C to 24 °C, yet the yields decreased to 36% and 51%, respectively. Attempted modification of directing groups were made to increase reaction efficiency. Interestingly, electron releasing substituent on DG increased activity and **107** was obtained in 54% yield at room temperature. Meanwhile, electron withdrawing substituent on DG shut down reaction completely, and **108** was not formed. Unfortunately, we were unable to measure enantiomeric excess of **107**.

Scheme 5.21. Reactions at room temperature.

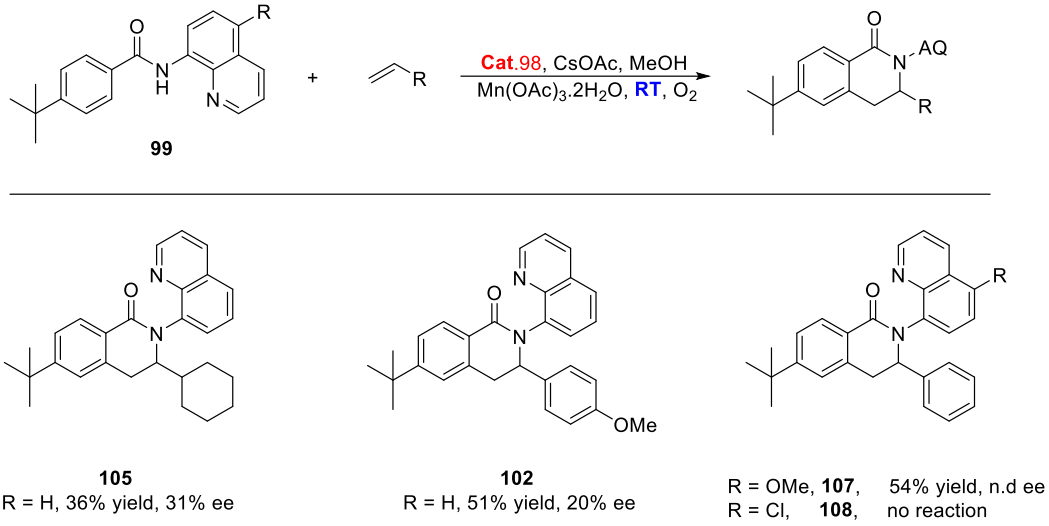

Another factor that can contribute to low enantioslectivity is the affinity of solvent molecules that may strongly bind and saturate coordination sites on metal center, preventing the incorporation of chiral ligand. We added stoichiometric amount of free ligand **96** to reaction mixture and changed solvent to less coordinating, 1,1,1-trifluoroethanol (TFE) (**Scheme 5.22**). The results show that 66% of **105** was obtained with methanol solvent and 44% was observed when TFE was used. Interestingly, the enantiomeric excess of **105** was lower if TFE solvent

was used, at 17% while reaction in methanol gave product in 26% ee. These results suggests that solvent does not compete with ligand at coordination sphere of metal. More electron deficient substituents on both amides and styrenes were tested and the yield of **109** was dropped to 15% with 21% ee while no formation of **110** was observed.

Scheme 5.22. Solvent and external ligands testing.

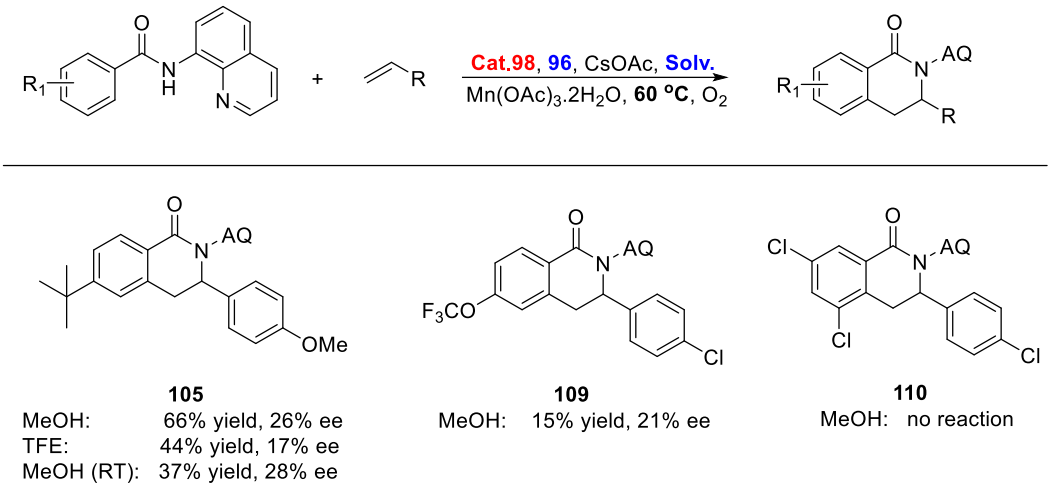

Generally, chiral catalyst **98** showed impressive results on asymmetric synthesis of isoquinolones derivatives, giving moderate to good yields of product. However, the enantioselectivities of reaction are still low. Thus, modifications of both catalyst and reaction conditions are essential to improve enantioselectivity of this reaction.

5.2.3 Experimental Section

General

Reactions were performed using standard glassware or were run in 2-dram vials with PTFE/Liner screw caps and 8-dram vials w/polyseal screw caps. Column chromatography was performed on 60Å silica gel (Dynamic Adsorbents Inc.). ^{1}H, ^{13}C-NMR spectra were recorded on JEOL EC-400, JEOL EC-500, or JEOL EC-600 spectrometers. Analytical thin layer chromatography was performed on silica gel IB-F (Baker-flex) by J. T. Baker. Purification by preparative HPLC was performed on a Shimadzu Prominence LC (LC-20AB) equipped with a SPD-20A UV-Vis detector and a DAICEL-Chiralpark AS-H (4.6 mmI.D x 250 mmL) column. All procedures were performed under ambient air unless otherwise noted. Reagents and starting materials were obtained from commercial sources and used without further purification unless otherwise noted.

Substrate synthesis

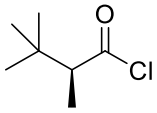

(S)-2,3,3-Trimethylbutanoyl chloride 93.

A round bottom flask (100 mL) equipped with a magnetic stir bar and connected to Schlenk line, was charged with **65** (1.95 g, 15 mmol), CH_2Cl_2 (40 mL), and DMF (0.15 mL, 2.0 mmol). The flask was then cooled down to 0 °C using ice bath. To the mixture, oxalyl chloride (4.28 mL, 50 mmol) was added dropwise in 5 min. Then the ice bath was removed and mixture was stirred at room temperature overnight. Subsequently, mixture was concentrated to

ca. 3 mL using rotovap at 35 °C under 500 mm Hg. Precipitate was formed after 2 minutes and liquid, containing **93** and CH_2Cl_2, was transferred to a 2-dram vial using pipet. This product was kept in CH_2Cl_2 due to high volatile property and used for next step. Concentration was estimated based on integration of NMR signals. This compound is known.[212]

^{1}H NMR (400 MHz, $CDCl_3$) δ 2.78 (q, *J* = 7.2 Hz, 1H), 1.25 (d, *J* = 7.2 Hz, 3H), 1.01 (s, 9H).

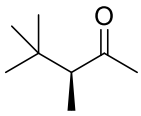

(S)-3,4,4-trimethylpentan-2-one 95.

A flame-dried Schlenk flask (50 mL) equipped with a magnetic stir bar, was charged with **64** (2.08 g, 16 mmol) and diethyl ether (25 mL). The flask was cooled to 0 °C using ice bath. To the mixture, methyl lithium (1.6 M in diethyl ether) (21 mL, 33.6 mmol) was added dropwise in 10 minutes. Then, ice bath was removed and the flask was stirred at room temperature overnight. After that, solution was diluted in diethyl ether (30 mL) and extracted with HCl 1 M (20 mL) then $NaHCO_3$ aq. (20 mL) and NaCl aq. (30 mL). Organic layer was dried over $MgSO_4$, filtered and concentrated to 2 mL using rotovap at 35 °C under 500 mm Hg. Product **95** remained in diethyl ether solution. Concentration was estimated based on integration of NMR signals. This compound is known.[213]

^{1}H NMR (400 MHz, $CDCl_3$) δ 2.40 (q, *J* = 7.5 Hz, 1H), 2.09 (s, 3H), 1.01 (d, *J* = 7.5 Hz, 3H), 0.89 (s, 3H).

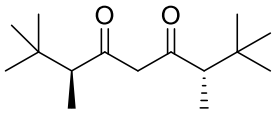

Compound 96.

A round bottom flask (100 mL) equipped with magnetic stir bar and connected to Schlenk line, was charged with $MgBr_2.OEt_2$ (6.04 g, 23.4 mmol) and CH_2Cl_2 (40 mL). The flask was cooled to 0 °C using ice bath. To the mixture was added compound **93** (7.8 mmol) and **95** (7.8 mmol) and the mixture was stirred for 10 minutes. Subsequently, diisopropylethylamine (5.39 mL, 31.2 mmol) was added dropwise to solution. Then ice bath was removed and the flask was stirred at room temperature overnight. After that, the mixture was diluted with CH_2Cl_2 (30 mL) and extracted with HCl 1 M (30 mL) then NaCl aq. (3 x 30 mL). Organic layer was dried over $MgSO_4$, filtered and solvent was removed. Product was purified using column chromatography in hexane/EtOAc (10/1), Rf = 0.75 (SiO_2, hexane/EtOAc = 10/1). Yield 0.77 g (41%) of a yellow liquid.

^{1}H NMR (600 MHz, $CDCl_3$) δ 16.09 (s, 1H), 5.38 (s, 1H), 2.13 – 2.05 (m, 2H), 1.10 – 1.08 (m, 6H), 0.94 (s, 18H).

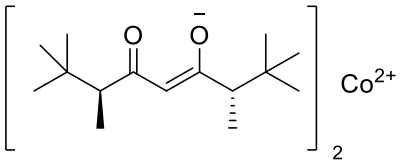

Compound 98.

A 20-dram vial equipped with a magnetic stir bar was charged with $Co(NO_3)_2.6H_2O$ (0.18 g, 0.6 mmol), ligand **96** (0.29 g, 1.2 mmol), and methanol (6 mL). The mixture was stirred

at room temperature for 10 minutes followed by addition of NaOH solution (48 mg in 0.6 mL). Precipitate was formed and the vial was sealed with a cap and placed in oil bath at 80 °C overnight. After cooling down to room temperature, mixture was filtered to remove solvent and solids were washed with water (5 x 10 mL) and then dried under vacuum. Yield 0.2 g (63%) of a deep green solid. This compound is paramagnetic and thus was not characterized.

General procedure for the insertion reaction

A 2-dram vial equipped with a magnetic stir bar was charged with aminoquinoline protected amide (0.2 mmol), alkene (0.3 mmol, 1.5 equiv), catalyst **98** (21.5 mg, 20 mol%), $Mn(OAc)_3.2H_2O$ (46.4 mg, 1.0 equiv), CsOAc (76.8 mg, 2.0 equiv), with or without ligand **96** (24 mg, 50 mol%), and methanol (2 mL). The mixture was flushed with oxygen for 3 minutes then capped and placed in hot plate at 60 °C with stirring. After indicated amount of time, the vial was taken out and cooled to room temperature. Mixture was diluted with CH_2Cl_2 (30 mL), silica was added and solvent was removed using rotovap. Product was purified using column chromatography with hexane/EtOAc (gradient from 0% to 20% then 50%). All compounds are known.[210] The enantiomeric ratio (%) of products were determined using chiral column.

3-Phenyl-2-(quinolin-8-yl)-6-(*tert*-butyl)-3,4-dihydroisoquinolin-1(2H)-one 100.

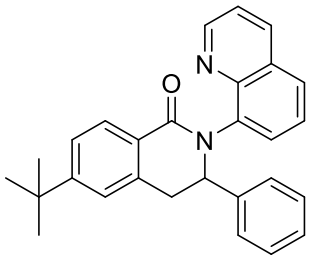

4-tert-Butyl-N-(quinolin-8-yl)benzamide (60.8 mg, 0.2 mmol), styrene (27.5 μL, 0.24 mmol, 1.2 equiv), catalyst **98** (21.5 mg, 20 mol%), CsOAc (76.8 mg, 0.4 mmol, 2 equiv),

$Mn(OAc)_3.2H_2O$ (46.4 mg, 0.2 mmol, 1.0 equiv), and MeOH (2.0 mL), 36 h, 60 °C. After column chromatography (gradient hexanes/EtOAc from 4:1 to 2:1) 42.2 mg (52%) of a white solid was obtained. Rf = 0.55 (hexanes/EtOAc 1:1), ee = 26%

Enantiomeric excess was determined by DAICEL Chiralpak AH-H, 899 psi, 1.0 mL min^{-1}, hexane/isopropanol (10/1), room temperature, t_1 = 30.8 min, t_2 = 52.4 min.

^1H NMR (400 MHz, $CDCl_3$) δ 8.90 (s, 1H), 8.16 – 8.12 (m, 2H), 7.70 (d, J = 8.4 Hz, 1H), 7.50 (d, J = 7.2 Hz, 1H), 7.41 – 7.38 (m, 3H), 7.25 – 7.14 (m, 6H), 5.48 – 5.46 (m, 1H), 4.15 – 4.09 (m, 1H), 3.25 – 3.22 (m, 1H), 1.29 (s, 9H).

3-(p-Methoxyphenyl)-2-(quinolin-8-yl)-6-(*tert*-butyl)-3,4-dihydroisoquinolin-1(2H)-one 102.

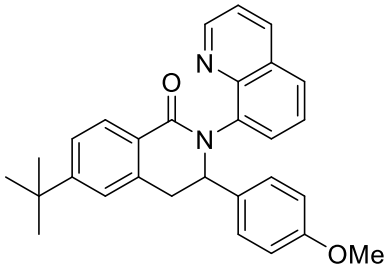

4-tert-Butyl-N-(quinolin-8-yl)benzamide (60.8 mg, 0.2 mmol), 4-vinyl anisole (40 μL, 0.24 mmol, 1.2 equiv), catalyst **98** (21.5 mg, 20 mol%), CsOAc (76.8 mg, 0.4 mmol, 2 equiv), $Mn(OAc)_3.2H_2O$ (46.4 mg, 0.2 mmol, 1.0 equiv), and MeOH (2.0 mL), 36 h, 60 °C. After column chromatography (gradient hexanes/EtOAc from 4:1 to 2:1) 72.9 mg (84%) of a white solid was obtained. Rf = 0.50 (hexanes/EtOAc 1:1), ee = 16%

Enantiomeric excess was determined by DAICEL Chiralpak AH-H, 1080 psi, 2.0 mL min^{-1}, hexane/isopropanol (10/1), room temperature, t_1 = 48.4 min, t_2 = 66.8 min.

^{1}H NMR (600 MHz, $CDCl_3$) δ 8.91 (d, *J* = 4.2 Hz, 1H), 8.13 (d, *J* = 1.8 Hz, 2H), 7.71 – 7.69 (m, 1H), 7.47 – 7.44 (m, 1H), 7.40 – 7.38 (m, 3H), 7.16 – 7.04 (m, 3H), 6.68 – 6.62 (m, 2H), 5.42 – 5.40 (m, 1H), 4.13 – 4.08 (m, 1H), 3.69 (s, 3H), 3.21 – 3.10 (m, 1H), 1.32 (s, 9H).

3-(p-Chlorophenyl)-2-(quinolin-8-yl)-6-(*tert*-butyl)-3,4-dihydroisoquinolin-1(2H)-one 103.

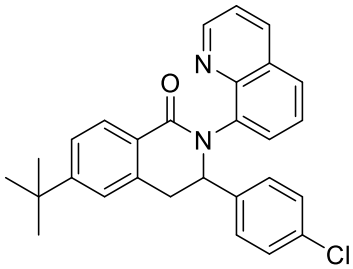

4-tert-Butyl-N-(quinolin-8-yl)benzamide (60.8 mg, 0.2 mmol), 4-vinyl anisole (40 μL, 0.24 mmol, 1.2 equiv), catalyst **98** (21.5 mg, 20 mol%), CsOAc (76.8 mg, 0.4 mmol, 2 equiv), $Mn(OAc)_3.2H_2O$ (46.4 mg, 0.2 mmol, 1.0 equiv), and MeOH (2.0 mL), 36 h, 60 °C. After column chromatography (gradient hexanes/EtOAc from 4:1 to 2:1) 68.6 mg (78%) of a white solid was obtained. Rf = 0.65 (hexanes/EtOAc 1:1).

Enantiomeric excess of this compound was not determined.

^{1}H NMR (400 MHz, $CDCl_3$) δ 8.91 (d, *J* = 6 Hz, 1H), 8.15 – 8.11 (m, 2H), 7.75 – 7.70 (m, 1H), 7.48 – 7.40 (m, 4H), 7.13 – 7.12 (m, 5H), 5.51 – 5.44 (m, 1H), 4.14 – 4.08 (m, 1H), 3.19 – 3.15 (m, 1H), 1.27 (s, 9H).

3-Butyl-2-(quinolin-8-yl)-6-(*tert*-butyl)-3,4-dihydroisoquinolin-1(2H)-one 104.

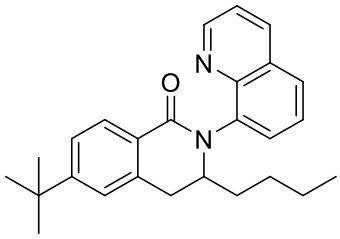

4-tert-Butyl-N-(quinolin-8-yl)benzamide (60.8 mg, 0.2 mmol), 1 - hexene (30 μL, 0.24 mmol, 1.2 equiv), catalyst **98** (21.5 mg, 20 mol%), CsOAc (76.8 mg, 0.4 mmol, 2 equiv), $Mn(OAc)_3.2H_2O$ (46.4 mg, 0.2 mmol, 1.0 equiv), and MeOH (2.0 mL), 36 h, 60 °C. After column chromatography (gradient hexanes/EtOAc from 4:1 to 2:1) 62.5 mg (81%) of a white solid was obtained. Rf = 0.70 (hexanes/EtOAc 1:1) ee = 16%

Enantiomeric excess was determined by DAICEL Chiralpak AH-H, 1000 psi, 2.0 mL min^{-1}, hexane/isopropanol (10/1), room temperature, t_1 = 22.1 min, t_2 = 24.5 min.

^{1}H NMR (600 MHz, $CDCl_3$) δ 8.89 – 8.87 (m, 1H), 8.18 (d, *J* = 8.4 Hz, 1H), 8.04 (d, *J* = 8.4 Hz, 1H), 7.82 (d, *J* = 7.8 Hz, 1H), 7.76 – 7.75 (m, 1H), 7.59 (t, *J* = 7.8 Hz, 1H), 7.41 – 7.36 (m, 2H), 7.27 – 7.25 (m, 1H), 4.15 – 4.01 (m, 1H), 4.00 – 3.82 (m, 1H), 3.04 – 2.85 (m, 1H), 1.62 – 1.59 (m, 2H), 1.35 (s, 9H), 1.28 – 0.99 (m, 4H), 0.75 – 0.68 (m, 3H).

3-Cyclohexyl-2-(quinolin-8-yl)-6-(*tert*-butyl)-3,4-dihydroisoquinolin-1(2H)-one 105.

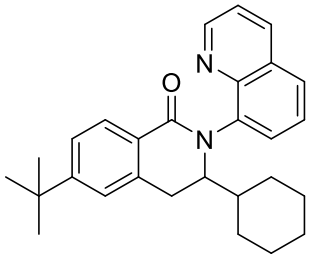

4-tert-Butyl-N-(quinolin-8-yl)benzamide (60.8 mg, 0.2 mmol), vinyl cyclohexane (41 μL, 0.24 mmol, 1.2 equiv), catalyst **98** (21.5 mg, 20 mol%), CsOAc (76.8 mg, 0.4 mmol, 2

equiv), $Mn(OAc)_3.2H_2O$ (46.4 mg, 0.2 mmol, 1.0 equiv), and MeOH (2.0 mL), 36 h, 60 °C. After column chromatography (gradient hexanes/EtOAc from 4:1 to 2:1) 52.6 mg (64%) of a white solid was obtained. Rf = 0.70 (hexanes/EtOAc 1:1), ee = 25%

Enantiomeric excess was determined by DAICEL Chiralpak AH-H, 1071 psi, 2.0 mL min^{-1}, hexane/isopropanol (10/1), room temperature, t_1 = 17.5 min, t_2 = 30.5 min.

^{1}H NMR (600 MHz, $CDCl_3$) δ 8.88 – 8.85 (m, 1H), 8.18 (d, *J* = 8.4 Hz, 1H), 8.01 (d, *J* = 8.4 Hz, 1H), 7.81 (d, *J* = 8.4 Hz, 2H), 7.60 (t, *J* = 8.4 Hz, 1H), 7.39 (dd, *J* = 4.2 Hz, *J* = 7.8 Hz, 1H), 7.35 (d, J = 7.8 Hz, 1H), 7.23 (s, 1H), 4.09 – 3.92 (m, 2H), 3.04 (d, *J* = 15 Hz, 1H), 1.70 – 1.50 (m, 6H), 1.36 (s, 9H), 1.06 – 0.95 (m, 3H).

9-(*tert*-Butyl)-5-(quinolin-8-yl)-1,3,4,4a,5,10b-hexahydrophenanthridin-6(2H)-one 106.

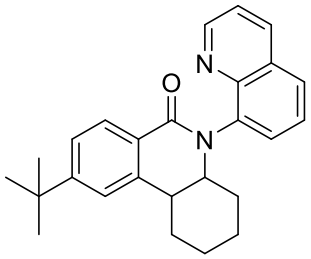

4-tert-Butyl-N-(quinolin-8-yl)benzamide (60.8 mg, 0.2 mmol), cyclohexene (41 μL, 0.24 mmol, 1.2 equiv), catalyst **98** (21.5 mg, 20 mol%), CsOAc (76.8 mg, 0.4 mmol, 2 equiv), $Mn(OAc)_3.2H_2O$ (46.4 mg, 0.2 mmol, 1.0 equiv), and MeOH (2.0 mL), 36 h, 60 °C. After column chromatography (gradient hexanes/EtOAc from 4:1 to 2:1) 25.2 mg (33%) of a white solid was obtained. Rf = 0.70 (hexanes/EtOAc 1:1), ee = 21%

Enantiomeric excess was determined by DAICEL Chiralpak AH-H, 1110 psi, 2.0 mL min^{-1}, hexane/isopropanol (10/1), room temperature, t_1 = 30.5 min, t_2 = 42.0 min.

^{1}H NMR (500 MHz, $CDCl_3$) δ 8.90 – 8.86 (m, 1H), 8.18 (d, *J* = 7.5 Hz, 1H), 8.09 (d, *J* = 7.5 Hz, 1H), 7.83 (d, *J* = 7 Hz, 1H), 7.82 – 7.70 (m, 1H), 7.60 – 7.53 (m, 1H), 7.39 - 7.35 (m, 3H), 4.37 – 3.71 (m, 2H), 1.76 – 1.36 (m, 7H), 1.37 (s, 9H), 1.25 – 1.18 (m, 1H).

Bibliography

(1) Reichenbächer, K.; Süss, H. I.; Hulliger, J. *Chem. Soc. Rev.* **2005**, *34*, 22-30.

(2) O'Hagan, D. *Chem. Soc. Rev.* **2008**, *37*, 308-319.

(3) Kuehnel, M. F.; Lentz, D.; Braun, T. *Angew. Chem. Int. Ed.* **2013**, *52*, 3328-3348.

(4) Stevenson, A. J.; Serier-Brault, H.; Gredin, P.; Mortier, M. *J. Fluorine Chem.* **2011**, *132*, 1165-1173.

(5) Han, J.; Kiss, L.; Mei, H.; Remete, A. M.; Ponikvar-Svet, M.; Sedgwick, D. M.; Roman, R.; Fustero, S.; Moriwaki, H.; Soloshonok, V. A. *Chem. Rev.* **2021**, *121*, 4678-4742.

(6) Oliver, A. J. O. z., E. *In Uranium for Nuclear Power; Ian, H.-L., Ed.; Woodhead Publishing,* **2016**.

(7) Ameduri, B. *Macromol. Chem. Phys.* **2020**, *221*, 1900573.

(8) Han, J.; Remete, A. M.; Dobson, L. S.; Kiss, L.; Izawa, K.; Moriwaki, H.; Soloshonok, V. A.; O'Hagan, D. *J. Fluorine Chem.* **2020**, 109639.

(9) Jeschke, P. *ChemBioChem* **2004**, *5*, 570-589.

(10) Carvalho, M. F.; Oliveira, R. S. *Crit. Rev. Biotechnol.* **2017**, *37*, 880-897.

(11) Chaney, R. L. *Adv. Agron.* **2012**, *117*, 51-116.

(12) Strunecka, A.; Strunecky, O. *Appl. Sci.* **2020**, *10*, 7100.

(13) Lim, X. *Nature* **2019**, *566*, 26-30.

(14) Kirsch, P. *Modern fluoroorganic chemistry: synthesis, reactivity, applications*; John Wiley & Sons, 2013.

(15) Jepson, P. D.; Law, R. J. *Science* **2016**, *352*, 1388-1389.

(16) Lucas, R. E.; Wheeler, D.; Hettige, H. *Economic development, environmental regulation, and the international migration of toxic industrial pollution, 1960-88*; World Bank Publications, 1992; Vol. 1062.

(17) Bandosz, T. J. *Catal. Today* **2012**, *186*, 20-28.

(18) Marrs, T. C. *Chemical warfare agents: toxicology and treatment* **2007**, *2*.

(19) Horike, S.; Shimomura, S.; Kitagawa, S. 2009.

(20) Guillerm, V.; Kim, D.; Eubank, J. F.; Luebke, R.; Liu, X.; Adil, K.; Lah, M. S.; Eddaoudi, M. *Chem. Soc. Rev.* **2014**, *43*, 6141-6172.

(21) Eddaoudi, M.; Moler, D. B.; Li, H.; Chen, B.; Reineke, T. M.; O'keeffe, M.; Yaghi, O. M. *Acc. Chem. Res.* **2001**, *34*, 319-330.

(22) Britt, D.; Tranchemontagne, D.; Yaghi, O. M. *Proc. Natl. Acad. Sci* **2008**, *105*, 11623-11627.

(23) Gelfand, B. S.; Shimizu, G. K. *Dalton Trans* **2016**, *45*, 3668-3678.

(24) Morris, R. E.; Brammer, L. *Chem. Soc. Rev.* **2017**, *46*, 5444-5462.

(25) Low, J. J.; Benin, A. I.; Jakubczak, P.; Abrahamian, J. F.; Faheem, S. A.; Willis, R. R. *J. Am. Chem. Soc.* **2009**, *131*, 15834-15842.

(26) Mukherjee, S.; Sharma, S.; Ghosh, S. K. *APL Materials* **2019**, *7*, 050701.

(27) Dhanumalayan, E.; Joshi, G. M. *Adv. Compos. Hybrid Mater.* **2018**, *1*, 247-268.

(28) O'Hagan, D. *J. Fluorine Chem.* **2010**, *131*, 1071-1081.

(29) Yang, C.; Wang, X.; Omary, M. A. *J. Am. Chem. Soc.* **2007**, *129*, 15454-15455.

(30) Fischer, R. A.; Wöll, C. *Angew. Chem. Int. Ed.* **2008**, *47*, 8164-8168.

(31) Serre, C. *Angew. Chem. Int. Ed.* **2012**, *51*, 6048-6050.

(32) Chen, T.-H.; Popov, I.; Zenasni, O.; Daugulis, O.; Miljanić, O. Š. *Chem. Commun.* **2013**, *49*, 6846-6848.

(33) Do, H.-Q.; Daugulis, O. *J. Am. Chem. Soc.* **2008**, *130*, 1128-1129.

(34) Yang, C.; Kaipa, U.; Mather, Q. Z.; Wang, X.; Nesterov, V.; Venero, A. F.; Omary, M. A. *J. Am. Chem. Soc.* **2011**, *133*, 18094-18097.

(35) DeFuria, M. D.; Zeller, M.; Genna, D. T. *Cryst. Growth Des.* **2016**, *16*, 3530-3534.

(36) Cheplakova, A. M.; Kovalenko, K. A.; Samsonenko, D. G.; Lazarenko, V. A.; Khrustalev, V. N.; Vinogradov, A. S.; Karpov, V. M.; Platonov, V. E.; Fedin, V. P. *Dalton Trans.* **2018**, *47*, 3283-3297.

(37) Cote, A. P.; Benin, A. I.; Ockwig, N. W.; O'Keeffe, M.; Matzger, A. J.; Yaghi, O. M. *Science.* **2005**, *310*, 1166-1170.

(38) Wan, S.; Guo, J.; Kim, J.; Ihee, H.; Jiang, D. *Angew. Chem. Int. Ed.* **2009**, *48*, 5439-5442.

(39) El-Kaderi, H. M.; Hunt, J. R.; Mendoza-Cortés, J. L.; Côté, A. P.; Taylor, R. E.; O'Keeffe, M.; Yaghi, O. M. *Science.* **2007**, *316*, 268-272.

(40) Tilford, R. W.; Mugavero III, S. J.; Pellechia, P. J.; Lavigne, J. J. *Adv. Mater.* **2008**, *20*, 2741-2746.

(41) Spitler, E. L.; Dichtel, W. R. *Nat. Chem.* **2010**, *2*, 672-677.

(42) Bojdys, M. J.; Jeromenok, J.; Thomas, A.; Antonietti, M. *Adv. Mater.* **2010**, *22*, 2202-2205.

(43) Kuhn, P.; Antonietti, M.; Thomas, A. *Angew. Chem. Int. Ed.* **2008**, *47*, 3450-3453.

(44) Beaudoin, D.; Maris, T.; Wuest, J. D. *Nat. Chem.* **2013**, *5*, 830-834.

(45) Chen, T.-H.; Popov, I.; Kaveevivitchai, W.; Chuang, Y.-C.; Chen, Y.-S.; Daugulis, O.; Jacobson, A. J.; Miljanić, O. Š. *Nat. Commun.* **2014**, *5*, 1-8.

(46) Wang, G.; Leus, K.; Jena, H. S.; Krishnaraj, C.; Zhao, S.; Depauw, H.; Tahir, N.; Liu, Y.-Y.; Van Der Voort, P. *J. Mater. Chem. A.* **2018**, *6*, 6370-6375.

(47) Braunecker, W. A.; Hurst, K. E.; Ray, K. G.; Owczarczyk, Z. R.; Martinez, M. B.; Leick, N.; Keuhlen, A.; Sellinger, A.; Johnson, J. C. *Cryst. Growth Des.* **2018**, *18*, 4160-4166.

(48) Doonan, C. J.; Tranchemontagne, D. J.; Glover, T. G.; Hunt, J. R.; Yaghi, O. M. *Nat. Chem.* **2010**, *2*, 235-238.

(49) Bloch, E. D.; Britt, D.; Lee, C.; Doonan, C. J.; Uribe-Romo, F. J.; Furukawa, H.; Long, J. R.; Yaghi, O. M. *J. Am. Chem. Soc.* **2010**, *132*, 14382-14384.

(50) Carson, F.; Agrawal, S.; Gustafsson, M.; Bartoszewicz, A.; Moraga, F.; Zou, X.; Martín-Matute, B. *Chem. - Eur. J.* **2012**, *18*, 15337-15344.

(51) Sun, D.; Gao, Y.; Fu, J.; Zeng, X.; Chen, Z.; Li, Z. *Chem. Commun.* **2015**, *51*, 2645-2648.

(52) Bruce, J. I.; Chambron, J.-C.; Kölle, P.; Sauvage, J.-P. *J. Chem. Soc., Perkin Trans. 1* **2002**, 1226-1231.

(53) Laev, S. S.; Evtefeev, V. U.; Shteingarts, V. D. *J. Fluorine Chem.* **2001**, *110*, 43-46.

(54) Naritomi, M.; Murofushi, H.; Nakashima, N. *Bull. Chem. Soc. Jpn.* **2004**, *77*, 2121-2127.

(55) Howarth, A. J.; Majewski, M. B.; Wolf, M. O. *Coord. Chem. Rev.* **2015**, *282*, 139-149.

(56) Kinik, F. P.; Ortega-Guerrero, A.; Ongari, D.; Ireland, C. P.; Smit, B. *Chem. Soc. Rev.* **2021**.

(57) Liu, Y.; Buru, C. T.; Howarth, A. J.; Mahle, J. J.; Buchanan, J. H.; DeCoste, J. B.; Hupp, J. T.; Farha, O. K. *J. Mater. Chem. A.* **2016**, *4*, 13809-13813.

(58) Okamoto, M.; Tanaka, F. *J. Phys. Chem. A.* **2002**, *106*, 3982-3990.

(59) Chen, X.; Huang, N.; Gao, J.; Xu, H.; Xu, F.; Jiang, D. *Chem. Commun.* **2014**, *50*, 6161-6163.

(60) Lin, G.; Ding, H.; Yuan, D.; Wang, B.; Wang, C. *J. Am. Chem. Soc.* **2016**, *138*, 3302-3305.

(61) Carter, T. S.; Mooibroek, T. J.; Stewart, P. F.; Crump, M. P.; Galan, M. C.; Davis, A. P. *Angew. Chem. Int. Ed.* **2016**, *55*, 9311-9315.

(62) Liu, Q.; Tang, Z.; Wu, M.; Liao, B.; Zhou, H.; Ou, B.; Yu, G.; Zhou, Z.; Li, X. *RSC Advances* **2015**, *5*, 8933-8937.

(63) Roemer, M.; Nijhuis, C. A. *Dalton Trans.* **2014**, *43*, 11815-11818.

(64) Miller, A. O.; Krasnov, V. I.; Peters, D.; Platonov, V. E.; Miethchen, R. *Tetrahedron Lett.* **2000**, *41*, 3817-3819.

(65) Sagara, Y.; Yamane, S.; Mitani, M.; Weder, C.; Kato, T. *Adv. Mater.* **2016**, *28*, 1073-1095.

(66) Qiu, Z.; Zhao, W.; Cao, M.; Wang, Y.; Lam, J. W.; Zhang, Z.; Chen, X.; Tang, B. Z. *Adv. Mater.* **2018**, *30*, 1803924.

(67) Bai, L.; Bose, P.; Gao, Q.; Li, Y.; Ganguly, R.; Zhao, Y. *J. Am. Chem. Soc.* **2017**, *139*, 436-441.

(68) Ren, Y.; Xie, S.; Svensson Grape, E.; Inge, A. K.; Ramstrom, O. *J. Am. Chem. Soc.* **2018**, *140*, 13640-13643.

(69) Ma, Z.; Wang, Z.; Meng, X.; Ma, Z.; Xu, Z.; Ma, Y.; Jia, X. *Angew. Chem. Int. Ed.* **2016**, *55*, 519-522.

(70) Wang, Z.; Ma, Z.; Wang, Y.; Xu, Z.; Luo, Y.; Wei, Y.; Jia, X. *Adv. Mater.* **2015**, *27*, 6469-6474.

(71) Shao, B.; Baroncini, M.; Qian, H.; Bussotti, L.; Di Donato, M.; Credi, A.; Aprahamian, I. *J. Am. Chem. Soc.* **2018**, *140*, 12323-12327.

(72) Sagara, Y.; Kato, T. *Angew. Chem.* **2008**, *120*, 5253-5256.

(73) Sagara, Y.; Kato, T. *Angew. Chem.* **2011**, *123*, 9294-9298.

(74) Liu, L.; Wang, X.; Wang, N.; Peng, T.; Wang, S. *Angew. Chem. Int. Ed.* **2017**, *56*, 9160-9164.

(75) Teng, M. J.; Jia, X. R.; Yang, S.; Chen, X. F.; Wei, Y. *Adv. Mater.* **2012**, *24*, 1255-1261.

(76) Park, S. K.; Cho, I.; Gierschner, J.; Kim, J. H.; Kim, J. H.; Kwon, J. E.; Kwon, O. K.; Whang, D. R.; Park, J. H.; An, B. K. *Angew. Chem. Int. Ed.* **2016**, *55*, 203-207.

(77) Sagara, Y.; Mutai, T.; Yoshikawa, I.; Araki, K. *J. Am. Chem. Soc.* **2007**, *129*, 1520-1521.

(78) Ito, H.; Saito, T.; Oshima, N.; Kitamura, N.; Ishizaka, S.; Hinatsu, Y.; Wakeshima, M.; Kato, M.; Tsuge, K.; Sawamura, M. *J. Am. Chem. Soc.* **2008**, *130*, 10044-10045.

(79) Yuan, W. Z.; Tan, Y.; Gong, Y.; Lu, P.; Lam, J. W.; Shen, X. Y.; Feng, C.; Sung, H. H. Y.; Lu, Y.; Williams, I. D. *Adv. Mater.* **2013**, *25*, 2837-2843.

(80) Luo, X.; Li, J.; Li, C.; Heng, L.; Dong, Y. Q.; Liu, Z.; Bo, Z.; Tang, B. Z. *Adv. Mater.* **2011**, *23*, 3261-3265.

(81) Zhao, Y.; Gao, H.; Fan, Y.; Zhou, T.; Su, Z.; Liu, Y.; Wang, Y. *Adv. Mater.* **2009**, *21*, 3165-3169.

(82) Balch, A. L. *Angew. Chem. Int. Ed.* **2009**, *48*, 2641-2644.

(83) Liu, Y.; Zeng, Q.; Zou, B.; Liu, Y.; Xu, B.; Tian, W. *Angew. Chem. Int. Ed.* **2018**, *57*, 15670-15674.

(84) Dong, Y.; Xu, B.; Zhang, J.; Tan, X.; Wang, L.; Chen, J.; Lv, H.; Wen, S.; Li, B.; Ye, L. *Angew. Chem. Int. Ed.* **2012**, *51*, 10782-10785.

(85) Yoon, S.-J.; Chung, J. W.; Gierschner, J.; Kim, K. S.; Choi, M.-G.; Kim, D.; Park, S. Y. *J. Am. Chem. Soc.* **2010**, *132*, 13675-13683.

(86) Strasser, C. E.; Catalano, V. J. *J. Am. Chem. Soc.* **2010**, *132*, 10009-10011.

(87) Lasanta, T.; Olmos, M. E.; Laguna, A.; López-de-Luzuriaga, J. M.; Naumov, P. *J. Am. Chem. Soc.* **2011**, *133*, 16358-16361.

(88) Laguna, A.; Lasanta, T.; López-de-Luzuriaga, J. M.; Monge, M.; Naumov, P.; Olmos, M. E. *J. Am. Chem. Soc.* **2010**, *132*, 456-457.

(89) England, K. R.; Lim, S. H.; Luong, L. M.; Olmstead, M. M.; Balch, A. L. *Chem. - Eur. J.* **2019**, *25*, 874-878.

(90) Nakajima, S.; Albrecht, K.; Kushida, S.; Nishibori, E.; Kitao, T.; Uemura, T.; Yamamoto, K.; Bunz, U. H.; Yamamoto, Y. *Chem. Commun.* **2018**, *54*, 2534-2537.

(91) Malwitz, M. A.; Lim, S. H.; White-Morris, R. L.; Pham, D. M.; Olmstead, M. M.; Balch, A. L. *J. Am. Chem. Soc.* **2012**, *134*, 10885-10893.

(92) Wadas, T. J.; Wang, Q.-M.; Kim, Y.-j.; Flaschenreim, C.; Blanton, T. N.; Eisenberg, R. *J. Am. Chem. Soc.* **2004**, *126*, 16841-16849.

(93) Mansour, M. A.; Connick, W. B.; Lachicotte, R. J.; Gysling, H. J.; Eisenberg, R. *J. Am. Chem. Soc* **1998**, *120*, 1329-1330.

(94) Lim, S. H.; Olmstead, M. M.; Balch, A. L. *J. Am. Chem. Soc.* **2011**, *133*, 10229-10238.

(95) Lim, S. H.; Olmstead, M. M.; Balch, A. L. *Chem. Sci.* **2013**, *4*, 311-318.

(96) Mei, J.; Leung, N. L.; Kwok, R. T.; Lam, J. W.; Tang, B. Z. *Chem. Rev.* **2015**, *115*, 11718-11940.

(97) Gao, M.; Tang, B. Z. *ACS sensors* **2017**, *2*, 1382-1399.

(98) Feng, H.-T.; Yuan, Y.-X.; Xiong, J.-B.; Zheng, Y.-S.; Tang, B. Z. *Chem. Soc. Rev.* **2018**, *47*, 7452-7476.

(99) Hong, Y.; Lam, J. W. Y.; Tang, B. Z. *Chem. Commun.* **2009**, 4332-4353.

(100) Hong, Y.; Lam, J. W.; Tang, B. Z. *Chem. Soc. Rev.* **2011**, *40*, 5361-5388.

(101) Sharber, S. A.; Shih, K.-C.; Mann, A.; Frausto, F.; Haas, T. E.; Nieh, M.-P.; Thomas, S. W. *Chem. Sci.* **2018**, *9*, 5415-5426.

(102) Wang, J.; Mei, J.; Hu, R.; Sun, J. Z.; Qin, A.; Tang, B. Z. *J. Am. Chem. Soc.* **2012**, *134*, 9956-9966.

(103) Wu, Z.; Mo, S.; Tan, L.; Fang, B.; Su, Z.; Zhang, Y.; Yin, M. *Small* **2018**, *14*, 1802524.

(104) Wei, Z.; Gu, Z.-Y.; Arvapally, R. K.; Chen, Y.-P.; McDougald Jr, R. N.; Ivy, J. F.; Yakovenko, A. A.; Feng, D.; Omary, M. A.; Zhou, H.-C. *J. Am. Chem. Soc.* **2014**, *136*, 8269-8276.

(105) Sun, Y.-P.; Bunker, C. E. *J. Am. Chem. Soc.* **1994**, *116*, 2430-2433.

(106) Schuddeboom, W.; Jonker, S. A.; Warman, J. M.; de Haas, M. P.; Vermeulen, M. J.; Jager, W. F.; de Lange, B.; Feringa, B. L.; Fessenden, R. W. *J. Am. Chem. Soc.* **1993**, *115*, 3286-3290.

(107) Ma, J.; Zimmt, M. B. *J. Am. Chem. Soc.* **1992**, *114*, 9723-9724.

(108) Kokado, K.; Sada, K. *Angew. Chem.* **2019**, *131*, 8724-8731.

(109) Würthner, F. *Angew. Chem. Int. Ed.* **2020**, *59*, 14192-14196.

(110) Cai, X.; Liu, B. *Angew. Chem.* **2020**, *132*, 9952-9970.

(111) La, D. D.; Bhosale, S. V.; Jones, L. A.; Bhosale, S. V. *ACS Appl. Mater. Interfaces.* **2017**, *10*, 12189-12216.

(112) Yang, Z.; Chi, Z.; Mao, Z.; Zhang, Y.; Liu, S.; Zhao, J.; Aldred, M. P.; Chi, Z. *Materials Chemistry Frontiers* **2018**, *2*, 861-890.

(113) Shultz, D. A.; Fox, M. A. *J. Am. Chem. Soc.* **1989**, *111*, 6311-6320.

(114) Vyas, V. S.; Rathore, R. *Chem. Commun.* **2010**, *46*, 1065-1067.

(115) Wang, W.; Lin, T.; Wang, M.; Liu, T.-X.; Ren, L.; Chen, D.; Huang, S. *J. Phys. Chem. B.* **2010**, *114*, 5983-5988.

(116) Huang, G.; Ma, B.; Chen, J.; Peng, Q.; Zhang, G.; Fan, Q.; Zhang, D. *Chem. - Eur. J.* **2012**, *18*, 3886-3892.

(117) Mallory, F. B.; Mallory, C. W. *Org. React.* **2004**, *30*, 1-456.

(118) Zhang, Z.; Miljanić, O. Š. *Org. Mater.* **2019**, *1*, 019-029.

(119) Tao, P.; Zhang, Y.; Wang, J.; Wei, L.; Li, H.; Li, X.; Zhao, Q.; Zhang, X.; Liu, S.; Wang, H. *J. Mater. Chem. C.* **2017**, *5*, 9306-9314.

(120) Babudri, F.; Farinola, G. M.; Naso, F.; Ragni, R. *Chem. Commun.* **2007**, 1003-1022.

(121) Lin, Y.; Chen, G.; Zhao, L.; Yuan, W. Z.; Zhang, Y.; Tang, B. Z. *J. Mater. Chem. C.* **2015**, *3*, 112-120.

(122) Zhang, H.; Nie, Y.; Miao, J.; Zhang, D.; Li, Y.; Liu, G.; Sun, G.; Jiang, X. *J. Mater. Chem. C.* **2019**, *7*, 3306-3314.

(123) Yang, Z.; Qin, W.; Leung, N. L.; Arseneault, M.; Lam, J. W.; Liang, G.; Sung, H. H.; Williams, I. D.; Tang, B. Z. *J. Mater. Chem. C.* **2016**, *4*, 99-107.

(124) Suzuki, H.; Aihara, M.; Yamamoto, H.; Takamoto, Y.; Ogawa, T. *Synthesis (Stuttgart)* **1988**, 236-238.

(125) Yao, M.-L.; Kabalka, G. W.; Blevins, D. W.; Reddy, M. S.; Yong, L. *Tetrahedron* **2012**, *68*, 3738-3743.

(126) Zhang, G.-F.; Chen, Z.-Q.; Aldred, M. P.; Hu, Z.; Chen, T.; Huang, Z.; Meng, X.; Zhu, M.-Q. *Chem. Commun.* **2014**, *50*, 12058-12060.

(127) Parke, S. M.; Hupf, E.; Matharu, G. K.; de Aguiar, I.; Xu, L.; Yu, H.; Boone, M. P.; de Souza, G. L.; McDonald, R.; Ferguson, M. J. *Angew. Chem. Int. Ed.* **2018**, *57*, 14841-14846.

(128) Bunker, C. E.; Hamilton, N. B.; Sun, Y. P. *Anal. Chem.* **1993**, *65*, 3460-3465.

(129) Talele, H. R.; Gohil, M. J.; Bedekar, A. V. *Bull. Chem. Soc. Jpn.* **2009**, *82*, 1182-1186.

(130) Piou, T.; Rovis, T. *Acc. Chem. Res.* **2018**, *51*, 170-180.

(131) He, J.; Wasa, M.; Chan, K. S.; Shao, Q.; Yu, J.-Q. *Chem. Rev.* **2017**, *117*, 8754-8786.

(132) Kealy, T.; Pauson, P. *Nature* **1951**, *168*, 1039-1040.

(133) Evans, W. J. *Organometallics* **2016**, *35*, 3088-3100.

(134) Crabtree, R. H. John Wiley & Sons, 2009.

(135) Arndt, S.; Okuda, J. *Chem. Rev.* **2002**, *102*, 1953-1976.

(136) Jutzi, P.; Burford, N. *Chem. Rev.* **1999**, *99*.

(137) Hartwig, J.; University Science Books, Sausalito: 2010.

(138) Elschenbroich, C. *Wiley-VCH, Weinheim. J. Am. Chem. Soc.* **2006**, *128*, 12029-12030.

(139) Piou, T.; Romanov-Michailidis, F.; Romanova-Michaelides, M.; Jackson, K. E.; Semakul, N.; Taggart, T. D.; Newell, B. S.; Rithner, C. D.; Paton, R. S.; Rovis, T. *J. Am. Chem. Soc.* **2017**, *139*, 1296-1310.

(140) Dunwoody, N.; Sun, S.-S.; Lees, A. J. *Inorg. Chem.* **2000**, *39*, 4442-4451.

(141) Janiak, C.; Versteeg, U.; Lange, K. C.; Weimann, R.; Hahn, E. *J. Organomet. Chem.* **1995**, *501*, 219-234.

(142) Okuda, J. *Transition Metall Coordination Chemistry* **1992**, 97-145.

(143) King, R.; Bisnette, M. *J. Organomet. Chem.* **1967**, *8*, 287-297.

(144) Janowicz, A. H.; Bergman, R. G. *J. Am. Chem. Soc.* **1982**, *104*, 352-354.

(145) Jones, W. D.; Feher, F. J. *J. Am. Chem. Soc.* **1982**, *104*, 4240-4242.

(146) Bolig, A. D.; Brookhart, M. *J. Am. Chem. Soc.* **2007**, *129*, 14544-14545.

(147) Hyster, T. K.; Rovis, T. *Chemical science* **2011**, *2*, 1606-1610.

(148) Romanov-Michailidis, F.; Sedillo, K. F.; Neely, J. M.; Rovis, T. *J. Am. Chem. Soc.* **2015**, *137*, 8892-8895.

(149) Blaser, H. U.; Federsel, H.-J. *Asymmetric catalysis on industrial scale: challenges, approaches and solutions*; John Wiley & Sons, 2011.

(150) Zhou, Q.-L. *Privileged chiral ligands and catalysts*; John Wiley & Sons, 2011.

(151) Yoon, T. P.; Jacobsen, E. N. *Science* **2003**, *299*, 1691-1693.

(152) Ye, B.; Cramer, N. *Acc. Chem. Res.* **2015**, *48*, 1308-1318.

(153) Halterman, R. L. *Chem. Rev.* **1992**, *92*, 965-994.

(154) Dai, L.-X.; Hou, X.-L. *Chiral ferrocenes in asymmetric catalysis: synthesis and applications*; John Wiley & Sons, 2010.

(155) Hoveyda, A. H.; Morken, J. P. *Angewandte Chemie International Edition in English* **1996**, *35*, 1262-1284.

(156) Wang, H.; Park, Y.; Bai, Z.; Chang, S.; He, G.; Chen, G. *J. Am. Chem. Soc.* **2019**, *141*, 7194-7201.

(157) Murata, K.; Ikariya, T.; Noyori, R. *J. Org. Chem.* **1999**, *64*, 2186-2187.

(158) Kündig, E. P.; Saudan, C. M.; Viton, F. *Adv. Synth. Catal.* **2001**, *343*, 51-56.

(159) Trost, B. M.; Rao, M.; Dieskau, A. P. *J. Am. Chem. Soc.* **2013**, *135*, 18697-18704.

(160) Matsushima, Y.; Onitsuka, K.; Kondo, T.; Mitsudo, T.-a.; Takahashi, S. *J. Am. Chem. Soc.* **2001**, *123*, 10405-10406.

(161) Newton, C. G.; Kossler, D.; Cramer, N. *J. Am. Chem. Soc.* **2016**, *138*, 3935-3941.

(162) Cesarotti, E.; Ugo, R.; Kagan, H. *Angew. Chem., Int. Ed. Engl.* **1979**, *18*, 779-780.

(163) Cesarotti, E.; Kagan, H.; Goddard, R.; Krüger, C. *J. Organomet. Chem.* **1978**, *162*, 297-309.

(164) Halterman, R. L.; Vollhardt, K. P. C. *Tetrahedron Lett.* **1986**, *27*, 1461-1464.

(165) Halterman, R. L.; Vollhardt, K. P. C. *Organometallics* **1988**, *7*, 883-892.

(166) Colletti, S. L.; Halterman, R. L. *Tetrahedron Lett.* **1989**, *30*, 3513-3516.

(167) Ye, B.; Cramer, N. *Science* **2012**, *338*, 504-506.

(168) Ye, B.; Cramer, N. *J. Am. Chem. Soc.* **2013**, *135*, 636-639.

(169) Mas-Roselló, J.; Herraiz, A. G.; Audic, B.; Laverny, A.; Cramer, N. *Angew. Chem.* **2021**, *133*, 13306-13332.

(170) Hyster, T. K.; Knörr, L.; Ward, T. R.; Rovis, T. *Science* **2012**, *338*, 500-503.

(171) Cui, W.-J.; Wu, Z.-J.; Gu, Q.; You, S.-L. *J. Am. Chem. Soc.* **2020**, *142*, 7379-7385.

(172) Sun, Y.; Cramer, N. *Chem. Sci.* **2018**, *9*, 2981-2985.

(173) Jia, Z. J.; Merten, C.; Gontla, R.; Daniliuc, C. G.; Antonchick, A. P.; Waldmann, H. *Angew. Chem.* **2017**, *129*, 2469-2474.

(174) Wang, S. G.; Park, S. H.; Cramer, N. *Angew. Chem.* **2018**, *130*, 5557-5560.

(175) Park, S. H.; Wang, S.-G.; Cramer, N. *Acs Catalysis* **2019**, *9*, 10226-10231.

(176) Liang, H.; Vasamsetty, L.; Li, T.; Jiang, J.; Pang, X.; Wang, J. *Chem. - Eur. J.* **2020**, *26*, 14546-14550.

(177) Phanopoulos, A.; Miller, P. W.; Long, N. J. *Coord. Chem. Rev.* **2015**, *299*, 39-60.

(178) Grabulosa, A.; P-Stereogenic Ligands in Enantioselective Catalysis; Wiley-VCH: Weinheim, Germany: 2008.

(179) Forcato, M.; Lake, F.; Mba Blazquez, M.; Renner, P.; Crisma, M.; Gade, L. H.; Licini, G.; Moberg, C.; Wiley Online Library: 2006.

(180) Fang, T.; Du, D.-M.; Lu, S.-F.; Xu, J. *Org. Lett.* **2005**, *7*, 2081-2084.

(181) Gibson, S. E.; Castaldi, M. P. *Angew. Chem. Int. Ed.* **2006**, *45*, 4718-4720.

(182) Moberg, C. *Angew. Chem. Int. Ed.* **1998**, *37*, 248-268.

(183) Gibson, S. E.; Castaldi, M. P. *Chem. Commun.* **2006**, 3045-3062.

(184) MacBeth, C. E.; Thomas, J. C.; Betley, T. A.; Peters, J. C. *Inorg. Chem.* **2004**, *43*, 4645-4662.

(185) Jenkins, D. M.; Di Bilio, A. J.; Allen, M. J.; Betley, T. A.; Peters, J. C. *J. Am. Chem. Soc.* **2002**, *124*, 15336-15350.

(186) Phanopoulos, A.; Brown, N. J.; White, A. J.; Long, N. J.; Miller, P. W. *Inorg. Chem.* **2014**, *53*, 3742-3752.

(187) Scherl, P.; Kruckenberg, A.; Mader, S.; Wadepohl, H.; Gade, L. H. *Organometallics* **2012**, *31*, 7024-7027.

(188) Bogza, M.; Oeser, T.; Blümel, J. *J. Organomet. Chem.* **2005**, *690*, 3383-3389.

(189) Herold, S.; Mezzetti, A.; Venanzi, L. M.; Albinati, A.; Lianza, F.; Gerfin, T.; Gramlich, V. *Inorg. Chim. Acta* **1995**, *235*, 215-231.

(190) Dau, M. T.; Shakirova, J. R.; Karttunen, A. J.; Grachova, E. V.; Tunik, S. P.; Melnikov, A. S.; Pakkanen, T. A.; Koshevoy, I. O. *Inorg. Chem.* **2014**, *53*, 4705-4715.

(191) Guenther, J.; Reibenspies, J.; Blümel, J. *Adv. Synth. Catal.* **2011**, *353*, 443-460.

(192) Mellah, M.; Voituriez, A.; Schulz, E. *Chem. Rev.* **2007**, *107*, 5133-5209.

(193) Abel, E.; Bhargava, S.; Orrell, K. *by SJ Lippard, An Interscience Publication, John Wiley & Sons, New York, Chichester, Brisbane, Toronto, Singapore* **1984**, *32*, 1-118.

(194) Dornan, P. K.; Leung, P. L.; Dong, V. M. *Tetrahedron* **2011**, *67*, 4378-4384.

(195) Krimmer, S. G.; Cramer, J.; Betz, M.; Fridh, V.; Karlsson, R.; Heine, A.; Klebe, G. *J. Med. Chem.* **2016**, *59*, 10530-10548.

(196) Cain, M. F.; Glueck, D. S.; Golen, J. A.; Rheingold, A. L. *Organometallics* **2012**, *31*, 775-778.

(197) Brodersen, K.; Rölz, W.; Jordan, G.; Gerbeth, R.; Ellermann, J. *Chem. Ber.* **1978**, *111*, 132-142.

(198) Yan, J.; Ouyang, R.; Jensen, P. S.; Ascic, E.; Tanner, D.; Mao, B.; Zhang, J.; Tang, C.; Hush, N. S.; Ulstrup, J.; Reimers, J. R. *J. Am. Chem. Soc.* **2014**, *136*, 17087-17094.

(199) Carey, F. A.; Sundberg, R. J.; Springer Science & Business Media, 2007.

(200) Krief, A.; Kremer, A. In *Comprehensive Organic Synthesis II (Second Edition)*; Pergamon, Elsevier Science Ltd: 2014, p 56-156.

(201) Fürstner, A. In *Alkene Metathesis in Organic Synthesis*; Springer: 1998, p 37-72.

(202) Zaitsev, V. G.; Shabashov, D.; Daugulis, O. *J. Am. Chem. Soc.* **2005**, *127*, 13154-13155.

(203) Kommagalla, Y.; Chatani, N. *Coord. Chem. Rev.* **2017**, *350*, 117-135.

(204) He, G.; Wang, B.; Nack, W. A.; Chen, G. *Acc. Chem. Res.* **2016**, *49*, 635-645.

(205) Castro, L. C. M.; Chatani, N. *Chem. Lett.* **2015**, *44*, 410-421.

(206) Daugulis, O.; Roane, J.; Tran, L. D. *Acc. Chem. Res.* **2015**, *48*, 1053-1064.

(207) Tong, H.-R.; Zheng, S.; Li, X.; Deng, Z.; Wang, H.; He, G.; Peng, Q.; Chen, G. *ACS Catalysis* **2018**, *8*, 11502-11512.

(208) Yan, S. Y.; Han, Y. Q.; Yao, Q. J.; Nie, X. L.; Liu, L.; Shi, B. F. *Angew. Chem. Int. Ed.* **2018**, *57*, 9093-9097.

(209) Yan, S.-B.; Zhang, S.; Duan, W.-L. *Org. Lett.* **2015**, *17*, 2458-2461.

(210) Grigorjeva, L.; Daugulis, O. *Org. Lett.* **2014**, *16*, 4684-4687.

(211) Aderibigbe, S. O.; Coltart, D. M. *J. Org. Chem.* **2019**, *84*, 9770-9777.

(212) Hu, J.; Lan, T.; Sun, Y.; Chen, H.; Yao, J.; Rao, Y. *Chem. Commun.* **2015**, *51*, 14929-14932.

(213) Saunders, W. H.; Carges, G. L. *J. Am. Chem. Soc.* **1960**, *82*, 3582-3585.